ISSN 1408-7073

RMZ – MATERIALS AND GEOENVIRONMENT

PERIODICAL FOR MINING, METALLURGY AND GEOLOGY

RMZ – MATERIALI IN GEOOKOLJE

REVIJA ZA RUDARSTVO, METALURGIJO IN GEOLOGIJO

RMZ-M&G, Vol. 55, No. 3 pp. 307-407 (2008)

Ljubljana, September 2008

Historical Review

More than 80 years have passed since in 1919 the University Ljubljana in Slovenia was founded. Technical fields were joint in the School of Engineering that included the Geologic and Mining Division while the Metallurgy Division was established in 1939 only. Today the Departments of Geology, Mining and Geotechnology, Materials and Metallurgy are part of the Faculty of Natural Sciences and Engineering, University of Ljubljana.

Before War II the members of the Mining Section together with the Association of Yugoslav Mining and Metallurgy Engineers began to publish the summaries of their research and studies in their technical periodical Rudarski zbornik (Mining Proceedings). Three volumes of Rudarski zbornik (1937, 1938 and 1939) were published. The War interrupted the publication and not until 1952 the first number of the new journal Rudarsko-metalurški zbornik - RMZ (Mining and Metallurgy Quarterly) has been published by the Division of Mining and Metallurgy, University of Ljubljana. Later the journal has been regularly published quarterly by the Departments of Geology, Mining and Geotechnology, Materials and Metallurgy, and the Institute for Mining, Geotechnology and Environment.

On the meeting of the Advisory and the Editorial Board on May 22nd 1998 Rudarsko-metalurški zbornik has been renamed into "RMZ - Materials and Geoenvironment (RMZ -Materiali in Geookolje)" or shortly RMZ - M&G.

RMZ - M&G is managed by an international advisory and editorial board and is exchanged with other world-known periodicals. All the papers are reviewed by the corresponding professionals and experts.

RMZ - M&G is the only scientific and professional periodical in Slovenia, which is published in the same form nearly 50 years. It incorporates the scientific and professional topics in geology, mining, and geotechnology, in materials and in metallurgy.

The wide range of topics inside the geosciences are welcome to be published in the RMZ -Materials and Geoenvironment. Research results in geology, hydrogeology, mining, geotechnology, materials, metallurgy, natural and antropogenic pollution of environment, biogeochemistry are proposed fields of work which the journal will handle. RMZ - M&G is co-issued and co-financed by the Faculty of Natural Sciences and Engineering Ljubljana, and the Institute for Mining, Geotechnology and Environment Ljubljana. In addition it is financially supported also by the Ministry of Higher Education, Science and Technology of Republic of Slovenia.

Editor in chief

Table of Contents – Kazalo

Aluminium alloys for cylinder heads

Aluminijeve zlitine za glave cilindrov

Stanislav Kores[1], Hennadiy Zak[2], Babette Tonn[2]

[1]University of Ljubljana, Faculty of Natural Sciences and Engineering, Department of Materials and Metallurgy, Aškerčeva cesta 12, SI-1000 Ljubljana, Slovenia;
E-mail: stanislav.kores@ntf.uni-lj.si
[2]TU Clausthal, Institute of Metallurgy, Department for Foundry Technology, Robert-Koch-Straße 42, D-38678 Clausthal-Zellerfeld, Germany;
E-mail: hennadiy.zak@tu-clausthal.de, babette.tonn@ tu-clausthal.de

Received: February 14, 2008 **Accepted:** July 17, 2008

Abstract: Nearly 100 % of all cylinder heads of the current light displacement vehicle production consist of aluminium cast alloys. The alloys have to sustain continuously growing requirements in terms of strength, ductility and heat resistance at an elevated temperature. Three different aluminium cylinder head alloys AlSi6Cu4, AlSi7MgCu0.5 and AlMg3Si1ScZr were examined and compared to each other with respect to fluidity, mechanical properties and hot cracking behaviour.

Izvleček: Skoraj 100 % vseh glav cilindrov aktualne proizvodnje avtomobilov je narejenih iz aluminijevih zlitin. Material glav cilindrov mora dosegati vedno večje zahteve po trdnosti, duktilnosti in obstojnosti pri visokih temperaturah. Preiskane so bile tri različne zlitine za izdelavo glav cilindrov AlSi6Cu4, AlSi7MgCu0.5 in AlMg3Si1ScZr ter med seboj primerjane glede livnosti, mehanskih lastnosti in nastanka razpok v vročem.

Key words: Al-Si alloy, cylinder heads, fluidity, mechanical properties
Ključne besede: Al-Si zlitine, glave cilindrov, livnost, mehanske lastnosti

Introduction

A contribution to reduce emission can be made by weight reduction, but at the same time an increase in power and torque are expected by the automotive customer[1].

Figure 1 shows the development of the power rating in diesel engine construction. Future developments will further aggravate this situation, because the next generation of diesel engines is likely to achieve a specific power rating of 75 kW/l and igniting pressures of 220 bars[2].

The cylinder head is one of the most complex and intensively loaded component in the engine (Figure 2). Not only camshaft

Scientific paper

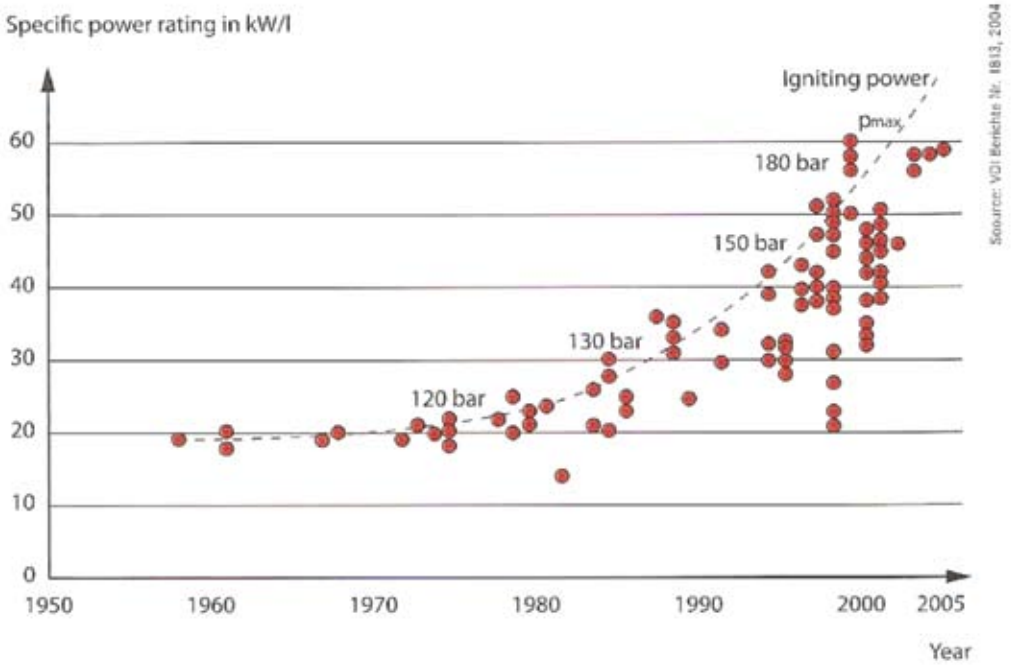

Figure 1. Development of the power rating and peak pressure in a car diesel engine[2]
Slika 1. Razvoj rasti moči in tlaka v avtomobilih z dizelskim motorjem[2]

Figure 2. Cylinder head[3]
Slika 2. Glava cilindra[3]

driven valves and combustion chamber, but also the camshaft bearing support is subjected to high stresses at high temperatures[2].

The aim of this research project was the comparison of two commercial heat resistant aluminium alloys AlSi7Mg0.5 and AlSi6Cu4, widely used in the production of cylinder heads, with a newly developed AlMg3Si1ScZr alloy. The following characteristics of the alloys were examined:

- mechanical properties at room temperature,
- mechanical properties at 250 °C,
- mechanical properties after 100 h preaging at 250 °C and tested at 250 °C,
- hot cracking behaviour,
- melt fluidity.

Experimental

Table 1 shows the chemical composition of the investigated alloys. For melting experiments an electric-resistance furnace with a crucible capacity of 3 kg was used. The melt was heated up to 720 °C and poured into several different test moulds.

Hot Cracking Behaviour

Hot cracking behaviour was defined with the star mould which is shown in Figure 3. The mould is made from gray cast iron and heated to 300 °C prior to casting.

Bars of different length are cast through a central gate in a star arrangement. These bars have thick portions at their ends, which obstruct shrinkage. The hot cracking behaviour was defined by evaluation of the cracks found[4]. For this, the castings were assessed visually by the number and relative importance of cracks or break-away bars using the following rating scheme (Figure 4):

- Number of full break-away rods × weighting factor 1,
- Number of wide circumferential cracks × weighting factor 0.75,
- Number of easily visible cracks × weighting factor 0.5 and,
- Number of hairline cracks (seen under the magnifying glass) × weighting factor 0.25.

Table 1. Chemical composition of investigated alloys in wt. % [3,4,5]
Tabela 1. Kemijska sestava preiskovanih zlitin v ut. % [3,4,5]

Alloy	Si	Fe	Cu	Mn	Mg	Zn	Ti	Al
AlSi7MgCu	7.0	0.30	0.50	0.20	0.30	0.10	0.15	rest
AlSi6Cu	7.21	0.36	3.84	0.45	0.33	0.88	0.16	rest
AlMg3Si1(Sc,Zr)	1.09	0.08	0.003	0.012	3.29	0.001	0.02	rest

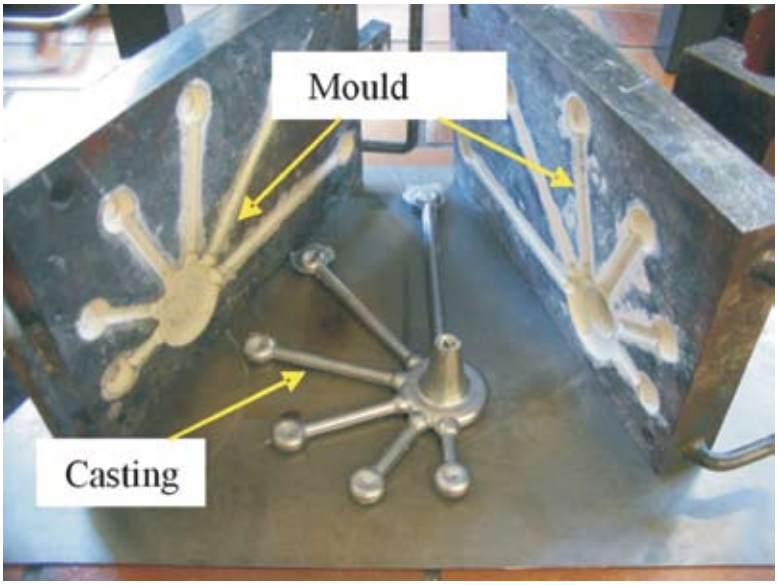

Figure 3. Star mould for assessment of hot cracking behaviour with star casting
Slika 3. Zvezdasta kokila z zvezdastim ulitkom za opazovanje razpok v vročem

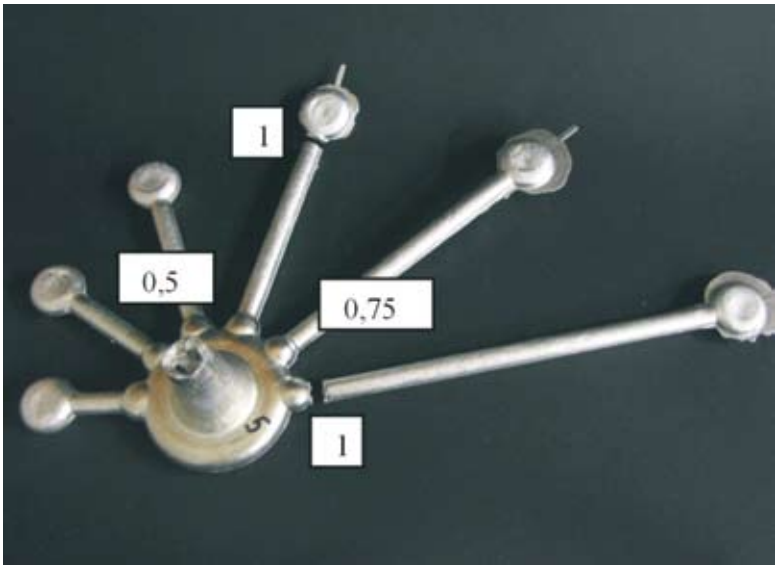

Figure 4. Star casting used to test hot cracking behaviour of the alloy
Slika 4. Zvezdasti ulitek za določitev razpok v vročem preiskovane zlitine

Definition of Fluidity

Fluidity is a material characteristic, telling how far a metal can flow in the mould and depends not only on the alloy's characteristics but also on the mould properties such as dimension, geometry, material, initial mould temperature, pouring temperature, etc. It is usually assessed as the total length of the branches filled with metal after solidification[6]. In this research an aluminium spiral mould heated up to 100 °C for determining the fluidity was used (Figure 5). The length of the spiral in cm after the experiment was measured.

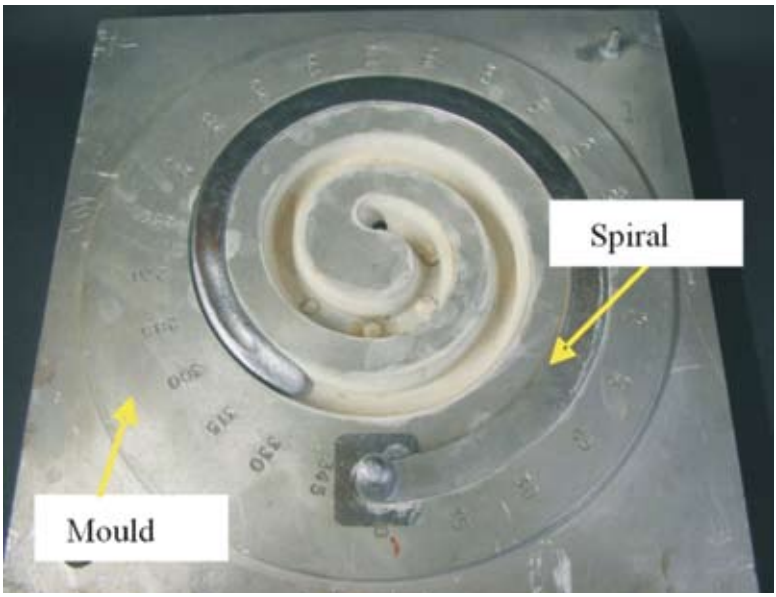

Figure 5. Mould for investigation of fluidity
Slika 5. Kokila za merjenje livnosti

Mechanical Properties

To study the mechanical properties a test specimen was used which was cast into a mould from gray cast iron according to DIN 29531 (Figure 6). The mould temperature was 300 °C. This mould provides castings that must be machined to the dimensions shown in Table 2. The tensile strength, yield strength and elongation were defined with tensile tests.

All alloys were T6 heat treated. Table 3 shows the heat treatment for each alloy. The samples were solution heat treated, quenched and hot age-hardened.

Table 2. Dimension of tensile test specimens
Tabela 2. Dimenzija vzorca za natezni preizkus

Specimens diameter d_0 [mm]	Coil d_1 [mm]	Head height h [mm]	Measurement length L_0 [mm]	Search length L_V [mm]	Total length L_T [mm]
6	M10	8	30	36	60

Table 3. Heat treatment for investigated alloys
Tabela 3. Toplotna obdelava preiskovanih zlitin

	AlSi7MgCu0,5		AlSi6Cu4		AlMg3Si1ScZr	
Solution treatment	Temperature [°C]	Time [h]	Temperature [°C]	Time [h]	Temperature [°C]	Time [h]
	530	6	505	6	505	10
	Water - quench		Water - quench		Water - quench	
Hot age-hardening	170	7	170	8	170	8

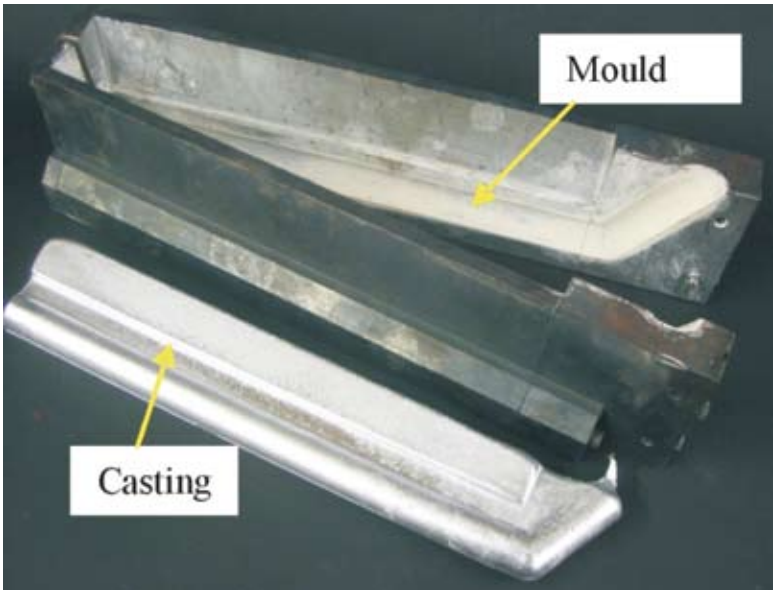

Figure 6. Mould and test bar according to DIN 29531
Slika 6. Kokila in preizkušanec po DIN 29531

RESULTS AND DISCUSSION

The results of the star mould casting are presented in Table 4. The higher the hot cracking index, the more likely is the alloy to develope hot cracks. The AlMg3Si1ScZr alloy reached the highest hot cracking index with 1.25.

Table 4. Hot cracking index of the investigated alloys
Tabela 4. Indeks razpok v vročem preiskovanih zlitin

Alloy	Hot cracking index
AlSi7MgCu0,5	0.75
AlSi6Cu4	0
AlMg3Si1ScZr	1.25

Table 5 shows the results of fluidity investigation. The best fluidity results show AlSi7MgCu0.5 alloy followed by AlMg3Si1ScZr and AlSi6Cu4 alloys.

Table 5. Fluidity of investigated alloys
Tabela 5. Livnost preiskovanih zlitin

Alloy	Length [cm]
AlSi7MgCu0,5	64.8
AlSi6Cu4	43.2
AlMg3Si1ScZr	52.5

The results of the tensile tests measured at room temperature are presented in Figures 7-9. Figure 7 evidently shows, that commercial alloys, AlSi6Cu4 and AlSi7MgCu0.5 and the newly developed AlMg3Si1ScZr alloy achieve similar values for tensile strength in as cast condition. After heat treatment the values for tensile strength of AlSi6Cu4 alloy rises to 408 MPa, AlSi7MgCu0.5 to 318 MPa and AlMg3Si1ScZr to 251 MPa.

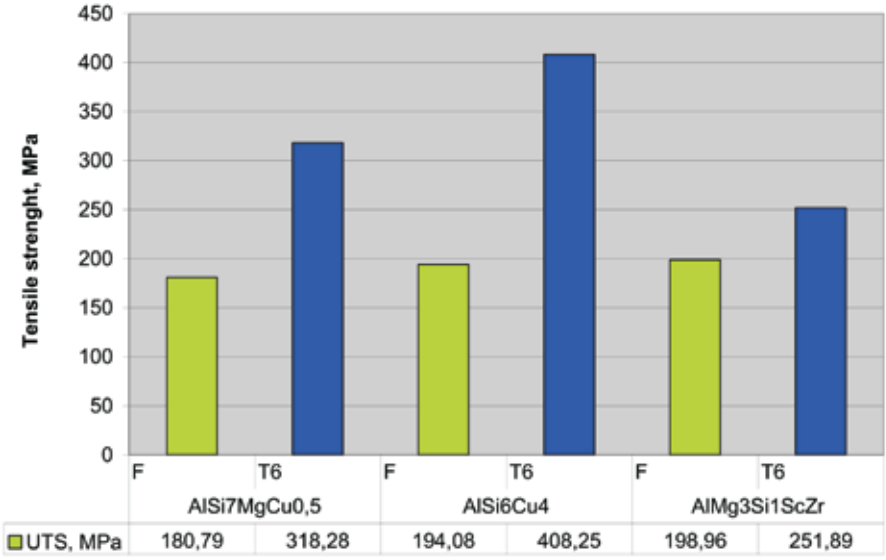

Figure 7. Tensile strength of investigated alloys, measured at room temperature (F – as-cast, T6 – heat treated)
Slika 7. Natezna trdost preiskovanih zlitin, merjena pri sobni temperature (F – lito stanje, T6 – toplotno obdelano stanje)

Figure 8 presents the yield strength of the investigated alloys. The AlSi6Cu4 alloy has a yield point of 136 MPa in as-cast condition. After heat treatment the yield point rises to 383 MPa. The yield point for AlMg3Si1Sc1Zr is 23 MPa higher then AlSi7MgCu0,5 in as-cast condition. But the yield point after heat treatment of the AlSi7MgCu0.5 alloy is higher than the AlMg3Si1ScZr alloy.

Figure 9 depicts the elongation of the investigated alloys. Obviously the best results in as-cast conditions showed the AlSi7MgCu0.5 alloy with an elongation of 6 %. After the heat treatment an increase of

elongation values of 8.7 % can be detected. The AlMg3Si1ScZr alloy shows the best results after heat treatment with 10.7 %. The high strength AlSi6Cu4 alloy shows the poorest ductility.

The results of tensile tests at 250 °C of the investigated alloys are shown in Figure 10. The newly developed alloy AlMg3Si1SCZr shows by far the best elongation results with 16 % at 250 °C. But the tensile strength and yield strength of this alloy are comparable with commercial AlSi7MgCu0.5 alloy. The best tensile strength and yield strength results show AlSi6Cu4 alloy.

After pre-aging 100 hours at 250 °C the material performance at 250 °C is quit different. This test simulates the working condition in a cylinder head for a long period of time. Figure 11 evidently shows that AlMg3Si1ScZr alloy has the best results of all three investigated alloys. This alloy achieves a tensile strength of 251 MPa and the highest yield strength of 162 MPa.

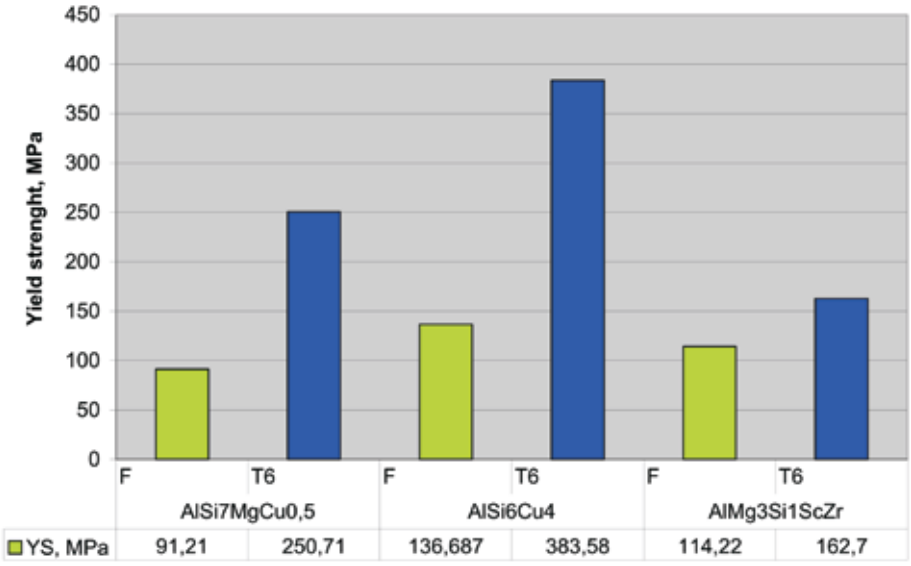

Figure 8. Yield strength of investigated alloys, measured at room temperature (F – as-cast, T6 – heat treated)
Slika 8. Meja tečenja preiskovanih zlitin, merjena pri sobni temperature (F – lito stanje, T6 – toplotno obdelano stanje)

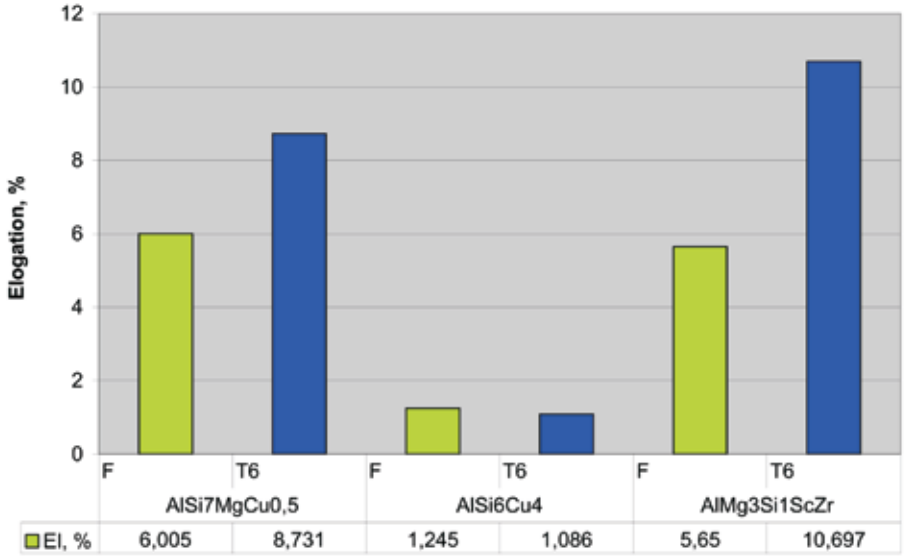

Figure 9. Elongation of investigated alloys, measured at room temperature (F – as-cast, T6 – heat treated)
Slika 9. Raztezek preiskovanih zlitin, merjen pri sobni temperature (F – lito stanje, T6 – toplotno obdelano stanje)

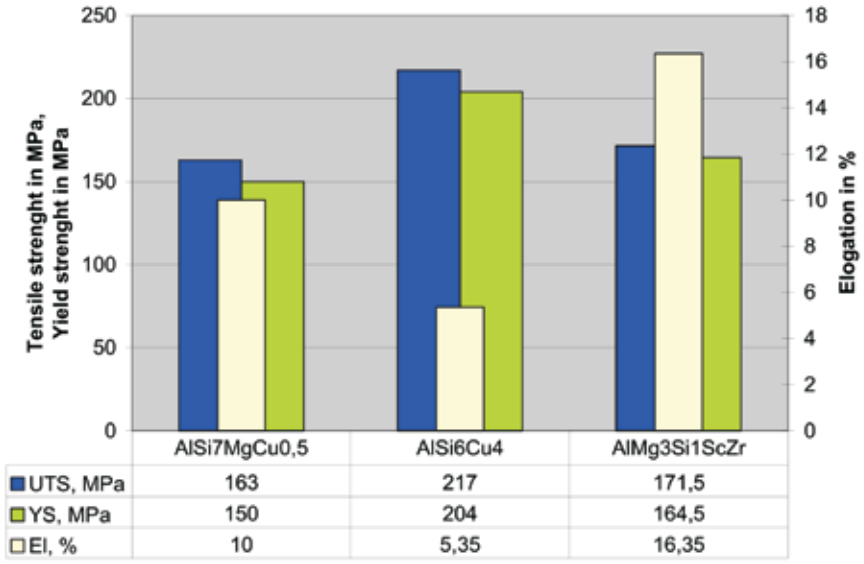

Figure 10. Tensile strength, yield strength and elongation of T6- heat treated alloys tested at 250 °C
Slika 10. Natezna trdnost, meja tečenja in raztezek T6 toplotno obdelanih zlitin, preizkus pri 250 °C

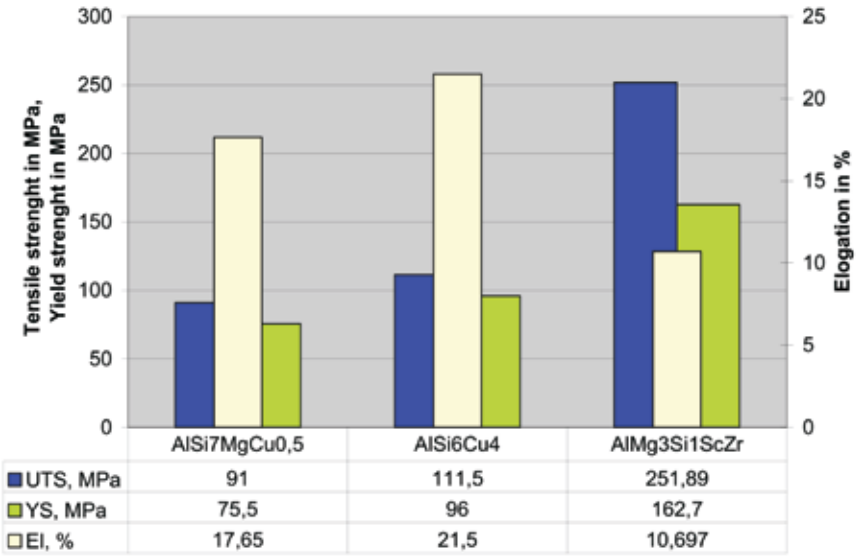

Figure 11. Tensile strength, yield strength and elongation T6-heat treated alloys tested at 250 °C, pre-aging 100 hours at 250 °C
Slika 11. Natezna trdnost, meja tečenja in raztezek T6 toplotno obdelanih zlitin staranih 100 ur na 250 °C, preizkus pri 250 °C

CONCLUSIONS

The AlMg3Si1ScZr alloy shows the best compromise of ductility and mechanical properties at 250 °C after pre-aging 100 hours at 250 °C, but it also shows the worst hot-tearing behaviour. The addition of Sc and Zr to the AlMg3Si1 base alloy has a positive effect on the mechanical properties, but on the other hand raises costs, which must be accepted by the industry. If 0.2 wt. % Sc is added to an alloy it will increase material cost to US$5/kg which, depending on the alloy, represents a doubling to quadrupling of the material cost[7].

The excellent tensile properties, fluidity and resistance to hot-tearing, allows the well known AlSi6Cu4 and AlSi7MgCu0.5 alloys to retain their leading position in the production of aluminium cylinder heads in the near future.

POVZETEK

Aluminijeve zlitine za glave cilindrov

Glave cilindrov so dan danes narejene izrecno iz aluminijevih zlitin in so ene izmed najbolj obremenjenih komponent v motorju. V tem delu so bile raziskane zlitine za izdelavo glav cilindrov. Preiskovale in primerjale so se dve poznani komercialni zlitini AlSi7MgCu0,5 in AlSi6Cu4 z novo razvito zlitino AlMg3Si1ScZr glede na mehanske lastnosti pri sobni temperaturi, po toplotni obdelavi in preizkusu pri 250°C

in po 100 urnem staranju na 250°C in preizkusu pri 250°C. Preiskovale so se tudi livarske lastnosti, kot so nastank razpok v vročem in livnost zlitin. Pri mehanskih lastnostih so se opazovale natezna trdnost, meja tečenja in raztezek zlitine. Zlitine so bile ulite v zato pripravljeno kokilo iz sive litine po standardu DIN 29531. Ulitek se je nato obdelal na dimenzije za natezni preizkus. Nastanek razpok se je opazovalo s pomočjo zvezdaste kokile. Kokila je bila opremljena z petimi različno dolgimi palicami katerih konci so odebeljeni. Pri strjevanju prihaja do krčenja in zato do napetosti, kar posledica so razpoke. Razpoke so bile razdeljene v štiri razrede ter jim dodeljene vrednosti, in sicer indeks 1 za popolnoma odlomljeno palico, indeks 0,75 za razpoko, ki je potekala okrog palice, 0,5 za razpoko, ki je bila tako velika, da je bila vidna s prostim očesom in 0,25 za razpoko, ki je bila vidna le pod povečevalnim steklom. Vsi indeksi so bili nato sešteti in dobljen je bil indeks nastanka razpok v vročem. Livnost se je določevala s pomočjo spiralaste kokile. Kokila je bila izdelana iz aluminija in ob vsakem litju ogreta na 100 °C. Po končanem preizkusu je bila izmerjena dolžina spirale.

Zlitina AlMg3Si1ScZr je pokazala najboljšo kombinacijo duktilnosti in mehanskih lastnosti pri 250 °C po 100 urnem staranju na 250 °C, vendar tudi visok indeks nastanka razpok v vročem. Dodatka Sc in Zr imata pozitiven učinek na mehanske lastnosti, vendar prinašata visoke stroške, kar mora biti sprejeto s strani industrije. Dodatek 0,2 ut. % Sc zlitini poveča ceno zlitine za 5 $/kg.

Odlične lastnosti pri nateznem preizkusu, livnost in obstojnost v vročem, prinašajo zlitinam AlSi6Cu4 in AlSi7MgCu0,5 vodilno mesto pri proizvodnji aluminijastih glav cilindrov v bližnji prihodnosti.

References

[1] Schneider, W. (2005): Highly stressed automotive engines of aluminium Challenges for the casting technology and material development. *Giessereiforschung 57*. No. 2, pp. 2-6.

[2] Mnich, F., Seawert, H.C., Bahr, R. (2007): NDCS-a new process for manufacturing Al automotive castings. *Casting, Plant and Technology*.; No. 1, pp. 34-37.

[3] VAW-IMCO, Guss und Recycling GmbH, 3. Auflage, 2004.

[4] Eigenfeld, K., Franke, A., Klan, S., Koch, H., Lenczowski, B., Pflege, B. (2004): New developments in heat resistant aluminium casting materials. *Casting Plant + Technology International*.; No. 4, pp. 4-9.

[5] Aluminium RHEINFELDEN, Ausgabe 6, 5/94.

[6] Vojtech, D., Šerak, J., Ekrt, O. (2004): Improving the casting properties of high-strength aluminium alloys. *Materials and Technology*.; Vol. 38, No. 1-2.

[7] Royset, J. (2007): Scandium in aluminium alloys overview: Physical metallurgy, properties and applications. *Metallurgical Science and Technology*. Vol. 25, No. 2, pp. 11-21.

Microstructure development of Nimonic 80A superalloy during hot deformation

Razvoj mikrostrukture superzlitine Nimonic 80 A med vročo deformacijo

David Bombač[1], Matevž Fazarinc[1], Goran Kugler[1], Savo Spajić[1]

[1]University of Ljubljana, Faculty of Natural Sciences and Engineering, Department of Materials and Metallurgy, Aškerčeva cesta 12, SI-1000 Ljubljana, Slovenia;
E-mail: david.bombac@ntf.uni-lj.si,
matevz.fazarinc@ntf.uni-lj.si, goran.kugler@ntf.uni-lj.si

Received: February 11, 2008 **Accepted:** July 31, 2008

Abstract: Uniaxial cylindrical compression tests at various temperatures and strain rates have been performed on the Nimonic 80A superalloy samples in order to define the best hot working characteristics. Evolution of the microstructure in correlation to the deformation temperatures, strain and strain rates has also been investigated by means of optical microscopy. The activation energy for hot deformation was derived with use of the Zener-Hollomon hyperbolic sine equation. Onset of dynamic recrystallization (DRX) was investigated with interrupted compression tests and metallographic analysis. Experimental data was also used for calculation of the processing maps on the basis of Dynamic Material Model.

Izvleček: Pri študiji najprimernejših karakteristik vroče predelave superzlitine Nimonic 80 A so bili izvedeni enoosni valjasti tlačni preizkusi pri različnih temperaturah in hitrostih deformacije. Razvoj mikrostrukture v odvisnosti od temperature deformacije, deformacije in hitrosti deformacije je bila raziskana z optično mikroskopijo. Aktivacijska energija za deformacijo je bila izračunana s pomočjo sinushiperbolične oblike Zener-Hollomonove enačbe. Začetek dinamične rekristalizacije je bil raziskan s prekinjenimi tlačnimi preizkusi in metalografsko analizo. Podatki dobljeni s preizkusi so služili tudi izračunu procesnih map.

Key words: Nimonic 80A, hot working, compression tests, optical microscopy, processing maps
Ključne besede: Nimonic 80A, vroče preoblikovanje, tlačni preizkus, optična mikroskopija, procesne mape

Scientific paper

INTRODUCTION

Design of new products with nickel-based superalloys and wide field of their use is in constant raise because of very specific material properties. Nickel-based superalloy Nimonic is a group of high temperature alloys intended for sophisticated parts used in high temperature applications. Unfortunately complex system of phases makes them very difficult to deform plastically. Further studies are necessary to predict the best hot workability and final microstructure and therefore a detailed understanding of interactions between hot deformation behavior and softening mechanisms i.e. recrystallization and recovery[1-3].

The Nimonic 80A superalloy is nonmagnetic at room temperature and does not go through any phase transformations when cooled from liquid phase. It contains Ti and Al, that form an ordered g' phase with composition of $Ni_3(Al,Ti)$ along with MC type primary carbides and Cr rich grain-boundary carbides of $M_{23}C_6$ type. Carbides of MC and $M_{23}C_6$ type were found to precipitate from the matrix at temperatures between 760 °C and 1000 °C, while above 1000 °C main carbides of M_6C type and less stable M_7C_3 will precipitate on grain boundaries where M is usually Cr, and less commonly W, Ta, Nb[4-6, 12].

Best mechanical properties of products made from Nimonic grade superalloy are achieved with homogenous fine grain microstructure. During hot forming metals experience strain hardening as the dislocation density increases. As deformation advances the energy during hot working causes upstart of the softening mechanism like dynamic recovery (DRV) and dynamic recrystallization (DRX). The hot workability of alloy is limited because carbides inhibit DRX and accelerate rupture. To execute the best hot working conditions one needs to select and use correct plastic deformation degree, suitable cool down period and also oversee softening mechanisms.

In this study laboratory compression tests at different temperatures have been performed to define best hot forming characteristics. Evolution of microstructure is investigated with optical microscopy in correlation to temperature, strain and strain rate. Also critical strain for DRX onset is determined from micrographs for various strains. From compression tests processing maps were calculated using dynamic material model.

EXPERIMENTAL PROCEDURE

The polycrystalline wrought nickel-based super-alloy with it's chemical composition after electro slag remelting presented in Table 1, was supplied by Metal Ravne d.o.o., Ravne, Slovenia. From a forged billet of dimensions 90 mm × 90 mm, which was later rolled to diameter Ø 11 mm and quenched in water from 1030 °C, cylindrical specimens were machined. Size of the

Table 1. Chemical composition of the Nimonic 80A alloy in wt.%
Tabela 1. Kemična sestava zlitine Nimonic 80A v mas.%

	C	Si	Cu	Mn	Cr	Ti	Al	Fe	P	S	N_2 pmm	O_2 pmm
NIMONIC 80A	0.07	0.08	0.02	0.03	19.54	2.38	1.51	0.21	0.002	0.002	70	100

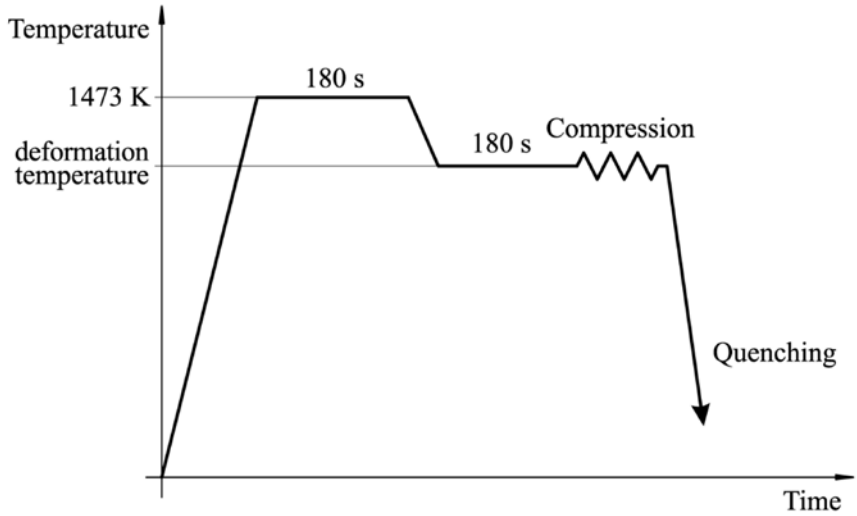

Figure 1. Schematic diagram of the hot compression process
Slika 1. Shematski prikaz procesa toplega tlačnega testa

compression specimens was Ø 10 mm and height 10 mm with measured hardness of approximately 330 HB.

Hot forming parameters and DRX start were studied by means of hot compression tests carried out on Gleeble 1500D thermo-mechanical simulator. Simulation conditions were as follows: temperature 950 °C, 1000 °C, 1040 °C, 1080 °C and 1120 °C and strain rates for all temperatures 0.01 s^{-1}, 0.1 s^{-1}, 1 s^{-1} and 5 s^{-1}. To avoid inhomogeneous deformation, tantalum follies of 0.05 mm thickness were inserted between cylindrical specimen and compression tool–anvil. After deformation the specimens were water quenched to freeze their microstructure. Figure 1 shows schematic time–temperature diagram of the hot compression tests.

Deformed, water quenched samples were visually inspected, cut and prepared for optical microscopy and analysis.

Results and discussion

The development of any process modeling capability requires a description of the viscoplastic flow behavior of the material in question. Results of the hot compression tests are depicted in Figure 2. Figure 2a depicts the effect of strain rate on stress-strain curves at 1080 °C. The flow stress decreases with lower strain rates, as does the strain at which the stress peak appears. Typical stress-strain curves for different temperatures and strain rate for strain rate 0.1 s^{-1} are presented in Figure 2b. A clear increase of flow stress with lowered testing temperature can be observed. In general, increase of force is required to deform the specimen at lower temperature and tendency for the phenomenon of interest to occur at higher temperature as strain rate increases.

Initial microstructure of the specimens is shown in Figure 3, where nonuniform grain arrangement with typical anneal twins can

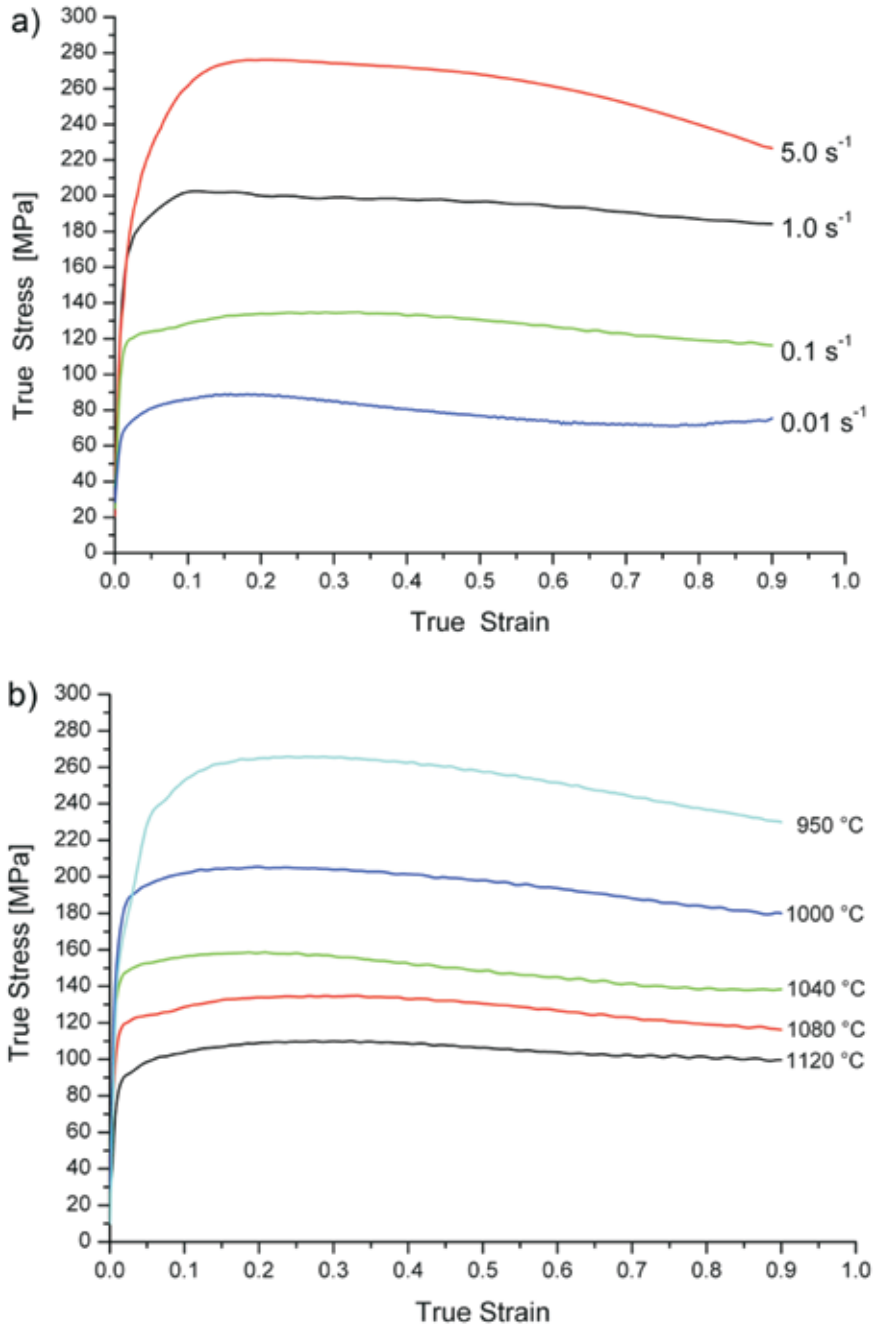

Figure 2. Flow curves; a) at temperature 1080 °C, b) at strain rate 0.1 s^{-1}
Slika 2. Krivulje tečenja; a) pri temperaturi 1080 °C, b) za hitrost deformacije 0,1 s^{-1}

be seen. Grain size varies regarding to the position from where micrograph is collected. On the diagonal and edge of the specimen grains of initial microstructure are finer than in the center.

Values for the peak stress for all deformation conditions were collected and analyzed. The peak stresses exhibits a clear decay trend with higher temperature. As expected, at any given temperature peak stress values also increases with higher strain rate. The activation energy for hot deformation is 379.28 kJ/mol and was derived with the Zener-Hollomon hyperbolic sine equation[7].

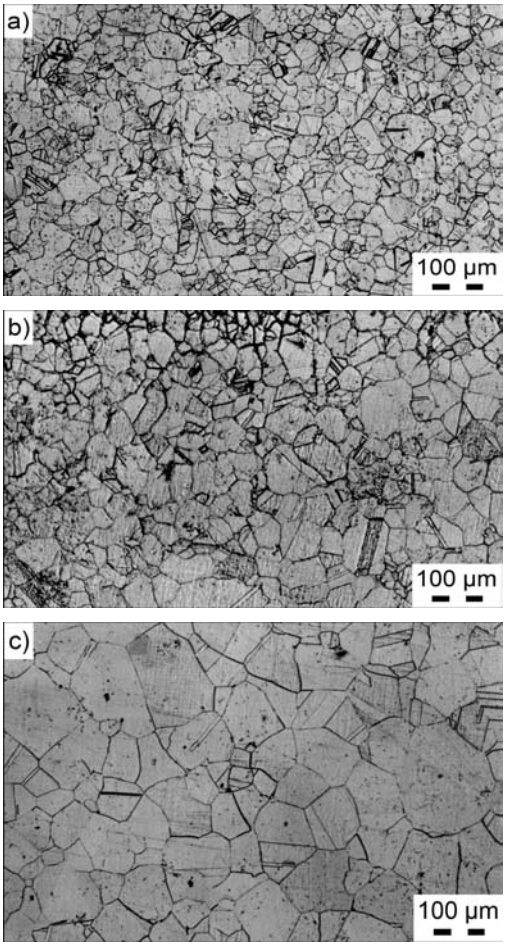

Figure 3. Initial microstructure at different specimen positions; a) diagonal , b) edge, c) center

Slika 3. Začetna mikrostruktura na različnih pozicijah vzorca; a) diagonala, b) rob, c) sredina

Flow curves in Figure 2 exhibits pronounced stress peaks which indicate occurrence of the dynamic recrystallization (DRX), but they does not provide information about the onset of DRX. The critical strain for DRX occurrence can be determined metallographically from grain development at various strains. For this purpose compression test at 1080 °C and strain rate 0.1 s^{-1} was interrupted and microstructure frozen at strain values of 0.0175, 0.175 and 0.40. In Figure 4 micrographs for these strains are depicted. The critical strain for DRX initiation depends on chemical composition, initial grain size, temperature and strain rate. A flow stress increase at diminished rate beyond critical strain, until the work hardening and dynamic softening becomes balanced, climaxing in a peak stress. Grain boundaries are preferential positions for initiation of the DRX[8, 9]. In Figure 4b onset of DRX at grain boundaries with bulging mechanism can be seen. Bulged boundaries later grow into new recrystallized grains as seen in Figure 4c.

Vickers micro-hardness measurements show a difference between recrystallized and non-recrystallized hardness. Microhardness of recrystallized grains was between 270 $HV_{0.1}$ and 280 $HV_{0.1}$, while for non-recrystallized grains the value was between 310 $HV_{0.1}$ and 320 $HV_{0.1}$.

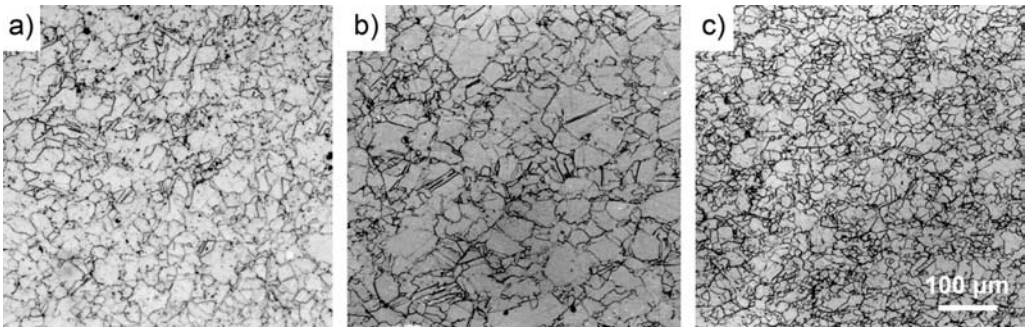

Figure 4. Microstructure observation of DRX onset from quenched samples at temperature of 1080 °C and strain rate of 0.1 s^{-1} at strain; a) 0.0175; b) 0.175 and c) 0.40
Slika 4. Mikrostruktura gašenih vzorcev pri opazovanju začetka dinamične rekristalizacije pri temperaturi 1080 °C in hitrosti deformacije 0,1 s^{-1} za deformacijo; a) 0,0175; b) 0,175 and c) 0,40

Evolution of microstructure obtained with hot compression tests and optical microscopy is shown in Figure 5. Micrographs have been taken from the center part of the specimens. Differences in microstructures can be explained with unequal deformation and stress distribution. At strain rate 0.01 s^{-1}, dynamic recrystallization has been visible at 950 °C, while carbides rearrangement process did not start to this point because of the low temperature and short time cycle. Rearrangement process is clearly visible at other temperatures. At middle temperatures and strain rates, the large un-recrystallized grains are surrounded by small grains, exhibiting a so-called necklace structure. New recrystallized grains nucleate on the boundaries of old ones and grow until energy for grain boundary movement is positive or until they colide with other grains. Start of the DRX with very small amount of recrystallized material volume is visible at highest strain rate. DRX start depends on temperature and strain rate and is shifted to lower temperatures if the strain rate is lowered. Critical deformation for DRX is first obtained at the center of the specimen. These results was also confirmed with findings of other authors[6,10].

Best hot working conditions were established using processing maps calculated on the basis of the Dynamic Material Model[11]. Maps obtained at strains 0.1, 0.2, 0.3 and 0.6 are similar to each other, indicating the limited influence of strain. Processing maps revealed unstable regions at high temperatures and strain rates at strains 0.1 and 0.2 as shown in Figure 6a and Figure 6b, respectively. Nimonic 80A has a prominent high temperature domain with the peak efficiency of power dissipation being about 40 % at 1000 °C and stain rate of 0.01 s^{-1}. For industrial praxis where are higher strain rates, optimal forming interval is between 1000 °C and 1080 °C.

CONCLUSIONS

Retrieved results can be usefully implemented into hot forming process. With

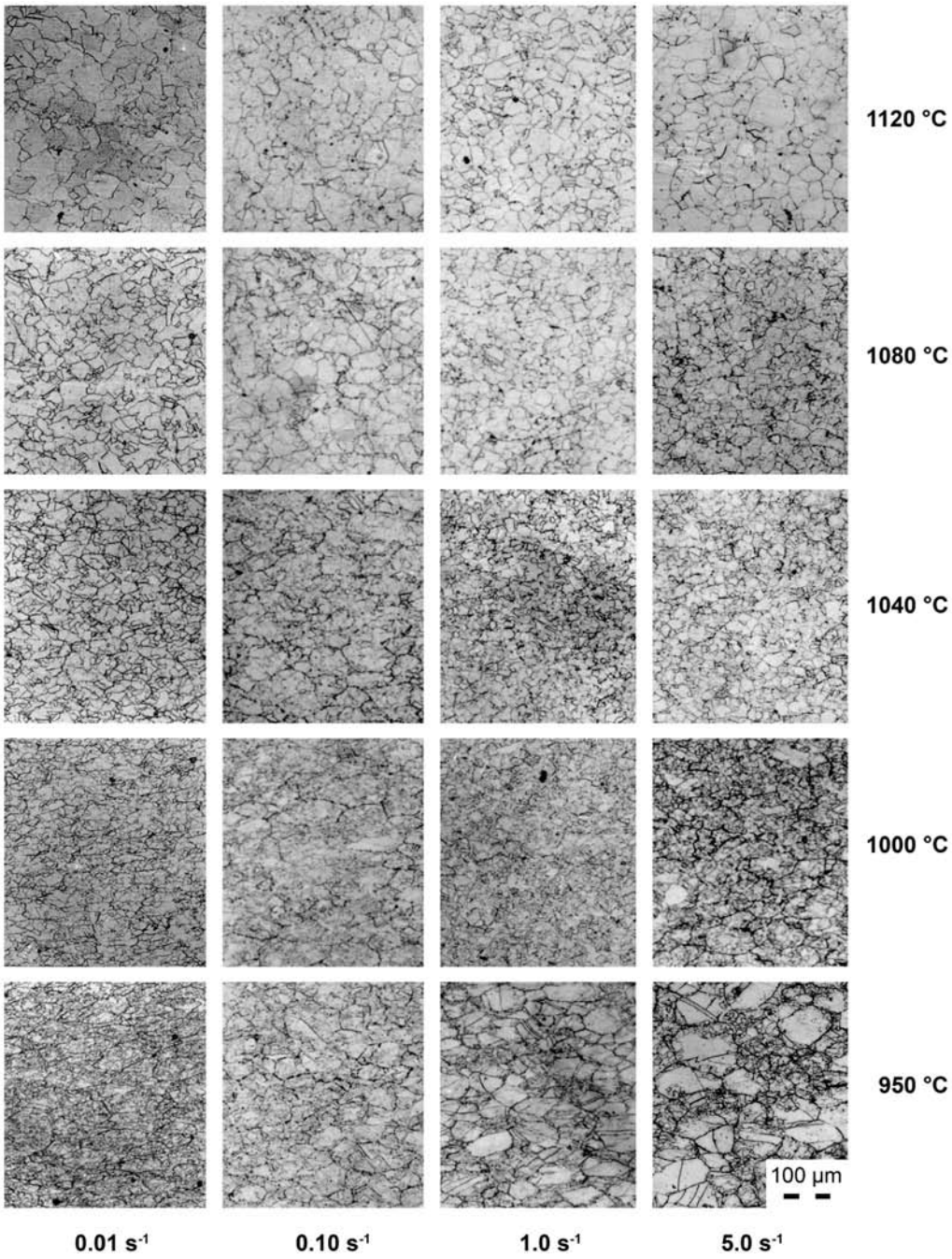

Figure 5. Microstructure development from hot compression tests dependent on the temperature and strain rate, taken from the middle of the specimen
Slika 5. Razvoj mikrostrukture vročega tlačnega preizkusa v odvisnosti od temperature in hitrosti deformacije, s sredine vzorcev

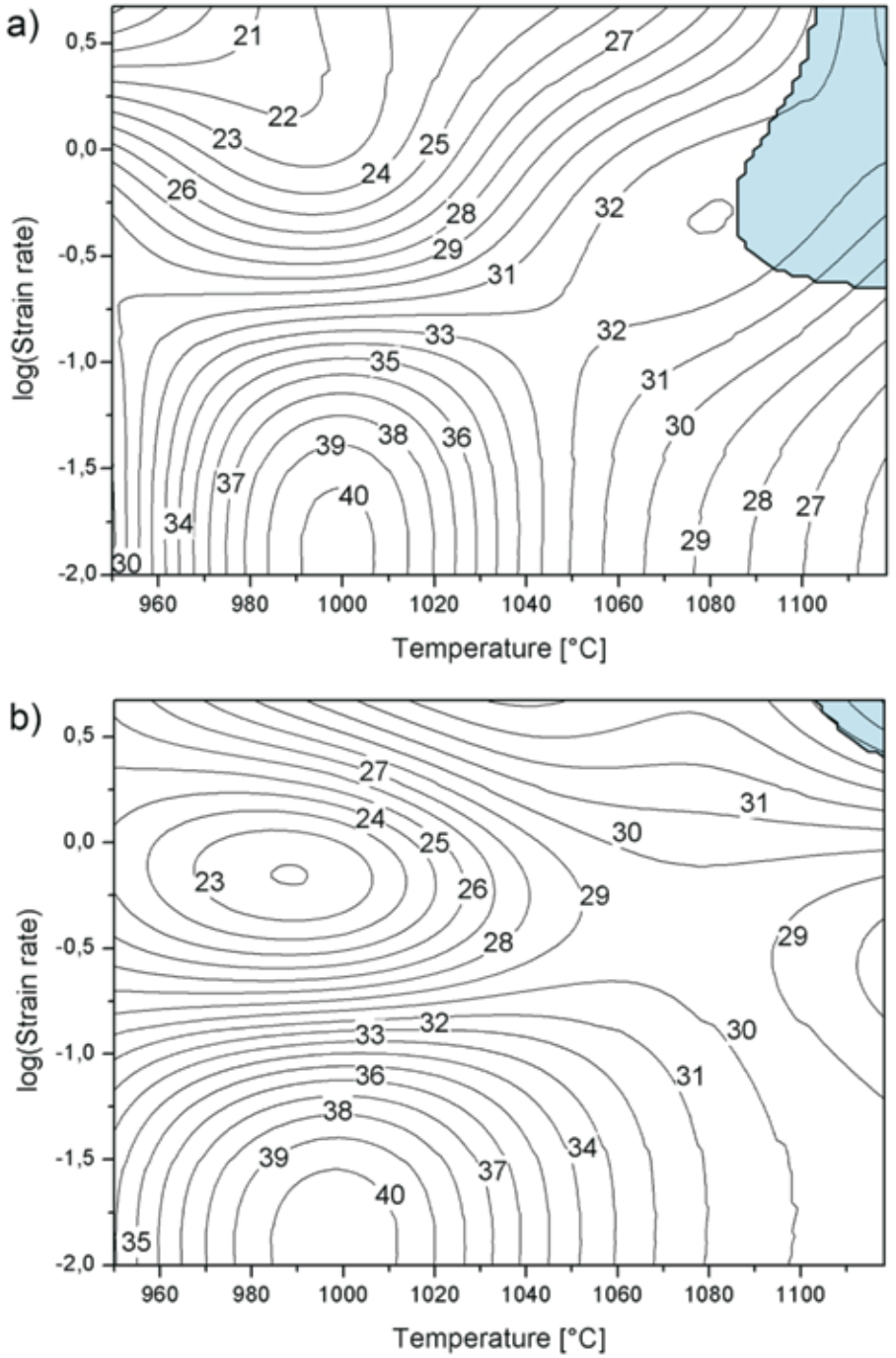

Figure 6. Processing maps for strain; a) of 0.1 and b) of 0.2
Slika 6. Procesna mapa pri deformaciji; a) 0,1 in b) 0,2

correct reductions at the end of the manufacturing process, homogenously recrystallized fine grain microstructure can be assured as has been proved in this paper with hot compression tests at various temperatures and strain rates. The following conclusions can be drawn as a result of this paper.

- When strain rate is increased or temperature lowered, the apex of stress is shifted to higher strain.
- The fraction of recrystallized material is higher at increased temperatures and lowered strain rates. DRX starts at a strain rate 0.01 s^{-1} at 900 °C.
- The optimum hot working conditions for industrial praxis lie between 1000 °C and 1080 °C.
- Unstable regions for hot working conditions were found at strains of 0.1 and 0.2 at high temperatures and high strain rates.

Povzetek

Razvoj mikrostrukture superzlitine Nimonic 80 A med vročo deformacijo

Pri študiji najprimernejših karakteristik vroče predelave superzlitine Nimonic 80 A so bili izvedeni enoosni valjasti tlačni preizkusi pri različnih temperaturah in hitrostih deformacije. Razvoj mikrostrukture v odvisnosti od temperature deformacije, deformacije in hitrosti deformacije je bila raziskana z optično mikroskopijo. Aktivacijska energija za deformacijo je bila izračunana s pomočjo sinushiperbolične oblike Zener-Hollomonove enačbe. Začetek dinamične rekristalizacije je bil raziskan s prekinjenimi tlačnimi preizkusi in metalografsko analizo. Podatki dobljeni s preizkusi so služili tudi izračunu procesnih map.

Pridobljene rezultate je možno uporabno vključiti v procese vroče predelave. S pravilno izbiro redukcije, še posebej pri koncu proizvodnega procesa lahko zagotovimo homogeno rekristalizirano mikrostrukturo, kot je bilo prikazano s pomočjo tlačnega preizkusa pri različnih temperaturah in hitrostih deformacije v tej študiji. Iz rezultatov študije je možno zaključiti, da kadar je hitrost deformacije povečana ali temperatura znižana, se vrh napetosti premakne proti večji deformaciji. Delež rekristaliziranega materiala je večji pri višjih temperaturah in nižjih hitrostih deformacije. Dinamična rekristalizacija se začne pri hitrosti deformacije 0,01 s^{-1} že pri 900 °C. Optimalni pogoji vroče predelave za industrijsko prakso ležijo med 1000 °C in 1080 °C. Nestabilna področja vroče predelave, je mogoče najti samo pri deformacijah 0,1 in 0,2 pri visokih temperaturah in velikih hitrostih deformacije.

References

[1] Sakai, T., Ohashi, M., China, K., Jonas, J.J. (1988): Recovery and recrystallization of polycrystalline nickel after hot working. *Acta Metallurgica*.; Vol. 7, pp. 1781-1790.

[2] Myshlyaev, M.M., McQueen, H.J., Mwembela, A., Konopleva, E. (2002): Twinning, dynamic recovery and recrystallization in hot worked Mg-Al-Zn alloy. *Ma-*

terials science & engineering. A, Structural materials: properties, microstructure and processing.; Vol 337, No. 1-2, pp. 121-133.

[3] Whillock, R.T.J., Buckley, R.A., Sellars, C.M. (2000): The influence of thermomechanical processing on recrystallization and precipitation in austenitic alloys with particular reference to the effects of deformation and ageing conditions. *Materials science & engineering. A, Structural materials: properties, microstructure and processing*.; Vol 276, No. 1-2, pp. 124-132.

[4] Bariani, P.F., Bruschi, S., Dal Negro, T. (2004): Prediction of nickel-base superalloys' rheological behaviour under hot forging conditions using artificial neural networks. *Journal of Materials Processing Technology*.; Vol. 3, pp. 395-400.

[5] Wilthan, B., Tanzer, R., Schützenhöfer, W., Pottlacher, G. (2007): Thermophysical properties of the Ni-based alloy Nimonic 80A up to 2400 K, III. *Thermochimica Acta*.; No. 1-2, pp. 83-87.

[6] Srinivasa, N., Prasad, Y.V.R.K. (1995): Hot working characteristics of Nimonic 75, 80A and 90 superalloys: a comparison using processing maps. *Journal of Materials Processing Technology*.; No. 1-4, pp. 171-192.

[7] Kugler, G., Knap, M., Palkowski, H., Turk, R. (2004): Estimation of activation energy for calculating the hot workability properties of metals. *Metalurgija*.; Vol. 43, No. 4, pp. 267-272.

[8] Kugler, G., Turk, R. (2004): Modeling the dynamic recrystallization under multi-stage hot deformation. *Acta Materialia*.; Vol. 15, pp. 4659-4668.

[9] Elwazri, A.M., Wanjara, P., Yue, S. (2004): Critical condition for dynamic recrystallisation of high carbon steels. *Materials Science and Technology*.; Vol. 20, No. 11, pp. 1469-1473.

[10] Tian, B., Lind, C., Paris, O. (2003): Influence of $Cr_{23}C_6$ carbides on dynamic recrystallization in hot deformed Nimonic 80a alloys. *Materials science & engineering. A, Structural materials: properties, microstructure and processing*.; No. 1-2, pp. 44-51.

[11] Prasad, Y.V.R.K., Sasidhara, S. (1997): *Hot Working Guide: A Compendium of Processing Maps*. ASM International, Materials Park, Ohio, 545 p.

[12] Novotnik, G. (1994): *Razvoj mikrostrukture zlitine nimonic 80a v temperaturnem območju toplega plastične predelave: magistrsko delo.* Naravoslovnotehniška fakulteta.

Microencapsulation technology and its applications in building construction materials

Tehnologija mikrokapsuliranja in njena uporaba v gradbenih materialih

Bojana Boh[1], Boštjan Šumiga[1,2]

[1]University of Ljubljana, Faculty of Natural Sciences and Engineering, Aškerčeva cesta 12, SI-1000 Ljubljana, Slovenia; E-mail: bojana.boh@ntf.uni-lj.si
[2]AERO, Chemical, Graphic and Paper Manufacturers, d.d. Celje, Ipavčeva ulica 32, SI-3000 Celje, Slovenia; E-mail: bostjan.sumiga@aero.si

Received: April 14, 2008 **Accepted:** August 25, 2008

Abstract: The article is a review of microencapsulation types, technologies, purposes of microencapsulation, release mechanisms, and application fields, with special emphasis on microencapsulated additives in building construction materials. The following improvements have been described in patents as a result of microencapsulated additives in the construction materials: increased fireproofing; improved freeze- and freeze-thaw resistance; reduced expansion and degradation of concrete and mortar; better hydration of concrete and mortar mixes in the compression-molding production of building elements; reduction of thermal cracking due to the heat release by cement hydration; decrease of water absorption of hydraulic cement sheets; insulation or absorption of noise; protection of building materials against mildew, bacteria, insects, rodents and environmental corrosion; fragranced / deodorising effect; and reversible thermochromic colour changes of cement-based materials for darker building exteriors in winter and lighter colours in summer. The fastest growing segment is that of insulating materials based on microencapsulated phase change materials (PCM) for active accumulation and release of heat. Microcapsules with a good mechanical resistance are essential to enable reversible liquid-solid-liquid phase transitions, and to protect the PCM during the whole product life.

Izvleček: Pregledni članek podaja tipe, tehnologije in namene mikrokapsuliranja, mehanizme sproščanja ter področja uporabe s podrobnejšim pregledom uporabe mikrokapsuliranih dodatkov v gradbenih materialih. V patentih so opisane naslednje izboljšave, dosežene s pomočjo mikrokapsuliranih aktivnih komponent: izboljšana protipožarna zaščita in negorljivost materialov; zmanjšano raztezanje in propadanje betona; preprečevanje razpok zaradi sproščanja toplote med hidracijo cementa; omogočanje hidracije cementnih izdelkov med proizvodnjo v stiskalnicah; zmanjšana vodna

Rewiew scientific paper

vpojnost cementnih plošč; zvočna izolacija in absorpcija zvoka; varovanje gradbenih materialov pred pojavom plesni, bakterij, insektov, glodalcev; zaščita pred korozijo; odišavnjenje in deodoriranje materialov; reverzibilne toplotne spremembe barv, ki omogočajo temnejšo barvo fasade pozimi in svetlejšo barvo poleti. Najhitreje razvijajoči se segment uporabe mikrokapsul so izolacijski materiali, ki temeljijo na fazno spremenljivih materialih (PCM) za aktivno akumulacijo in sproščanje toplote pri prehodih agregatnega stanja tekoče-trdno-tekoče. Mikrokapsule z dobro mehansko odpornostjo premoščajo problem reverzibilnih faznih prehodov in omogočajo varno zadrževanje PCM v gradbenem materialu skozi vso življensko dobo izdelka.

Key words: microencapsulation, microcapsules, applications, building, construction, materials

Ključne besede: mikrokapsuliranje, mikrokapsule, uporaba, gradbeništvo, materiali

MICROENCAPSULATION TECHNOLOGY

Microencapsulation is a technology of coating small particles of finely ground solids, drops of liquids, or gaseous components, with protective membranes – microcapsule walls (DEASY, 1984; ARSHADY & BOH, 2003). Industrial applications of microencapsulation were first introduced at the end of the 1950s in the production of pressure-sensitive copying papers for the encapsulation of hydrophobic solutions of leuco dyes (FANGER, 1974). Since then, microencapsulation has been constantly improved, modified and adapted for a variety of purposes and uses. As a consequence, it has become an example of a knowledge-intensive and dynamic technology (BOH & KARDOŠ, 2003), characterised by a rapid growth of patent applications, reflecting industrial research and development, as well as by an increasing number of new scientific articles, deriving from the basic research (Figure 1). In addition to the graphic and printing industries, microcapsules have been used for pharmaceutical and medical purposes, in cosmetic and food products, agricultural formulations, as well as in the chemical, textile and construction materials industries, biotechnology, photography, electronics, and waste treatment (BOH et al., 2003; BOH, 2007; PONCELET & BOH, 2008).

Several physical and chemical methods have been developed for the production of microcapsules (ARSHADY, 1999; VANDAMME et al., 2007). The most often used microencapsulation methods are (BOH, 1996a,b):

- **mechanical methods** (e.g. spray drying, pan coating, and solvent evaporation from emulsions), where the microcapsule wall is mechanically applied or condensed around the microcapsule core;
- **coacervation,** a phenomenon taking place in colloid systems, where macromolecular colloid rich coacervate droplets surround dispersed microcapsule cores, and form a viscous microcapsule wall, which is solidified with cross-linking agents (Figure 2), and

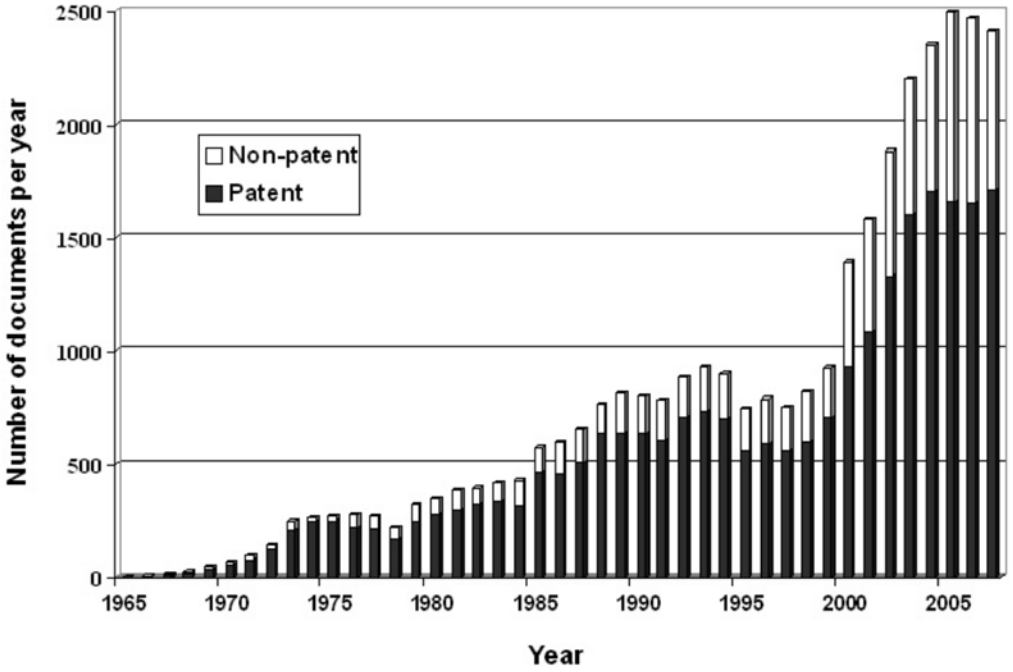

Figure 1. Growth of new patent documents and scientific articles on microencapsulation (CA Plus database)
Slika 1. Rast števila patentnih dokumentov in znanstvenih člankov na področju mikrokapsuliranja

- **polymerisation methods**, where monomers polymerise around droplets of an emulsion and form a solid polymeric wall. In **polymerisation *in situ*** monomers or precondensates are added only to the aqueous phase of emulsion (Figure 3), while in **interfacial polymerisation,** one of the monomers is dissolved in the aqueous phase and the other in a lypophylic solvent (Figure 4).

Due to the development and specialisation of microencapsulation technologies and applications, microencapsulation products differ in structure and terminology (Table 1), (Boh, 1996a,b).

Purposes of microencapsulation and release mechanisms

Different purposes of microcapsule-based final products require different characteristics of microcapsules. The size and shape of microcapsules, chemical properties of microcapsule walls, and their degradability, biocompatibility and permeability have to be considered in the selection of raw materials and microencapsulation processes. The purpose of microencapsulation is usually defined by the permeability. Microcapsules with **impermeable walls** are used in products where isolation of active substances is needed, followed by a quick release under defined conditions.

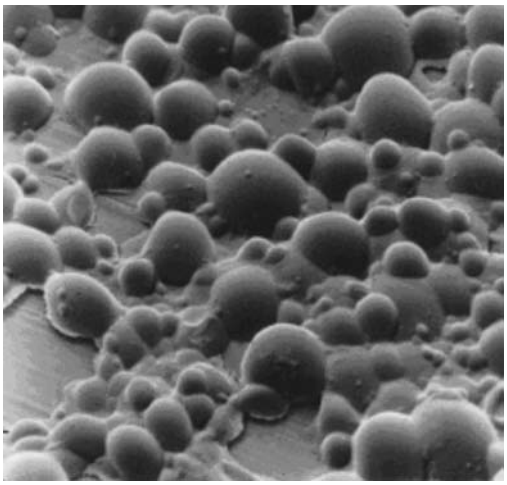

Figure 2. Coating of microcapsules, produced by complex coacervation of gelatin and carboxymethyl cellulose (scanning electron micrograph, 630 x), (BOH, 1986)
Slika 2. Premaz mikrokapsul, izdelanih po postopku kompleksne koacervacije želatine in karboksimetil celuloze (elektronski mikroskop, 630x), (BOH, 1986)

The effects achieved with impermeable microcapsules include: separation of reactive components, protection of sensitive substances against environmental effects, reduced volatility of highly volatile substances, conversion of liquid ingredients into a solid state, taste and odour masking, and toxicity reduction. On the other hand, microcapsules with **permeable walls** enable prolonged release of active components into the environment, such as in the case of prolonged release drugs, perfumes, deodorants, repellents, etc., or immobilisation with locally limited activity of microencapsulated substances. Examples of later include microencapsulated fertilizers and pesticides with locally limited release to reduce leaching into the ground water, or microencapsulated catalysts and enzymes for chemical and biotechnological processes (BOH, 1996a,b).

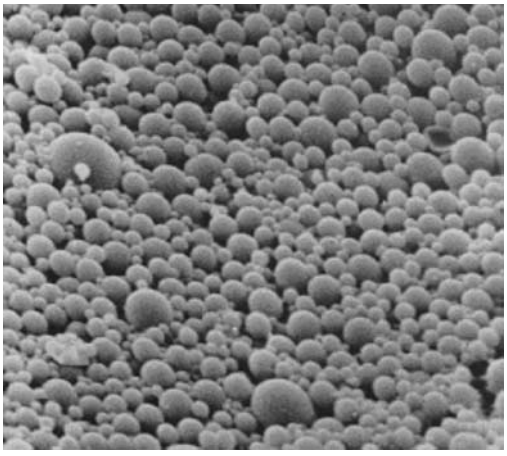

Figure 3. Coating of microcapsules, produced by in situ polymerization of aminoaldehyde precondensates (scanning electron micrograph, 1900x), (KNEZ, 1988; KUKOVIČ & KNEZ, 1996)
Slika 3. Premaz mikrokapsul, izdelanih z in situ polimerizacijo aminoaldehidnih predkondenzatov (elektronski mikroskop, 1900x), (KNEZ, 1988; KUKOVIČ & KNEZ, 1996)

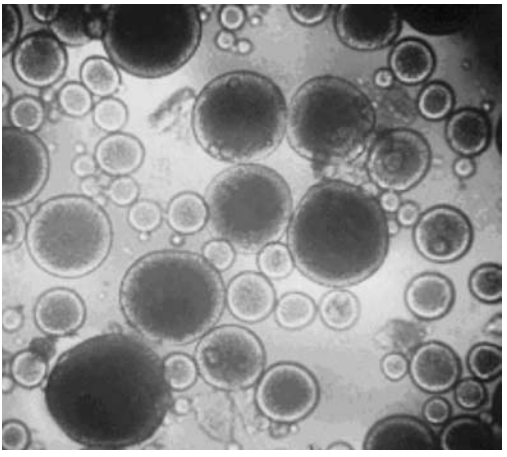

Figure 4. Suspension of microcapsules, produced by interfacial polymerization - crosslinking of proteins in a water-in-oil emulsion (light microscopy, 100x), (BOH, 1991)
Slika 4. Suspenzija mikrokapsul, izdelanih po postopku medpovršinske polimerizacije z zamreževanjem beljakovin v emulziji tipa voda v olju (optični mikroskop, 100x), (BOH, 1991)

Table 1. Terminology of microencapsulation products
Tabela 1. Poimenovanje produktov mikrokapsuliranja

Terminology	Description	Size range	Schematic illustration
Microcapsules (narrow sense of meaning)	Products of coating liquid nuclei with solid walls.	µm	
Nanocapsules	Same structure as microcapsules, but smaller.	nm	
Microspheres or microparticles	The cores and walls are both solid. Often, there is no clear distinction between them: the thick solid wall functions as a porous matrix where active substances are embedded.	µm	
Nanospheres or nanoparticles	Same structure as microspheres, but smaller.	nm	
Liposomes	Lipid wall, often made of phospholipids and cholesterol. Subtypes: unilamellar (one lipid layer) and multilamellar (several lipid layers).	µm to nm	
Niosomes	Similar to liposomes but their membranes are made of synthetic amphiphylic molecules (detergents).		

The **mechanisms of releasing encapsulated materials** are planned in advance and depend on the purpose of microencapsulation. An analysis of several hundred patent documents (BOH, 1996a,b; PONCELET & BOH, 2008) revealed that the first developed and still often used is the mechanism of **external pressure** which breaks the microcapsule wall and releases the liquid from the core. This principle is applied in pressure-sensitive copying papers (pressure of the pen-ball or typewriter head), multi-component adhesives (activation in a press), deodorants and fungicides for shoes (mechanical pressure caused by walking), polishing pastes (rubbing) and aromas and sweeteners in chewing gums (chewing). In some applications, the microcapsule wall breaks because of **inner pressure**, e.g. for blowing agents in the production of light plastic materials and synthetic leather. In instant drinks, microcapsules **dissolve** in water. Dissolution at the selected pH value is useful for microencapsulated catalysts and pharmaceuticals. Drugs, vitamins, minerals, essential amino acids, fatty acids, or even whole diets, can be released into the gastro-intestinal tract by **enzymatic degradation** of digestible microcapsules. The core substance can be released by **abrasion** of the microcapsule wall, e.g. in antistatics and fragrances for textiles (abrasion in washing machines and dryers), or for grinding and cutting additives. In many applications, core materials are released by **heat.** Heat-sensitive recording papers (e.g. telefax paper), temperature indicators for frozen food, heat-sensitive adhesives, textile softeners and fragrances in formulations for dryers, cosmetic components to be released at body temperature and aromas for tea and baking, are based on the effect of melting of the microcapsule wall. Microencapsulated fire retardants or extinguishers, based on release caused by **burning** of microcapsule walls, are used in fire-proof materials. These types of microcapsules are used for wall paper, carpets, curtains, fire-protecting clothes, and added to plastics and coatings for electric devices and wires. Microcapsules in special photographic emulsions, light-sensitive papers and toners for photocopiers are decomposed (or hardened) by **light**. If the wall is **permeable**, it **slowly releases** the content of the core. This mechanism can be applied in controlled drug release products, aromas, fragrances, insecticides and fertilisers. In the case of microencapsulated cells and enzymes in biotechnology, high-molecular weight components can be retained in microcapsules, while low-molecular by-products and substrate residues are **extracted** through **semi-permeable** microcapsule walls. A special example is that of microencapsulated phase change materials for active accumulation and release of heat in textiles, shoes and building insulation materials. To remain functional over numerous phase transition cycles, they have to **remain encapsulated** within the impermeable and mechanically resistant microcapsule wall for the whole product life.

APPLICATIONS OF MICROCAPSULES IN BUILDING CONSTRUCTION MATERIALS

An analysis of scientific articles and patents shows numerous possibilities of adding microencapsulated active ingredients into construction materials, such as cement, lime, concrete, mortar, artificial

marble, sealants, paints and other coatings, and functionalised textiles. A summary of applications is presented in Figure 5.

Fireproofing

Composite fire-resistant and lightweight building boards were patented (Adachi, 2005), containing a flammable substrate and a fireproofing Portland cement, which contained a foaming agent for generating an incombustible gas, a carbide layer precursor, and a microencapsulated carbide formation catalyst. The product was suitable for interior and/or exterior building boards. In another invention (Parthy, 2003) microencapsulated water was used for increasing fire resistance of construction materials. Microencapsulated water was added to gypsum plaster boards, paints, or thermal insulating materials.

Freeze and freeze-thaw resistance

To improve freeze and/or freeze-thaw resistance, microencapsulated sterically or electrostatically repelling monomers were added into hydraulically setting building materials, such as cement, lime, gypsum, anhydrite binders, as well as mortar or concrete mixtures (Schattka et al., 2007). Zhang (2005) patented the manufacture of an efficient and environmentally friendly snow-thawing composition, containing microencapsulated percarbamide as a snow-thawing active component.

Expansion and degradation resistance

To reduce expansion and to prevent degradation of concrete and mortar by alkali-aggregate reaction, a patent by Miyazawa and Akiyama (1988) suggested an addition of microcapsulated mineral oils or surfactants into construction material mixes. In a test, the expansion of the mortar product after 3 months was 0.127 %, vs. 0.41 % without the microcapsules.

Hydration of concrete and mortar mixes

Tomiuchi and Nishihama (1986) patented applications of microencapsulated water in the production of building boards with uniform strength. Typical compositions consisted of cement, mixed with fiber (e.g., asbestos, synthetic fiber) and microcapsules containing water for hardening. Building boards with uniform strength were manufactured on a belt conveyer by compression-molding, resulting in cement hardening. In another invention (Noda Plywood Mfg. Co., Ltd, 1985) high strength building boards were manufactured from a mixture of hydraulic material (gypsum), fibrous material, additives, and gelatine microcapsules containing water glass as a setting accelerator. Setting retardant and excess water were added, the mixture was poured into molds, pressed to remove access water and release the accelerator, and set. Microencapsulated or gelled water was used in cartridges of quick-setting cement (Heinen & Babcock, 1988). A premixed mortar mixture was patented, consisting of cement and microcapsules containing water (Origasa et al., 1988). In a patent by Okamoto et al., (1989) on manufacturing concrete and mortar mixes, water was encapsulated in an acrylate superabsorbent polymer. In the production of concrete or mortar, the water was released from the superabsorbent by molding to promote hydration of the surrounding cement.

Reduction of hydration heat release

Mass concrete suffers from thermal cracking due to heat release by cement hydra-

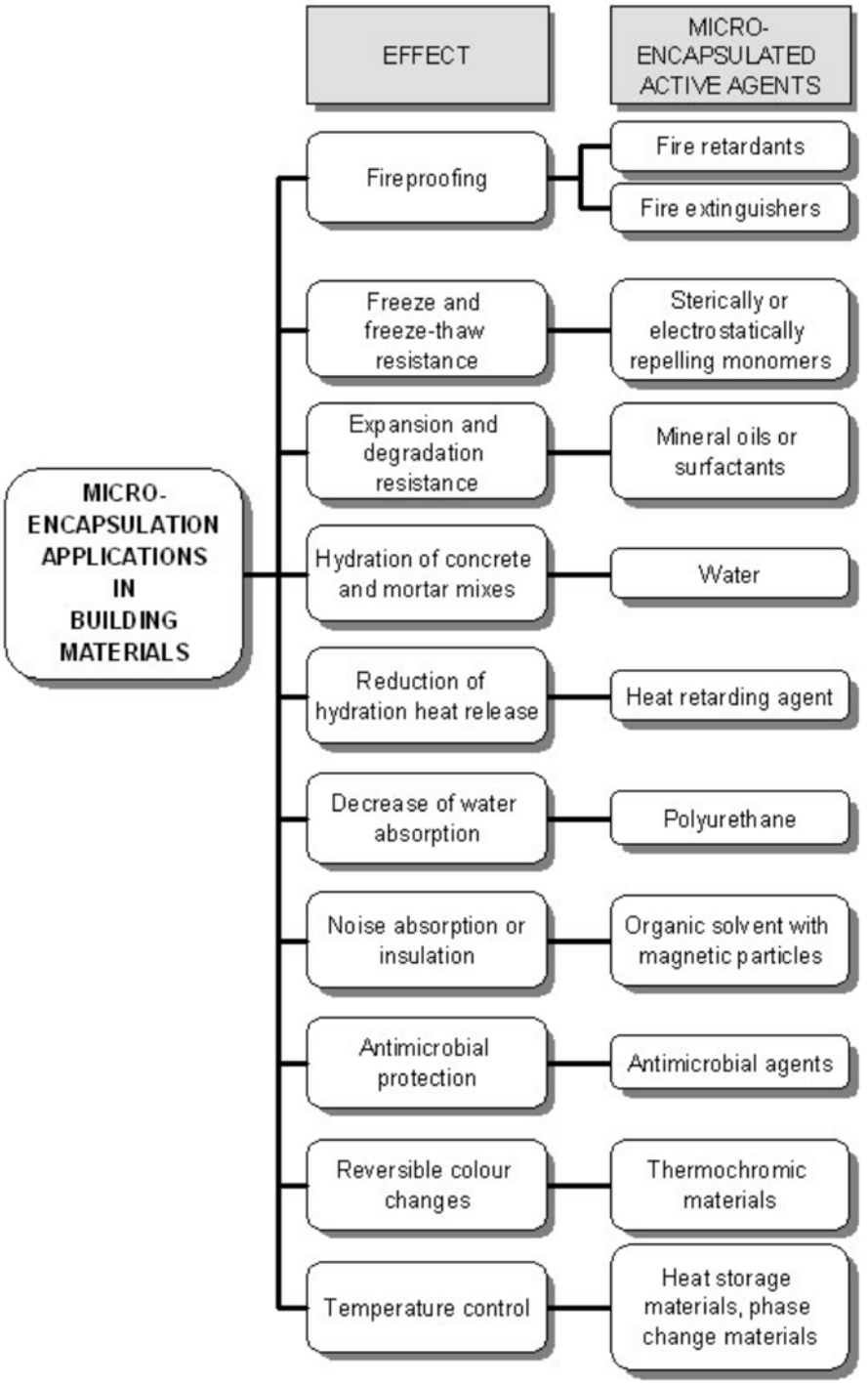

Figure 5. Applications of microcapsules in building construction materials
Slika 5. Uporaba mikrokapsul v gradbeništvu

tion. Using low heat Portland cement or fly ash cement was proposed as a countermeasure against this problem. The problem was also addressed in a study by Takeuchi et al., (2007). Wax microcapsules were developed, in which very fine solid particles of a retarder were included. When wax microcapsules melted at a designed temperature, the retarder was released into the cement matrix and it controlled the rate of heat release by cement hydration. Microcapsules remarkably reduced the hydration heat release rate and the adiabatic temperature rise speed of the cement mortar.

Decrease of water absorption

In the production of hydraulic inorganic sheets, 5-20 % of microcapsules containing polyurethane resin were added to the aqueous slurry of a blast-furnace slag cement and ettringite. The sheets were molded and hardened. Microencapsulated additive decreased the water absorption by 15-20 % (Matsushita Electric Works, Ltd., 1982).

Noise absorption or insulation

Microcapsules containing a magnetic fluid were used to absorb or insulate noise. Examples included noise-absorbing thermally expanding microcapsules, made of a thermoplastic resin, which contained a hydrophobic organic solvent with 5-200 nm magnetic particles, and a hydrophobic liquid foaming agent. The noise-absorbing microcapsules were incorporated into paints, and mixed in or adhesively attached to construction materials (Tanaka et al., 1997).

Antimicrobial protection

Microcapsulated essential oils of a white cedar were used in a mixture with a binder to protect building walls against generation of mildew (Arai, 2001). In a patent by Higashizaka (2002a,b, 2004), sustained release microcapsules containing hinokithiol were applied to protect leveling or base concrete in building construction against insects, bacteria, and corrosion, and to achieve a deodorising effect. A patent by Nishiguchi et al., (1998) described incorporation of microencapsulated fragrances, deodorants, antibacterial agents or insecticides into Calcium silicate shaped products for building interiors and exteriors.

Reversible colour changes

Several patents by Ma (2006a,b,c, 2007) described reversibly thermochromic cement-based materials, prepared by adding reversibly thermochromic microcapsules into a white Portland cement. Microencapsulated special thermochromic agents changed reversibly from blue, red or green colour at a lower temperature to white at a higher temperature. The system enabled a reversible change of colours: buildings were darker in winter, to absorb heat, and white in summer, to reflect the light energy.

Temperature control

Microcapsules containing latent heat storage materials, especially phase change materials, have been used to improve the heat storage capacity of buildings.

Phase Change Materials (PCMs) are a subgroup of heat Storage Materials (HSMs), with a dynamic heat exchange process taking place at the melting point temperature. When a PCM undergoes a phase change transition from solid to liquid, energy is

stored in the form of latent heat at a constant temperature. Accumulated latent thermal energy is released when the PCM solidifies again. In general, the higher the PCM's latent heat of phase change is, the more thermal energy a material can store. The transition process is completely reversible.

Typical organic PCMs are higher hydrocarbons (paraffins and their narrow fractions) (He & Setterwall, 2002; Hawlader et al., 2002; Hummel & Stich, 2003), as well as waxes, higher alcohols and higher fatty acids (Feldman et al., 1986, 1989; Suppes et al., 2003). The melting points of straight chain higher hydrocarbon PCMs depend on the length of the carbon atom chains, i.e. on the number of carbon atoms in the molecule. Higher hydrocarbons with 13 to 28 carbon atoms have phase change temperatures ranging from – 5.5 °C to + 61 °C. Compared to other PCMs, they have a high energy storage density, high boiling points and stability up to 250 °C. They are chemically inert, non-corrosive, long-lasting, inexpensive, ecologically harmless and non-toxic. These characteristics have made them the preferred PCMs for many commercial applications.

To overcome practical problems of solid-liquid phase transitions, PCMs have to be microencapsulated and turned into solid formulations for applications in various thermal management applications. To remain functional over numerous phase transition cycles, microencapsulated PCMs have to remain encapsulated within the impermeable microcapsule walls for the whole product life. PCM microcapsules need to be highly resistant to mechanical and thermal stress, which is achieved by improved or new microencapsulation methods. Holman (2001) patented gel-coated microencapsulated PCMs, consisting of a polymeric wall and a continuous metal oxide gel, resulting in an improved mechanical stress and flame resistance. Momoda and Phelps (2002) reported that nanoencapsulated PCMs with reversible high thermal transport properties at elevated temperatures can be used in low viscosity heat transfer fluids at sub-freezing temperatures. Another method of making microcapsules has been developed (Vasishtha, 2003), using microwaves as a source of electromagnetic energy, in combination with core and wall materials of different dielectric constants and dissipation factors.

Several temperature management systems have been developed and patented with microencapsulated PCMs for building applications. Examples include building elements for reduction of temperature oscillations in buildings, containing microencapsulated PCMs sealed within the concrete or plaster matrix structure (Chahroudi, 1981), and building conditioning systems for ceiling and floor surfaces (Pause, 2001). Tanaka and Suzuki (1997) patented microencapsulated paraffin phase change materials as additives to fresh concrete mix, mortar, or cement paste in the production of molded building products.

Inventions by Ishiguro (1998, 2003, 2004a,b, 2005, 2006) were based on the incorporation of microencapsulated heat storage materials into building insulation materials, such as laminated gypsum boards. In a typical example, one or both sides of the gypsum board were laminated

with a heat-storage sheet, obtained by dipping the board into a microencapsulated heat storage material. Patents by Matsushita and co-workers (Matsushita et al., 2002a,b; Matsushita & Ishiguro, 2003; Matsushita & Sato, 2003) described hydraulic compositions for production of latent heat-storable building materials. Typical compositions contained cement or gypsum, and microencapsulated latent heat storage materials. Iguchi et al., (2005) patented the application of microencapsulated heat storage materials in road construction materials, suitable especially for bridges, to suppress freezing in the winter time, or the heat island phenomenon in the summer time. Patents by Schmidt and co-workers (Schmidt & Volkmann, 2005; Schmidt & Schmidt, 2006) described a composite element made from a rigid polyurethane foam and two outer layers. At least one outer layer was molded (made of gypsum, lignocellulose, aminoplast resin, phenolic resin, urea-formaldehyde resin, and/or melamine-formaldehyde resin), and contained microencapsulated latent heat storage material. Hu and co-workers (Hu et al., 2007) patented sodium alginate for the microencapsulation of heat storage materials. Microcapsules were incorporated into gypsum.

Conclusions

Microencapsulation is a knowledge-intensive technology with a rapid growth of publications. A bibliometric analysis in the Chemical Abstracts Pus database shows that per each new scientific article on microencapsulation there are at least two patent applications, which illustrates the intensity of industrial research and innovation in the field. Microcapsules have been used in paper and printing industries, adhesives for technical purposes, textiles, pharmaceutical and medical applications, food industry, biotechnology, chemical industries, agrichemicals, photography, and electronics.

Microencapsulation applications are also entering into the field of building construction materials. Analysis of patents identified the following improvements achieved by microencapsulated additives in the construction materials: fireproofing by microencapsulated fire retardants or fire extinguishers; improved freeze- and freeze-thaw resistance; reduced expansion and degradation of concrete and mortar; hydration of concrete and mortar mixes in the compression-molding production of building elements; reduction of thermal cracking due to heat release by cement hydration; decrease of water absorption of hydraulic cement sheets; insulation or absorption of noise; protection of building materials against mildew, bacteria, insects, rodents and environmental corrosion, and achieving a fragranced / deodorising effect.

Special applications are microencapsulated thermochromic agents, which enable reversible colour changes of cement-based materials, e.g. for darker building exteriors in winter, to absorb heat, and for white colour in summer, to reflect the light energy. The fastest growing segment of microencapsulated additives in construction materials are latent heat storage materials for temperature control, especially the paraffinic phase change materials with a high energy storage density. Microcapsules with a good mechanical resistance are essential

to enable reversible liquid-solid-liquid phase transitions and to protect the PCM during the whole product life.

Povzetek

Tehnologija mikrokapsuliranja in njena uporaba v gradbenih materialih

Mikrokapsuliranje je tehnologija z velikim deležem znanja in hitrim naraščanjem števila publikacij. Bibliografska analiza v podatkovni bazi Chemical Abstracts Plus kaže več kot dvakrat večje število patentnih prijav v primerjavi z znanstvenimi članki, kar nakazuje intenzivnost industrijskih raziskav in aplikacij mikrokapsuliranja. Mikrokapsule uporabljajo v industriji papirja in tiska, v tekstilstvu, v farmacevtskih in medicinskih izdelkih, v živilski industriji, biotehnologiji, kemiji, za večkomponentna lepila, v proizvodnji fitofarmacevtskih sredstev, v fotografiji in elektrotehniki.

Aplikacije tehnologije mikrokapsuliranja se širijo tudi na področje gradbeništva. Analiza patentnih dokumentov je identificirala naslednje možnosti izboljšav, ki jih prinaša uporaba mikrokapsuliranih dodatkov v gradbenih materialih: negorljivi materiali z vsebnostjo mikrokapsuliranih zaviralcev gorenja; izboljšana odpornost proti zamrzovanju, taljenju in korozivnemu razpadu; zmanjšano raztezanje in krčenje ter posledično pokanje betona in ometov zaradi dejavnikov okolja ali zaradi termičnih sprememb ob hidraciji cementa; vlaženje suhih zmesi betona in malte z mikrokapsulirano vodo pod pritiskom v kalupih; cementni izdelki z manjšo absorptivnostjo vode; izboljšana zvočna izolacija oz. močnejša absorpcija zvoka; zaščita gradbenih materialov pred glivami, bakterijami, insekti, glodalci, korozijo zaradi okoljskih dejavnikov; odišavljenje in deodoriranje materialov.

Posebne aplikacije tehnologije mikrokapsuliranja so termokromni dodatki, ki omogočajo reverzibilne barvne spremembe cementnih izdelkov. Primer so zunanje površine zgradb, ki so pozimi temne, da absorbirajo več toplotne energije, ter bele poleti, da sončno svetlobo čim močneje odbijajo. Najhitreje rastoči segment mikrokapsuliranih aditivov v gradbenih materialih so materiali za latentno akumulacijo toplote. Med njimi so v ospredju parafinski fazno spremenljivi materiali (PCM – Phase Change Materials) z visoko toplotno kapaciteto. Zaradi nenehnih reverzibilnih prehodov agregatnega stanja trdno-tekoče je za praktično uporabo PCM ključnega pomena mikrokapsuliranje v mikrokapsule z dobro mehansko in termično odpornostjo.

References

Adachi, K. (2005): Composite fire-resistant and lightweight building board. *JP patent 2005120646*. Nihon Kankyo Kenkyusho K. K.

Arai, K. (2001): Wall material for applying to building walls. *JP patent 2001348306*. Sanribu Y. K.

Arshady, R. (1999): Microcapsule patents and products. *Preparation & Chemical Application*.; The MML series, Vol. 1, Citus reference series, London.

Arshady, R., Boh, B. (2003): Microcapsule

patents and products: introduction and overview. In: Arshady, R., Boh, B. (Eds.): *Microcapsule patents and products*.; The MML series, Vol. 6, Citus reference series, London, pp. 1-45.

Boh, B. (1986): *Mikroenkapsulacija olj s koacervacijo (Microencapsulation of oils with coacervation): Master Thesis*. University of Ljubljana, 198 pp.

Boh, B. (1991): *Kombinacija informacijskih in laboratorijskih metod v preučevanju mikrokapsuliranja proteinov z medpovršinsko polimerizacijo (Combination of Information and Laboratory Methods in the Study of Microencapsulation of Proteins by Interfacial Polymerisation): Ph.D. Thesis*. University of Ljubljana.

Boh, B. (1996a): Microencapsulation technology applications: with special reference to biotechnology: developing support for introducing knowledge intensive technologies. In: Kornhauser, A., Dasilva, E. (Eds.): *The integrating triangle: research - education - development: a challenge for higher education*. Ljubljana, International Centre for Chemical Studies: Slovenian National Commision for Unesco, pp. 51-76.

Boh, B. (1996b): Microencapsulation for pollution prevention: developing support for introducing clean(er) technologies and products. In: Kornhauser, A. (Ed.): *Developing information support for research and education in toxic waste management*. Ljubljana: International Centre for Chemical Studies: Slovenian National Commission for Unesco, pp. 205-222.

Boh, B. (2007): Developpements et applications industrielles des microcapsules. V: Vandamme, T.F. (ur.): *Microencapsulation: des sciences aux technologies*. Paris, Lavoisier, pp. 9-22.

Boh, B., Kardoš, D. (2003): Microcapsule patents and products: innovation and trend analysis. In: Arshady, R., Boh, B. (Eds.): *Microcapsule patents and products*.; The MML series, Vol. 6, Citus reference series, London, pp. 47-83.

Boh, B., Sajovic, I., Voda, K. (2003): Microcapsule applications: patent and literature analysis. In: Arshady, R., Boh, B. (Eds.): *Microcapsule patents and products*.; The MML series, Vol. 6, Citus reference series, London, pp. 85-156.

Chahroudi, D. (1981): Methods, apparatus, and compositions for storing heat for the heating and cooling of buildings. *US patent 4259401*. The Southwall Corporation.

Deasy, P.B. (1984): Microencapsulation and Related Drug Processes: General Introduction. *Microencapsulation and Related Drug Processes*. Mercel Dekker, pp. 1-19.

Fanger, G.O. (1974): Microencapsulation: A Brief History and Introduction. In: Vandegaer J.E. (Ed.): *Microencapsulation - Processes and Applications*). Plenum Press, New York, London, pp. 1-20.

Feldman, D., Shapiro, M. M., Banu, D. (1986): Organic phase change materials for thermal energy storage. *Solar Energy Materials*.; Vol. 13, pp. 1-10.

Feldman, D., Shapiro, M. M., Banu, D.,

Fuks, C. J. (1989): Fatty acids and their mixtures as phase-change materials for thermal energy storage. *Solar Energy Materials*.; Vol.18, pp. 201-216.

Hawlader, M.N.A., Uddin, M.S., Zhu, H.J. (2002): Encapsulated phase change materials for thermal energy storage: Experiments and simulation. *International Journal of Energy Research*.; Vol. 26, No. 2, pp. 159-171.

He, B., Setterwall, F. (2002): Technical grade paraffin waxes as phase change materials for cool thermal storage and cool storage systems capital cost estimation. *Energy Conversion and Management*.; Vol. 43, No. 13, pp. 1709-1723.

Heinen, J., Babcock, D.S. (1988): Cartridges of quick-setting cement and gelled water. *US patent 4772326*. Construction Products Research, Inc.

Higashizaka, E. (2002a): Foaming building material having microcapsules containing hinokithiols for antibacterial effect for applying to walls, floors and ceilings. *JP patent 2002146933*. Topics K. K.

Higashizaka, E. (2002b): Wall panels from plaster and microcapsules containing hinokithiol for insect killing effect and antibacterial effect. *JP patent 2002309688*. Topics K. K.

Higashizaka, E. (2004): Formation of leveling concrete or base concrete using hinoki oil in building construction for insect repelling, corrosion prevention, antibacterial action and deodorization. *JP patent 2004076402*. Topics K. K.

Holman, M. (2001): Gel-coated microcapsules. *US patent 6270836*. Frisby Technologies.

Hu, D.w., Hu, X.f., Lin, l.y. (2007): Preparation of phase transition microcapsule compound building material and heat storage/release research. *Jianzhu Cailiao Xuebao*.; Vol. 10, No. 6, pp. 664-670.

Hummel, H.U., Stich, D. (2003): Production of a gypsum-based construction board with microencapsulated paraffin core and glass fiber mats. *EP patent 1291475*. Gebr. Knauf Westdeutsche Gipswerke.

Iguchi, S., Iwasaki, M., Terao, K. (2005): Heat-storage-type road structure containing microcapsule. *JP patent 2005002597*. Yokogawa Bridge Co.

Ishiguro, M. (1998): Concrete for cold heat storage. *JP patent 10297950*. Mitsubishi Paper Mills, Ltd.

Ishiguro, M. (2003): Heat-storing building boards. *JP patent 2003155789*. Mitsubishi Paper Mills, Ltd.

Ishiguro, M. (2004a): Heat storing building material and its utilization method. *JP patent 2004324246*. Mitsubishi Paper Mills, Ltd.

Ishiguro, M. (2004b): Method for preventing the temperature rising of ground. *JP patent 2004316244*. Mitsubishi Paper Mills, Ltd.

Ishiguro, M. (2005): Heat-storing building materials having improved durability. *JP patent 2005061078*. Mitsubishi Paper Mills, Ltd.

Ishiguro, M. (2006): Heat storage material laminated gypsum board for construction. *JP patent 2006225986*. Mitsubishi Paper Mills, Ltd.

Knez, E. (1988): Postopek za pripravo mikrokapsul (Process for preparing microcapsules). *Patent SI A 8411319 (equivalent YU 1319/84)*. Aero Chemical, Graphic and printing Industry.

Kukovič, M., Knez, E. (1996): Process for preparing carriers saturated or coated with microencapsulated scents. *WO 96/09114*. Aero Chemical, Graphic and printing Industry.

Ma, Y. (2006a): Preparation of reversible thermochromic cement-based material at normal temperature. *Jianzhu Cailiao Xuebao*.; Vol. 9, No 6, pp. 700-704.

Ma, Y. (2006b): Research on normal temperature reversible thermochromic functional cement based composite. *Fuhe Cailiao Xuebao*.; Vol. 23, No. 4, pp. 106-111.

Ma, Y. (2006c): Research on the preparation of reversibly thermochromatic cement at normal temperature and the effect of temperature-control intelligently. *Gongneng Cailiao*.; Vol. 37, No. 7, pp. 1076-1077.

Ma, Y. (2007): Research on reversibly thermochromic cement-based material. *Tongji Daxue Xuebao, Ziran Kexueban*.; Vol. 35, No. 6, pp. 764-768.

Matsushita Electric Works, Ltd. (1982): Hydraulic inorganic sheets. *JP patent 57071843*. Matsushita Electric Works, Ltd.

Matsushita, S., Aoki, K., Ishiguro, M. (2002a): Latent heat storage cement type building materials having extremely small dimensional change at around phase transition temperature. *JP patent 2002114553*. Asahi Chemical Industry Co., Ltd., Mitsubishi Paper Mills, Ltd.

Matsushita, S., Aoki, K., Ishiguro, M. (2002b): Latent heat storage type gypsum based building material with microcapsules containing latent heat storage material. *JP patent 2002114560*. Asahi Chemical Industry Co., Ltd., Mitsubishi Paper Mills, Ltd.

Matsushita, S., Ishiguro, M. (2003): Hydraulic composition for production of latent heat-storable building materials. *JP patent 2003313062*. Asahi Kasei Corporation, Mitsubishi Paper Mills, Ltd.

Matsushita, S., Sato, H. (2003): Method for dewatering press molding of cement composition containing latent heat storage material. *JP patent 2003311724*. Asahi Kasei Corporation, Japan.

Miyazawa, T., Akiyama, I. (1988): Degradation prevention of concrete and mortar. *JP patent 63233031*. Takata K. K.

Momoda, L.A., Phelps, A.C. (2002): Nanometer sized phase change materials for enhanced heat transfer fluid performance. *US patent 6447692*. HRL Laboratories.

Nishiguchi, T., Takahashi, K., Yoshii, K., Kuroki, T., Arakawa, S. (1998): Calcium silicate shaped products containing microcapsules and their manufacture. *JP patent 10251052*. Konoshima Chemical Co., Ltd.

Noda Plywood Mfg. Co., Ltd (1985): Fabrication of hydraulic building boards. *JP patent 60028776*. Noda Plywood Mfg. Co., Ltd.

Okamoto, T., Sato, T., Kanbayashi, T., Kato, C. (1989): Preparation of

fine grain ice and dry clathrate water for manufacture of concrete and mortar, and manufacture of concrete and mortar. *EP patent 338739*. Mitsui Construction Co., Ltd., Shiiai Kemutekku K. K., Osaka Yuki Kagaku Kogyo Co., Ltd.

ORIGASA, W., YOSHIDA, A., KAWAMOTO, K. (1988): Premixed mortar. *JP patent 63260877*. Nippon Sogo Maintenance Co., Ltd., Nichie Yoshida K. K.

PARTHY, K. (2003): Use of microencapsulated water for increasing fire resistance of construction materials. *DE patent 10221939*. Germany.

PAUSE, B. (2001): Building conditioning technique using phase change materials. *US patent 6230444*. Outlast Technologies.

PONCELET, D., BOH, B. (2008): Microcapsules deliver. *Chemistry & Industry (Lond.)*.; No. 2, 28 January 2008, pp. 23-25.

SCHATTKA, J. H., KAUTZ, H., LOEHDEN, G. (2007): Additive for building material mixes comprising sterically or electrostatically repelling monomers in the shell of microparticles. *WO 2007096236*. Roehm G.m.b.H.

SCHMIDT, M., SCHMIDT, V. (2006): Composite thermal insulating layers made from rigid polyurethane foam. *WO 2006021306*. Basf Aktiengesellschaft.

SCHMIDT, M., VOLKMANN, B. (2005): Sound-absorbing molded shapes manufactured from porous concrete with plastic microcapsule. *DE patent 102004005912*. BASF A.G.

SUPPES, G.J., GOFF, M.J., LOPES, S. (2003): Latent heat characteristics of fatty acid derivatives pursuant phase change material applications. *Chemical Engineering Science*.; Vol. 58, pp. 1751-1763.

TAKEUCHI, T., NISHIYAMA, N., MIHASHI, H., SAKAI, E. (2007): Study on the hydration generation of heat control of cement by retarder inclusion microcapsule. *Semento, Konkurito Ronbunshu*.; Vol. 60, pp. 568-574.

TANAKA, I., SUZUKI, N. (1997): Microcapsule type cement hydration heat generation-preventing agent and manufacture of cement hardened products. *JP patent 09169554*. Shimizu Construction Co., Ltd.

TANAKA, K., SHIBAMOTO, T., NISHIZAKI, A. (1997): Microcapsule containing magnetic fluid and its manufacture and use. *WO 9733686*. Matsumoto Yushi-Seiyaku Co., Ltd., Nitto Boseki Co., Ltd., Tanaka, Koji, Shibamoto, Toshihiko, Nishizaki, Akihiko.

TOMIUCHI, S., NISHIHAMA, Y. (1986): Inorganic building boards with uniform strength. *JP patent 61031338*. Matsushita Electric Works, Ltd.

VANDAMME, T.F., PONCELET D., SUBRA-PATERNAULT, P. (Ed.) (2007): *Microencapsulation: des sciences aux technologies*. Paris, Lavoisier, 2007, 355 pp.

VASISHTHA, N. (2003): Microencapsulation using electromagnetic energy and core and shell materials with different dielectric constants and dissipation factors. *US patent 2003006264 1A1*. Vasishtha, N.

ZHANG, T. (2005): Manufacture of high-efficiency environmentally-friendly snow-thawing agent. *CN patent 1644646*. Peop. Rep. China.

Upper Triassic and Lower Jurassic limestones from Mt Kobla in the northern Tolmin Basin: tectonically repeated or continuous succession?

Zgornje triasni in spodnje jurski apnenci na Kobli v severnem Tolminskem bazenu: tektonsko ponovljeno ali zvezno zaporedje?

Boštjan Rožič[1]

[1]University of Ljubljana, Faculty of Natural Sciences and Engineering, Department of Geology, Privoz 11, SI-1000 Ljubljana, Slovenia; E-mail: bostjan.rozic@ntf.uni-lj.si

Received: February 27, 2008 **Accepted:** August 18, 2008

Abstract: Successions of the Tolmin Basin (western Slovenian Basin) structurally belong to the Tolmin Nappe of the Southern Alps. The Norian–Rhaetian succession of the Tolmin Basin is characterised mainly by bedded dolomite with chert nodules named the Bača Dolomite. It was recently discovered that in the northern part of the basin, the Upper Norian–Rhaetian limestone succession is preserved above the Bača Dolomite. This succession was studied on Mt Kobla, where it is composed of hemipelagic limestone alternating in the upper part with resedimented limestones. It ends with a distinct horizon of thin-bedded hemipelagic limestone that presumably records the end-Triassic carbonate productivity crisis. The overlying resedimented limestones of the Lower Jurassic Krikov Formation document the recovery of production on the adjacent Julian Carbonate Platform. The horizon of thin-bedded hemipelagic limestone therefore contains the Triassic–Jurassic boundary. The discovery of the succession brings an opportunity to study this boundary that recently attracted widespread scientific attention because it is marked by one of the five major extinction events of the Phanerozoic. The problem arises because the topmost part of the succession appears to be tectonically repeated on Mt Kobla and the distinct horizon of thin-bedded hemipelagic limestone is doubled. Alternatively, the overall succession on Mt Kobla could also be continuous and would in this case contain two horizons of thin-bedded hemipelagic limestone. This paper debates both possibilities and elucidates the data that indicate the first, i.e. tectonic, interpretation as more possible.

Izvleček: Razvoji Tolminskega bazena (zahodnega Slovenskega bazena) strukturno pripadajo Tolminskemu pokrovu Južnih Alp. Norijsko – retijsko zaporedje Tolminskega bazena označuje predvsem plastnat dolomit z gomolji

roženca, ki je znan pod imenom Baški dolomit. Nedavno je bilo ugotovljeno, da je v severnem delu bazena nad Baškim dolomitom ohranjeno zgornje norijsko – retijsko apnenčevo zaporedje. To zaporedje je bilo proučeno na Kobli, kjer ga sestavljajo hemipelagični apnenci, ki se v vrhnjem delu menjavajo s presedimentiranimi apnenci. Zaporedje se zaključi z značilnim horizontom tanko plastnatega hemipelagičnega apnenca, ki domnevno odraža krizo v karbonatni produkciji koncem triasa. Višje ležeči presedimentirani apnenci spodnje jurske Krikovske formacije pa odražajo ponovno obnovitev karbonatne produkcije na bližnji Julijski karbonatni platformi. Značilen horizont iz tanko plastnatega hemipelagičnega apnenca tako najverjetneje vsebuje triasno-jursko mejo. Odkritje tega zaporedja tako nudi priložnost za proučevanje te meje, katera je nedavno pritegnila pozornost široke geološke znanosti, saj jo označuje eno od petih velikih izumrtij v fanerozoiku. Vendar pa je vrhnji del zaporedja na Kobli najverjetneje tektonsko ponovljen, saj je horizont tanko plastnatega hemipelagičnega apnenca podvojen. Obstaja tudi možnost, da bi bilo celotno zaporedje na Kobli zvezno in bi v tem primeru vsebovalo dva horizonta tanko plastnatega hemipelagičnega apnenca. Ta prispevek tehta obe možnosti in osvetljuje podatke, ki kažejo, da je tektonska ponovitev zaporedja bolj verjetna.

Key words: Tolmin Basin, Late Triassic, facies analysis, Triassic-Jurassic boundary
Ključne besede: Tolminski bazen, zgornji trias, facielne analize, triasno-jurska meja

Introduction

The Norian–Rhaetian succession of the Tolmin Basin (western part of the Slovenian Basin) was considered to be represented only by Bača Dolomite, a bedded dolomite with chert nodules (Buser, 1986, 1989, 1996). Recently, it was proven that the part of the limestone succession that overlies the Bača Dolomite in the northern part of the basin is still Late Norian to Rhaetian in age (Rožič & Kolar-Jurkovšek, 2007; Rožič et al., in press). This limestone succession was studied in the eastern Bohinj Range; more precisely on Mt Kobla (Figure 1). The study is important for two reasons. Firstly, it contributes to a better understanding of the late Triassic sedimentary evolution of the Tolmin Basin. It is essential especially because the Bača Dolomite experienced intensive diagenetic overprinting (silification and dolomitisation) which reduced the exploration potential of the formation. Secondly, it most probably contains the Triassic–Jurassic boundary. Recently, this biostratigraphic boundary attracted scientific attention because it is marked by one of the five major extinction events of the Phanerozoic (Stanton & Flügel, 1987; Sepkoski, 1996; Tanner et al., 2004). Consequently, numerous sedimentological, paleontological, and geochemical studies have focused on this boundary with the aim of elucidating factors that forced the extensive crisis in the evolution of life that occurred approximately 200 million years ago (Palfy et al., 2001, 2007; Guex et al., 2004; Galli et al., 2005, 2007; and many others).

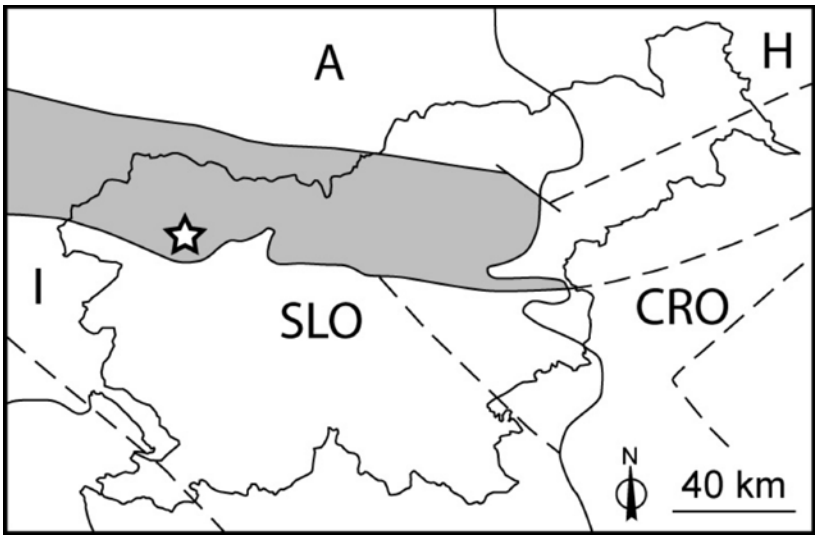

Figure 1. Location of the studied sections (star) and simplified macrotectonic subdivision of Slovenia (after Placer, 1999); the Southern Alps are shaded grey
Slika 1. Lokacija raziskanih profilov (zvezda) in poenostavljena makrotektonska rajonizacija Slovenije (po Placer-ju, 1999); Južne Alpe so obarvane sivo

The Upper Triassic–Lower Jurassic carbonate succession of the Tolmin Basin was investigated in the Kobla sections. It includes the uppermost part of the Bača Dolomite, the Late Triassic limestones and the base of the Early Jurassic Krikov Formation. The transition between the Upper Triassic limestones and the Krikov Formation is characterised by a distinct horizon of thin-bedded limestone with chert nodules, several metres thick. This horizon most probably contains the first known Triassic–Jurassic boundary within basinal succession in Slovenia and therefore offers great potential for boundary studies in this part of the world. The problem arises because this distinct horizon appears to be repeated within the studied succession. The aim of this paper is to distinguish whether the horizon is repeated tectonically or the Late Triassic–Early Jurassic succession is continuous and therefore marked by two horizons of thin-bedded limestone.

Geological setting

The studied succession is located in the eastern Bohinj Range that forms the southern orographic boundary of the Julian Alps (in northwest Slovenia). In the Late Triassic, the Julian Alps were part of the Adriatic continental margin. The whole of western Slovenia was divided into three paleogeographic domains: the Dinaric Carbonate Platform to the south, the approximately east–west extending Slovenian Basin in the middle, and the Julian Carbonate Platform to the north (Buser, 1989, 1996). In the early Jurassic the Julian Carbonate Platform drowned and became the pelagic plateau known as the Julian High (Buser, 1989, 1996; Šmuc, 2005).

In the Norian–Rhaetian both carbonate platforms were characterised by sedimentation on tidal flats, and thick successions of Dachstein Limestone and Main Dolomite formed (Ogorelec & Rothe, 1993; Buser, 1996; Verbovšek, 2008). In the Late Norian and Rhaetian, the southern margin of the Julian Carbonate Platform was locally dominated by coral reefs (Turnšek & Buser, 1991; Turnšek, 1997). The intermediate Slovenian Basin was filled with carbonate material shed from the surrounding carbonate platform. These deposits were mostly dolomitised and silicified during diagenesis, thus forming the Bača Dolomite (Buser, 1989, 1996; Buser et al., 2008). The exception was the northern part of the Tolmin Basin (western Slovenian Basin), where the Upper Norian–Rhaetian succession experienced less intense diagenetic alteration and the limestone succession studied in this paper was preserved.

Structurally, the Julian Alps form the eastern part of the Southern Alps (Figure 1) and consist of two large nappes characterised by southward thrusting: the lower Tolmin Nappe with successions of the Tolmin Basin and the overlying Julian Nappe composed predominantly of Dachstein Limestone of the Julian Carbonate Platform (Placer, 1999; Vrabec & Fodor, 2006). The Tolmin Nappe is thrust over the External Dinarides, which are marked by older, southwest directed thrust displacements (Placer, 1999) and composed of the Dinaric Carbonate Platform successions (Buser, 1989, 1996). The Tolmin Nappe is additionally divided into three lower-order nappes (Buser, 1987); the studied Late Norian to Rhaetian limestone succession is known only from the highest Kobla Nappe. The overall succession of the Kobla Nappe in the studied area ranges from the Carnian to the Lower Cretaceous. The topmost part of the succession (from the Pliensbachian upward) is repeated above a thrust north of Mt Krevl (Figure 2). This succession differs from the classical succession of the Kobla Nappe because it records a long stratigraphic gap (at least Toarcian to Bajocian) and most probably originated on the margins of the Julian High. Further north, shallow-water Late Triassic reef limestone, Jurassic ooidal limestone, the deeper-water Sedlo Formation (Šmuc, 2005; Šmuc & Goričan, 2005), and Biancone limestone of the Julian Carbonate Platform and Julian High are exposed. This succession belongs to the Julian Nappe but the tectonic contact with the regionally underlying Tolmin Nappe in the Mt Kobla area is exceptionally not a thrust but a normal or strike-slip fault (Figure 2).

Description of Kobla sections

The succession of Mt Kobla was included in some earlier geological surveys. The first extensive geological work of the area was carried out during the construction of the Bohinjska Bistrica–Podbrdo railway tunnel that penetrates the eastern Bohinj Range directly below Mt Kobla (Kossmat, 1907). The overall carbonate succession of the Tolmin Basin was described as Jurassic, although an Late Triassic Bača Dolomite had already been recognised in other parts of the basin. The Bača Dolomite in this area was recognised later, during geological mapping of the Julian Alps (Buser, 1986, 1987). On Mt Kobla, the same section as is

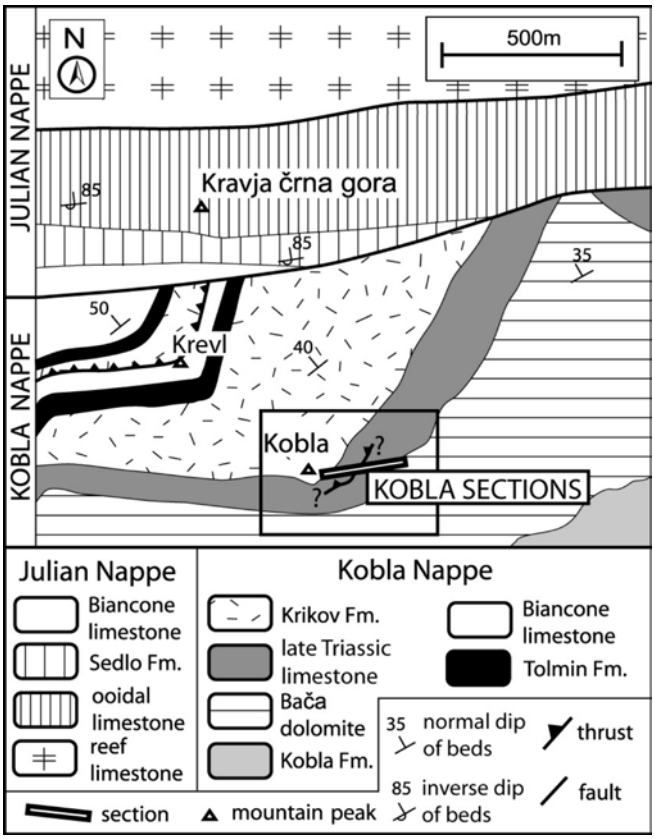

Figure 2. Geological map of the Mt Kobla area and the general location of the studied sections. The boxed area is enlarged in Figure 3.
Slika 2. Geološka karta območja Koble in približna lokacija preiskanih profilov. Del karte v okvirju je povečan na sliki 3.

described in the present paper was studied for the purpose of stratigraphic ordering. The overall limestone succession overlying the Bača Dolomite was assigned to the Jurassic, although Buser (1986) pointed out that no characteristic Jurassic fossils were found in the lower part of the succession. The author mentioned the foraminifers *Galeanella panticae*, *Ophtalmidium* sp. and the dasyclad alga *Thaumatoporella parvovesiculifera*, whereas the Jurassic *Involutina farinacciae* was found only in the topmost part of the section.

The studied succession is located on the old path that climbs the eastern slope of Mt Kobla (y = 5420550, x = 5121590, 1498 m above sea level) and was investigated in three sections (Figure 3 and Plate 1; Fig.1). The main section is 112 m thick and beds in this section dip towards the northwest (Figures 3 and 5). The second section investigates 18 m of beds that overlie the main section, are sub-vertical, and extend in an east–west direction (Figures 3 and 5). Sedimentary structures in these beds indicate that succession becomes younger towards

the south. The third section is 23 m thick and covers the uppermost beds exposed along the path. These beds dip similarly to beds in the main section (Figures 3 and 5).

Main section

The section begins with a few metres of the Bača Dolomite, a bedded dolomite with chert nodules (Figure 4). The boundary with the overlying limestone succession is covered but most probably sharp. The following 90 m are characterised by bedded (10 to 50 cm), grey, occasionally wavy, and even laminated hemipelagic limestone (Plate 1; Fig. 2). The microfacies is wackestone composed of pellets and fossils, of which the most abundant are calcified radiolarians. Other fossils are sponge spicules, echinoderms, bivalves, brachiopods, ostracods, benthic foraminifers, gastropods, and juvenile ammonites (Plate 1; Fig. 4). Beds usually contain replacement chert nodules. Especially in the upper part of this succession (above 70 m in the section), hemipelagic limestone alternates with coarser beds; i.e. calcarenite and limestone conglomerate (Plate 1; Fig. 3). Calcarenite is mostly medium- to

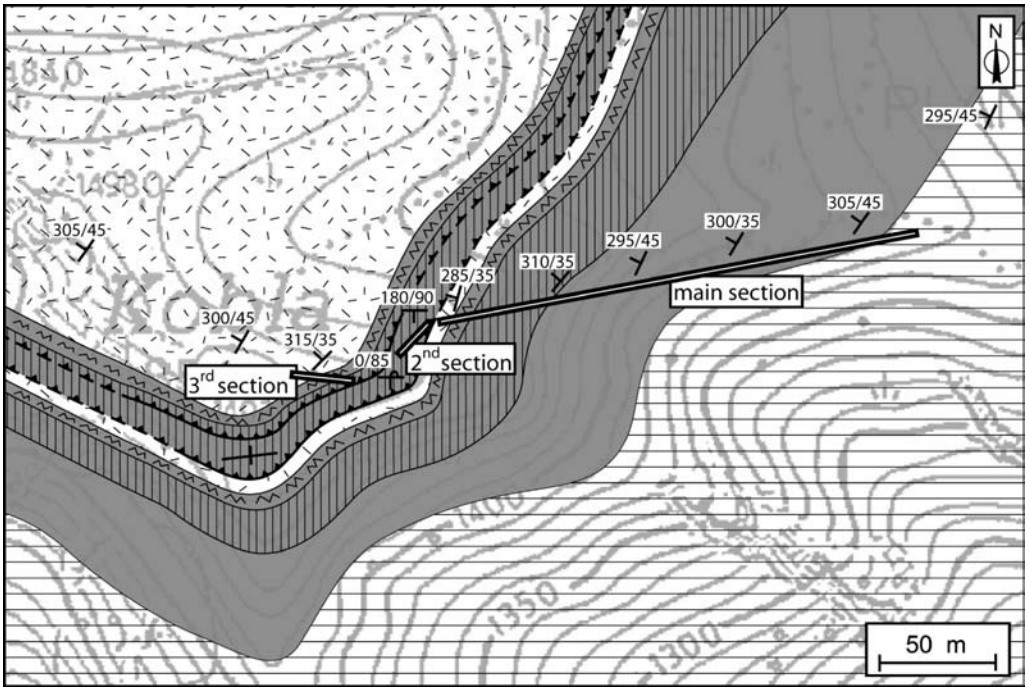

Figure 3. Detailed geological map of Mt Kobla with the exact position of sections. The legend is the same as for Figure 2. Within the Upper Triassic limestone succession the horizon with abundant resedimented limestones is outlined with vertical lines and the horizon of thin-bedded hemipelagic limestone with a zigzag pattern.
Slika 3. Natančna geološka karta Koble s točnimi lokacijami profilov. Legenda je ista kot pri sliki 2. Znotraj zgornje triasnega apnenčevega zaporedja je horizont z obilnimi presedimentiranimi apnenci izdvojen z navpičnimi črtami in horizont tanko plastnatega hemipelagičnega apnenca s cikcak vzorcem.

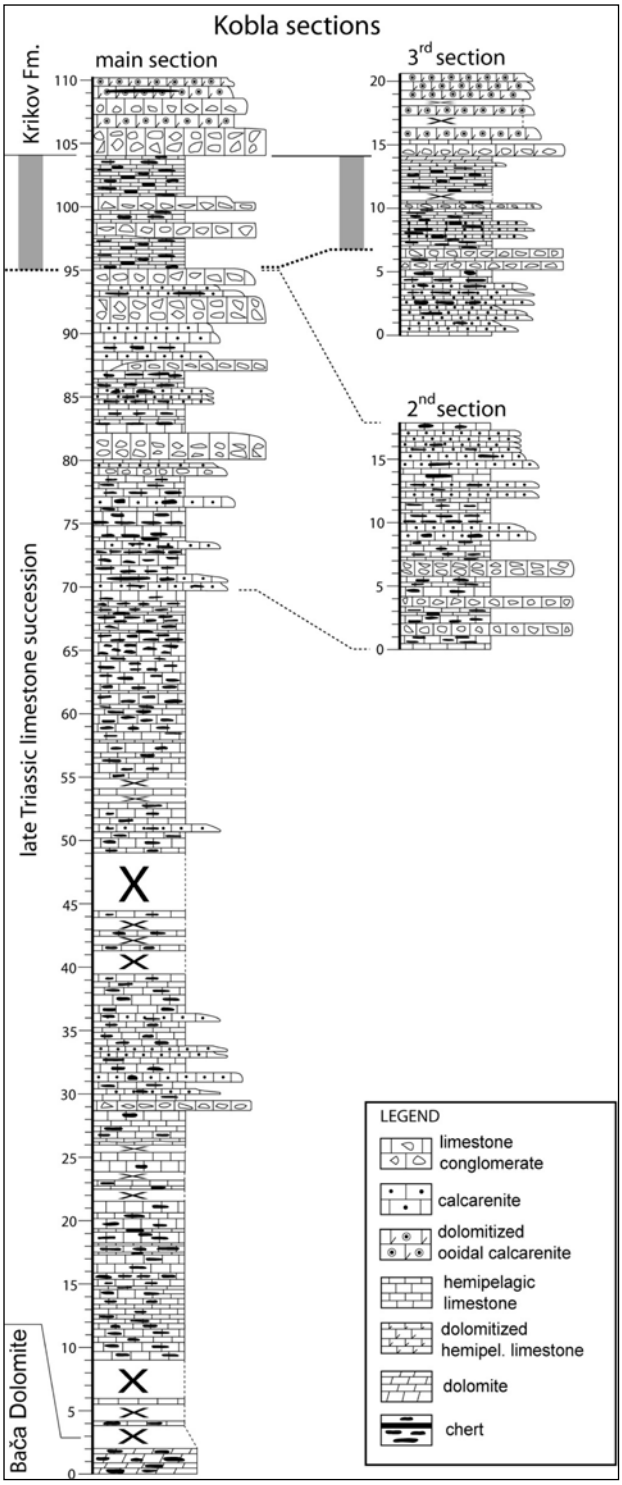

Figure 4. Kobla sections: the main section consists of the Bača Dolomite at the base, the Upper Triassic limestone succession in the major part, and the Krikov Formation at the top. The second section exhibits a similar composition to the main section between 70 and 95 m (where coarser limestone beds are abundant), whereas the third section generally correlates well to the topmost part of the main section. The distinctive horizon of thin-bedded hemipelagic limestone is indicated by grey stripes.

Slika 4. Profili Koble: glavni profil se začne z Baškim dolomitom, glavni del sestavlja zgornje triasno apnenčevo zaporedje, konča pa se s Krikovsko formacijo. Drugi profil je sestavljen podobno kot glavni profil med 70 in 95 m (kjer so pogosti presedimentirani apnenci), medtem ko tretji profil ustreza vrhnjemu delu glavnega profila. Značilen horizont tanko plastnatega hemipelagičnega apnenca je označen s sivima trakovoma.

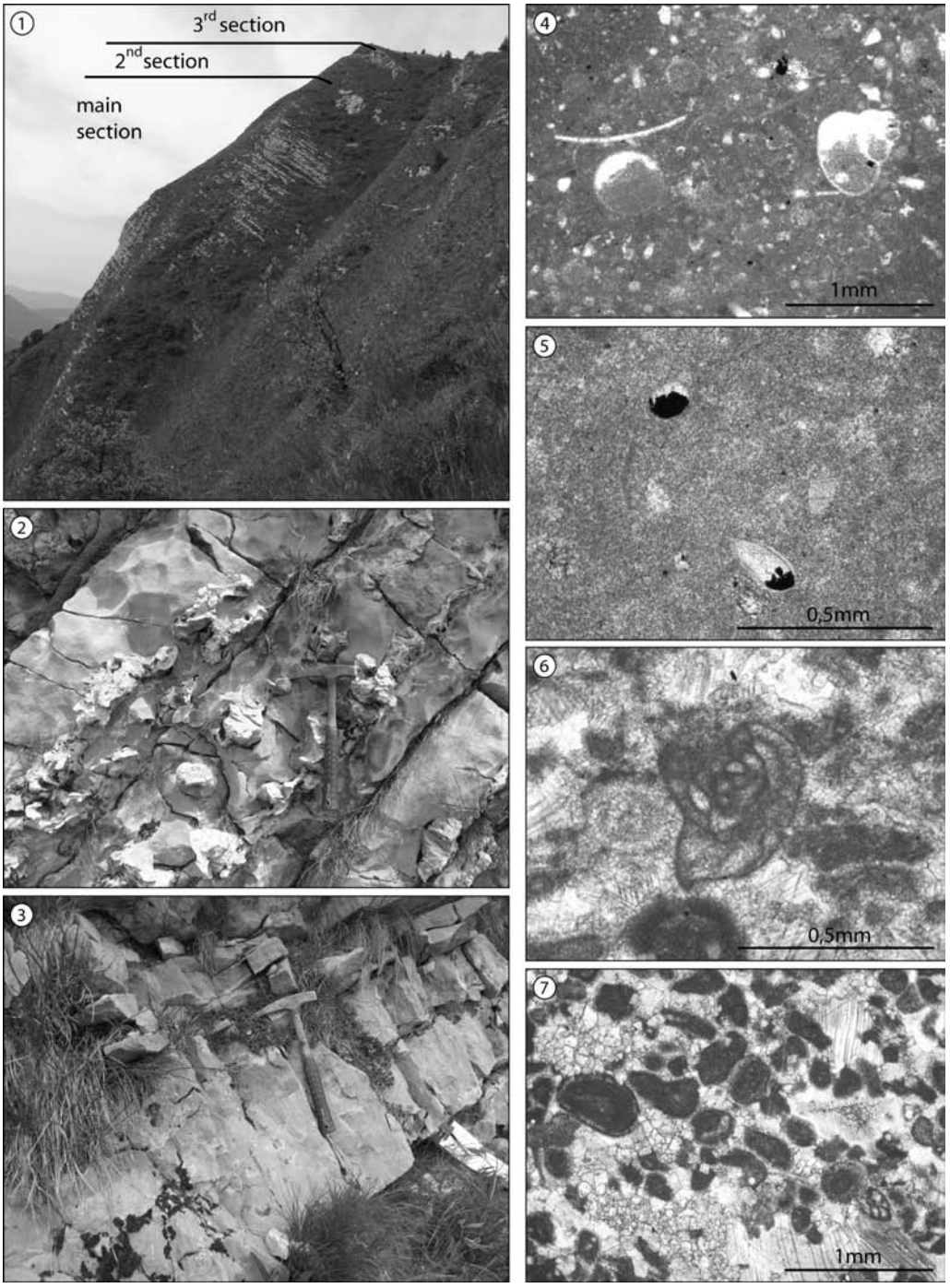
1
3rd section
2nd section
main
section
2
3
4
1mm
5
0,5mm
6
0,5mm
7
1mm

Plate 1. Fig. 1. View of Mt Kobla from the eastern side with the location of the studied sections; Fig. 2. Hemipelagic limestone with irregular chert nodules from the middle part of the main section; Fig. 3. Thicker limestone conglomerate beds alternating with thinner beds of hemipelagic limestone just below the distinct horizon of thin-bedded hemipelagic limestone (at approximately 95 m in the main section); Fig. 4. Wackestone composed of calcified radiolarians and sponge spicules, pellets, bivalve-shells, and gastropods with a geopetal structure (at 18.5 m in the main section); Fig. 5. Mudstone to wackestone with "ghosts" of calcified radiolarians, echinoderm fragments, and ostracods geopetally filled with an opaque mineral, most probably pyrite (at 102.3 m in the main section); Fig. 6. Medium-grained grainstone with foraminifer *Galeanella tollmanni* Kristan-Tollmann; other grains are echinoderm fragments, pellets, and intraclasts (at 1.8 m in the third section); Fig. 7. Medium-grained, partially dolomitised grainstone with ooids, peloids, and rarer fossils, predominantly echinoderm fragments and foraminifer (at 16.5 m in the third section).

Tabla 1. Sl. 1. Pogled na Koblo z vzhodne strani z lokacijami raziskanih profilov; Sl. 2. Hemipelagični apnenec z nepravilnimi roženčevimi gomolji v srednjem delu glavnega profila; Sl. 3. Menjavanje debelih plasti apnenčevega konglomerata s tanjšimi plastmi hemipelagičnega apnenca tik pod značilnim horizontom tanko plastnatega hemipelagičnega apnenca (približno 95 m glavnega profila); Sl. 4. Vekston s kalcitiziranimi radiolariji in spongijskimi spikulami, peleti, školjčnimi lupinami in polži z geopetalno teksturo (18,5 m glavnega profila); Sl. 5. Madston do vekston z "duhovi" kalcitiziranih radiolarijev, drobci iglokožcev in ostrakodi, ki so geopetalno zapolnjeni z neprosojnim mineralom, najverjetneje piritom (102,3 m glavnega profila); Sl. 6. Srednje zrnati greinston s foraminifero *Galeanella tollmanni* Kristan-Tollmann; preostala zrna so drobci iglokožcev, peleti in intraklasti (1,8 m tretjega profila); Sl. 7. Srednje zrnat, deloma dolomitiziran greinston z ooidi, peloidi in manj pogostimi fosili, predvsem drobci iglokožcev in foraminifer (16,5 m tretjega profila).

coarse-grained, grey, bedded (3 to 45 cm), normally graded, even, and wavy laminated grainstone composed predominantly of intraclasts and fossils; i.e. echinoderm fragments and rarer benthic foraminifers, fragmented shells of bivalves, brachiopods, and ostracods, gastropods, and codiaceans. The limestone conglomerate is bedded (12 to 150 cm) and occasionally graded. Beds are even or rarely channelised. The thickest beds are abruptly overlain by graded calcarenite. Clasts in the conglomerate are dm-sized, well rounded, elongated, and oriented parallel to the bedding planes. Clasts are almost exclusively basinal intraclasts (mud-chips) and of the same composition as the surrounding hemipelagic limestone, whereas the matrix consists of the calcarenite described above.

Above 95 m in the section, coarser beds become rare, while hemipelagic limestone becomes very thin-bedded and exhibits less diverse composition, with calcified radiolarians as predominant grains; other fossils are rare ostracods and echinoderm fragments (Plate 1; Fig. 5). This distinct, thin-bedded horizon is above 104 m in the section overlain by bedded (up to 80 cm) limestone conglomerate and calcarenite. Clasts in the conglomerate are again mostly basinal intraclasts, whereas the composition of calcarenite (which also forms the matrix in conglomerate) changes significantly. It is grainstone composed of ooids, peloids, and rare fossils, among which echinoderms and codiaceans prevail. These beds are partially dolomitised. The topmost bed in the main section is tectonically altered; i.e. dissected by numerous calcite veins and fissures oriented generally parallel to the bedding planes.

The main section was sampled for conodonts (Rožič & Kolar-Jurkovšek, 2007; Rožič et al., in press). The last conodonts were retrieved below the horizon of thin-bedded hemipelagic limestone. Conodont assemblages indicated that the limestone succession below this horizon was Late Norian to Rhaetian in age.

Second section

The second section consists of hemipelagic limestone alternating with limestone conglomerate and calcarenite (Figure 4). It is similar to the succession from 70 to 95 m in the main section, although limestone conglomerate beds are generally thinner (up to 90 cm). The composition of these beds is the same as that of corresponding beds from the main section.

Third section

The section begins with a 5 m thick horizon dominated by calcarenite (Figure 4). The microfacies and composition are equal to that of the calcarenite researched below 95 m in the main section (Plate 1; Fig. 6). Above this horizon hemipelagic limestone starts to prevail. In the first two metres, beds are still up to 25 cm thick and are overlain by rather thin limestone conglomerate beds. Upwards thin-bedded hemipelagic limestone dominates the succession. It is interbedded with very rare, thin calcarenite beds and composed similarly to the thin-bedded hemipelagic limestone from the main section. The thickness of this horizon is eight metres. It is overlain by 10 m of bedded (up to 50 cm) calcarenite and limestone conglomerate. The microfacies and composition are the same as those of the coarse beds of the topmost part of the main section (Plate 1; Fig. 7).

Similarly, these topmost beds also exhibit partial dolomitisation. Upwards the outcrops become poor, but it is evident that the following succession is dominated by ooidal/peloidal calcarenite while limestone conglomerate becomes rarer.

Discussion

The lower part of the main section is dominated by hemipelagic limestone. The composition of these beds indicates deposition in a deeper-water sedimentary environment. Because carbonate plankton was scarce until the late Jurassic (Bartolini et al., 2002; Pittet & Mattioli, 2002), the lime mud must have been shed especially from the adjacent Julian Carbonate Platform. Upwards the coarser beds start to occur more abundantly. Sedimentary textures in these beds indicate deposition by gravity flows, predominantly turbidites. In the calcarenite, the foraminifers *Galeanella panticae* Brönnimann and *G. tollmanni* Kristan-Tollmann were determined (Plate 1; Fig. 6). The presence of these foraminifers indicates that reefs were present in the source area (Schäfer, 1979; Senowbari-Daryan, 1980; Senowbari-Daryan et al., 1982). Coarser beds in the upper part of the main section indicate the progradation of the sedimentary environment. Namely, the facies association is characteristic of the basin plain and changes upwards to the lower slope.

The horizon of thin-bedded limestone records a sudden biotic decrease and may be related to the biocalcification crisis that marks the Triassic–Jurassic boundary (Palfy et al., 2001, 2007; Ward et al., 2004; Galli et al., 2005, 2007). Although no Jurassic fossils have yet been found in the overlying ooidal/peloidal calcarenite and limestone conglomerate, the ooidal beds most probably belong to the Hettangian–Pliensbachian Krikov Formation and

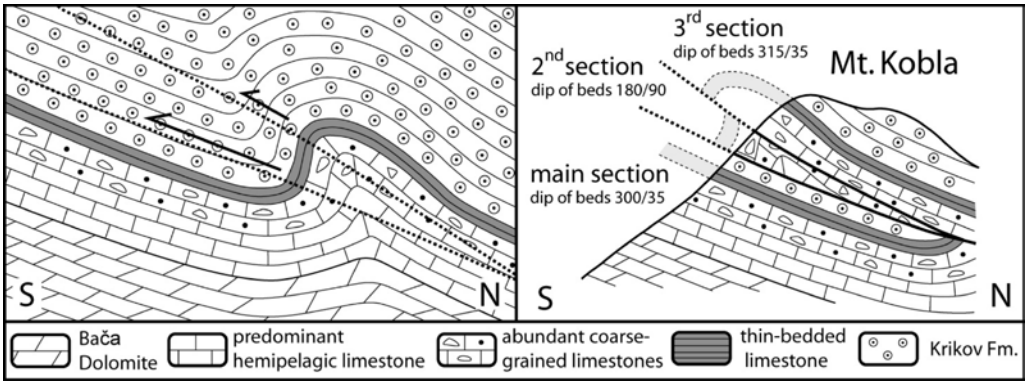

Figure 5. Sketch of the tectonic interpretation. Left: the tectonic compression resulted first in an asymmetric fold that was later dissected by minor thrusts. Right: a present-day geological cross-section of Mt Kobla with the position of the studied sections.

Slika 5. Skica tektonske interpretacije. Levo: kot posledica tektonske kompresije je najprej nastala nesimetrična guba, ki je bila kasneje pretrgana z manjšimi narivi. Desno: današnji geološki prerez Koble z lokacijami preiskanih profilov.

record the recovery of production on the adjacent Julian Carbonate Platform.

The main purpose of this paper is to determine whether the second and third sections represent a tectonically repeated upper part of the main section or form a continuous succession. It seems likely that the first, tectonic explanation is correct. The arguments for this interpretation are the presence of the following: a) the same superposition of different facies in the main and the third section, namely, from alternating hemipelagic and coarse-grained resedimented limestones through thin-bedded hemipelagic limestone to the subsequent change to ooidal/peloidal calcarenite and limestone conglomerate; b) the change in dips of beds from northwest dips in the main and third sections to sub-vertical, east–west extending beds in the second section; and c) the fissures and calcite veins at the top of the main section that indicate intense tectonic deformation oriented approximately parallel to the bedding plains; i.e. thrust displacement.

The repeated succession on Mt Kobla is explained as a consequence of compression that resulted in asymmetric fold originating during thrust fault propagation (Davis & Reynolds, 1996). The fold limbs were additionally displaced by minor thrust (Figure 5). East–west extending beds in the second section indicate that the compression is related to South-Alpine south-verging thrusting (Placer, 1999; Vrabec & Fodor, 2006; Kastelic et al., 2008). As indicated by numerous fissures and calcite veins at the top of the main section, the displacement was greater along the lower thrust. The second section is structurally located in the sub-vertical; i.e. southern fold limb. The succession investigated in this section corresponds to the succession between 70 and 95 m of the main section (Figures 4 and 5). Under such structural setting, the third section is located in the low-dip; i.e. northern fold limb. In this section the topmost part of the main section is repeated (Figures 4 and 5). The Triassic foraminifer *Galeanella tollmanni* Kristan-Tollmann was determined at the base of this section (Plate 1; Fig. 6). Because Buser (1986) reports Jurassic *Involutina farinacciae* at 140 m in his section, it seems likely that this occurrence corresponds to the top of the third section. Therefore, we can presume that the Triassic–Jurassic boundary lies within the horizon of thin-bedded hemipelagic limestone that marks the top of the main section but is repeated due to thrusting in the third section. Minor differences between the second and third sections with corresponding parts of the main section are explained by lateral variations caused by deposition in the lower slope sedimentary environment.

Alternatively, the second and third sections could represent a stratigraphically continuous succession above the main section. In this case, the sub-vertical dip in the second section would originate from a synsedimentary fold caused by slumping. The overall succession (comprising all three sections) would be marked by two horizons of thin-bedded hemipelagic limestone each overlain by ooidal/peloidal calcarenite and limestone conglomerate. Such an interpretation is less probable when the sedimentary succession of the Julian Carbonate Platform, which was a source area of resedimented carbonate

material, is taken into consideration. The Triassic–Jurassic boundary on the platform has not yet been studied in detail, but is generally placed below the first occurrence of ooidal limestone that overlies the Dachstein Limestone or, in platform margins, lies above the reef limestone (Buser 1986; Jurkovšek et al., 1990; Ogorelec & Buser, 1997). Similar Late Triassic to Early Jurassic depositional change is also observed in the Julian Carbonate Platform succession located in the northern part of the Mt Kobla area (Figure 2), where the Late Triassic is represented by reef limestone (Turnšek & Buser, 1991; Turnšek, 1997) and Early Jurassic by ooidal limestone. Although the contact in this area is tectonic, the fault dips parallel to the bedding and disruption of the sedimentary succession is most probably minor. Therefore the prominent change in the composition of resedimented limestones in the studied basinal sections records the main sedimentary change on the Julian Carbonate Platform: i.e. from tidal flats or reefs to ooidal shoals. A similar main change is reported from the Lombardian Basin located in the western Southern Alps. In the Lombardian Basin the Late Triassic Zu Limestone Formation is represented predominantly by marl/micritic limestone alternations, whereas in the upper part of the formation coral limestones are present as a consequence of the basin shallowing (Jadoul et al., 1994, 2007; Gaetani et al., 1998; Gianolla & Jacquin, 1998). Although rare ooidal limestone beds are reported already from the upper Zu Limestone Formation the main change is reserved for the Early Jurassic, when Bahamian-type carbonate platform peloidal and ooidal limestones of the Albenza Formation started to deposit (Jadoul et al., 2007). Furthermore, the interval between the Zu Limestone and Albenza Formations is marked by a succession that is very similar to thin-bedded limestone horizons from the Kobla sections. This distinct interval from the Lombardian Basin (which records a major transgression) is known as topmost Zu Limestone or Malanotte Formation and was proven to contain a Triassic–Jurassic boundary (Galli et al. 2005, 2007; Jadoul, 2007). The correlation with the Lombardian Basin additionally suggests only one, tectonically repeated thin-bedded limestone horizon in the Kobla sections and furthermore indicates that this horizon offers great potential for studies of the Triassic–Jurassic boundary in the Tolmin Basin.

Conclusions

In the northern part of the Tolmin Basin the Late Triassic succession is exceptionally represented by limestones, whereas in the major part of the basin the entire Norian–Rhaetian interval consists of dolomite (Bača Dolomite). This limestone succession was studied at Mt Kobla and is composed predominantly of hemipelagic limestone alternating in the upper part with resedimented limestones, i.e. calcarenite and limestone conglomerate. The change of facies association indicates a progradation of sedimentary environments from the basin plain to the lower slope. The Triassic succession ends with a distinct, few-metres-thick horizon of thin-bedded, hemipelagic limestone. This distinct horizon records the end-Triassic productivity crisis. The overlying resedimented limestones, mostly ooidal/peloidal calcarenites

of the Krikov Formation, document the early Jurassic recovery of carbonate production on the adjacent Julian Carbonate Platform. Apart from the main section, the uppermost Triassic–Early Jurassic succession was additionally studied in two sections that overlie the main section. Microfacies analysis, geological mapping data, brittle deformations of sections margins, and correlation with the Julian Carbonate Platform and the Lombardian Basin successions indicate that the studied succession at Mt Kobla is tectonically repeated due to minor thrust displacement.

Povzetek

Zgornje triasni in spodnje jurski apnenci na Kobli v severnem Tolminskem bazenu: tektonsko ponovljeno ali zvezno zaporedje?

V severnem delu Tolminskega bazena zgornje triasno zaporedje izjemoma sestavljajo apnenci, medtem ko v preostalih delih bazena celotno norijsko-retijsko obdobje predstavlja dolomit (Baški dolomit). Apnenčevo zaporedje je bilo raziskano na Kobli. Sestavljajo ga predvsem hemipelagični apnenci, ki se v zgornjem delu menjavajo s presedimentiranimi apnenci, in sicer kalkareniti in apnenčevimi konglomerati. Sprememba v faciesni združbi dokazuje progradacijo sedimentacijskega okolja iz bazenske ravnice v spodnje pobočje. Triasno zaporedje se konča z značilnim, nekaj metrov debelim, horizontom tanko plastnatega hemipelagičnega apnenca. Ta horizont odraža krizo v karbonatni produkciji, ki označuje konec triasa. Višje ležeči presedimentirani apnenci, predvsem ooidno/peloidni kalkareniti Krikovske formacije kažejo na obnovitev karbonatne produkcije na bližnji Julijski karbonatni platformi. Poleg glavnega sedimentološkega profila je bilo zgornje triasno do spodnje jursko zaporedje preučeno še v dveh profilih, ki se nahajajo neposredno nad glavnim profilom. Analiza mikrofaciesov, rezultati geološkega kartiranja, lomne deformacije na robovih profilov in korelacija z zaporedji Julijske karbonatne platforme ter Lombardijskega bazena kažejo, da je preučeno zaporedje na Kobli zaradi premikov ob manjših narivih tektonsko ponovljeno.

Acknowledgements

This study was financed by the Slovenian Research Agency. Stanko Buser is sincerely thanked for numerous consultations and Rajka Radoičić for the determination of foraminifers. Mirč Udovč is thanked for the preparation of thin sections. Petra Žvab and Nina Rman are acknowledged for assistance during the geological mapping. Boštjan Bradaškja and Andrej Šmuc are thanked for the help on the fieldwork. The final text corrections of Vanja Kastelic and the reviser Špela Goričan are kindly appreciated.

References

Bartolini, A., Pittet, B., Mattioli, E. & Hunziker, J.C. (2002): Shallow-platform palaeoenvironmental conditions recorded in deep-shelf sediments: C and O stable isotopes in Upper Jurassic sections of southern Germany (Oxfordian-Kimmeridgian). *Sedimentary Geology*.; Vol. 160, No. 1, pp. 107-130.

Buser, S. (1986): *Tolmač k Osnovni geološki karti SFRJ 1: 100 000 lista Tolmin in Videm (Udine)*. Zvezni geološki zavod, Beograd, Yugoslavia, 103 pp.

Buser, S. (1987): *Osnovna geološka karta SFRJ 1: 100 000, list Tolmin*. Zvezni geološki zavod, Beograd, Yugoslavia.

Buser, S. (1989): Development of the Dinaric and Julian carbonate platforms and the intermediate Slovenian basin (NW-Yugoslavia). In: Carulli, G.B., Cucchi, F., Radrizzani, C.P. (eds): Evolution of the Karstic carbonate platform: relation with other periadriatic carbonate platforms. *Mem. Soc. Geol. Ital*.: Vol. 40, pp. 313-320.

Buser, S. (1996): Geology of western Slovenia and its paleogeographic evolution. In: Drobne, K., Goričan, Š., Kotnik, B. (eds): *The role of Impact Processes in the Geological and Biological Evolution of Planet Earth*. International workshop, ZRC SAZU, Ljubljana, pp. 111-123.

Buser, S., Kolar-Jurkovšek, T. & Jurkovšek, B. (2008): Slovenian Basin during Triassic in the Light of Conodont Data. *Boll. Soc. Geol. Ital*.; Vol. 127, pp. 257-263.

Davis, G.H. & Reynolds, S. J. (1996): *Structural geology of rocks and regions*. 2nd ed, John Wiley & Sons, New York, 776 pp.

Gaetani, M., Gnaccolini, M., Jadoul, F. & Garzanti, E. (1998): Multiorder sequence stratigraphy in the Triassic system of the western Southern Alps. In: Graciansky, P., Hardenbol, J., Jacquin, T., Vail, P.R. (eds): Mesozoic and Cenozoic Sequence stratigraphy of European Basins. *SEMP Special Publications*.; No. 60, pp. 70-717.

Galli, M.T., Jadoul, F., Bernasconi, S.M. & Weissert, H. (2005): Anomalies in global carbon cycling and extinction at the Triassic/Jurassic boundary: evidence from a marine C-isotope record. *Palaeogeogr. Palaeoclimat. Palaeoeco*.; Vol. 216, pp. 203-214.

Galli, M.T., Jadoul, F., Bernasconi, S.M., Cirilli, S. & Weissert, H. (2007): Stratigraphy and palaeoenvironmental analysis of the Triassic–Jurassic transition in the western Southern Alps (Northern Italy). *Palaeogeogr. Palaeoclimat. Palaeoeco*.; Vol. 244, pp. 52-70.

Gianolla, P. & Jacquin, T. (1998): Triassic sequence stratigraphic framework of western European basins. In: Graciansky, P., Hardenbol, J., Jacquin, T., Vail, P.R. (eds): Mesozoic

and Cenozoic Sequence stratigraphy of European Basins. *SEMP Special Publications*.; No. 60, pp. 643-650.

Guex, J., Bartolini, A., Atuderoi, V. & Taylor, D. (2004): High – resolution ammonite and carbon isotope stratigraphy across the Triassic – Jurassic boundary at New York Canyon (Nevada). *Earth an Planetary Science Letters*.; Vol. 225, pp. 29-41.

Jadoul, F., Masetti, D., Cirilli, S., Berra, F., Claps, M. & Frisia, S. (1994): Norian–Rhaetian stratigraphy and paleogeographic evolution of the Lombardy Basin (Bergamasc Alps). *Excursion B1, 15th IAS Regional Meeting*.; pp. 5-38.

Jadoul, F., Galli, M.T., Muttoni, G., Rigo, M. & Cirilli, S. (2007): The late Norian–Hettangian stratigraphic and paleographic evolution of the Bergamasc Alps. *Geoitalia 2007, Pre–Congress Field Trip Guide Book–FW02*. Rimini, pp. 1-33.

Jurkovšek, B., Šribar, L., Ogorelec, B. & Jurkovšek-Kolar, T. (1990): Pelagic Jurassic and Cretaceous beds in the western part of the Julian Alps. *Geologija.*; Vol. 31/32, pp. 285-328.

Kastelic, V., Vrabec, M., Cunningham, D. & Gosar, A. (2008): Neo-Alpine structural evolution and present-day tectonic activity of the eastern Southern Alps: The case of the Ravne Fault, NW Slovenia. *Journal of Structural Geology*.; Vol. 30; pp. 963-975.

Kossmat, F. (1907): Geologie des Wocheiner Tunnels und der Sudlichen Anschluslinie. *Denkschriften mathem naturwis K1*.; Vol. 83, pp. 6-140.

Ogorelec, B. & Rothe, P. (1993): Mikrofazies, Diagenese und Geochemie des Dachsteinkalkes und Hauptdolomits in Süd – West Slowenien. *Geologija*.; Vol. 35, pp. 81-182.

Ogorelec, B. & Buser, S. (1997): Dachstein Limestone from Krn in Julian Alps. *Geologija*.; Vol. 39, pp. 133-144.

Pálfy, J., Demény, A., Haas, J., Hetényi, M., Orchard, M.J. & Vető, I. (2001): Carbon isotope anomaly and other geochemical changes at the Triassic–Jurassic boundary from a marine section in Hungary. *Geology*.; Vol. 29, pp. 1047-1050.

Pálfy, J., Demény, A., Haas, J., Carter, E.S., Görög, A., Halász, D., Oravecz-Scheffer, A., Hetényi, M., Márton, E., Orchard, M.J., Ozsvárt, P., Vető, I. & Zajzon, N. (2007): Triassic–Jurassic boundary events inferred from integrated stratigraphy of the Csővár section, Hungary. *Palaeogeogr. Palaeoclimat. Palaeoeco*.; Vol. 244, pp. 11-33.

Pittet, B. & Mattioli, E. (2002): The carbonate signal and calcareous nannofossil distribution in an Upper Jurasic section (Balingen-Tieringen, Late Oxfordian, southern Germany). *Palaeogeogr. Palaeoclimat. Palaeoeco*.; Vol. 179, pp. 71-96.

Placer, L. (1999): Contribution to the macrotectonic subdivision of the border region between Southern Alps and External Dinarides. *Geologija*.; Vol. 41, pp. 223-255.

Rožič, B. & Kolar-Jurkovšek, T. (2007): Zgornjetriasni apnenčevi razvoji slovenskega bazena na Kobli in Slatniku. V: Horvat, A. (ur.): *18.*

posvetovanje slovenskih geologov, *(Geološki zbornik, 19)*. Ljubljana, Univerza v Ljubljani, Naravoslovnotehniška fakulteta, Oddelek za geologijo, pp. 96-99.

Rožič, B., Kolar-Jurkovšek, T. & Šmuc A. (in press): Late Triassic Sedimentary Evolution of Slovenian Basin (eastern Southern Alps): description and correlation of the Slatnik Formation. *Facies*.

Schäfer, P. (1979). Fazielle entwicklung und palökologische zonierung zweiter obertriadischer riffstrukturen in den Nördliche Kalkalpen (»Oberrhät«- Riff- Kalke, Salzburg). *Facies*.; Vol. 1, pp. 3-245.

Senowbari-Daryan, B. (1980): Fazielle und paläontologische Untersuchungen in oberrhätischen Riffen (Feichtenstein- und Gruberriff bei Hintersee, Salzburg, Nördliche Kalkalpen). *Facies*.; Vol. 3, pp. 1-237.

Senowbari-Daryan, B., Schäfer, P. & Abate, B. (1982): Obertriadische Riffe und Rifforganismen in Sizilien (Beiträge zur Paläontologie und Microfazies obertriadischer Riffe im alpin-mediterranen Raum, 27). *Facies*.; Vol. 6, pp. 165-184.

Sepkoski, Jr. J.J. (1996): Patterns of the Phanerozoic extinction: a perspective from global data bases. In: Walliser, O.H. (ed): *Global Events and Event Stratigraphy in the Phanerozoic*. Springer, Berlin, pp. 35-51.

Stanton, Jr. R.J. & Flügel, E. (1987): Paleoecology of Upper Triassic reefs in the Northern Calcareous Alps: reef communities. *Facies*.; Vol. 16, pp. 157-186.

Šmuc, A. (2005): *Jurassic and Cretaceous Stratigraphy and Sedimentary Evolution of the Julian Alps, NW Slovenia*. ZRC, ZRC SAZU, Ljubljana, 98 pp.

Šmuc, A. & Goričan, Š. (2005): Jurassic sedimentary evolution of a carbonate platform into a deep-water basin, Mt. Mangart (Slovenian-Italian border). *Rivista Italiana di Paleontologia e Stratigrafia*.; Vol. 111, pp. 45-70.

Tanner, L.H., Lucas, S.G. & Chapman, M.G. (2004): Assessing the record and causes of Late Triassic extinctions. *Earth-Sci. Rev.*; Vol. 65, pp. 103-139.

Turnšek, D. (1997): *Mezosoic Corals of Slovenia*. ZRC, ZRC SAZU, Ljubljana, 512 pp.

Turnšek, D. & Buser, S. (1991): Norian-Rhetian Coral Reef Buildups in Bohinj and Rdeči rob in Southern Julian Alps (Slovenia). *Razprave IV razreda SAZU* .; Vol. 32, pp. 215-257.

Verbovšek, T. (2008). Diagenetic effects on well yield of dolomite aquifers in Slovenia. *Environmental Geology*.; Vol. 53, pp. 1173-1182.

Vrabec, M. & Fodor, L. (2006): Late Cenozoic tectonics of Slovenia: structural styles at the Northeastern corner of the Adriatic microplate. In: Pinter, N., Grenerczy, G., Weber, J., Stein, S., Medak, D. (eds): The Adria microplate: GPS geodesy, tectonics and hazards. NATO Science Series, IV. *Earth and Environmental Sciences*.; Vol. 61, pp. 151-168.

Ward, P.D., Garrison, G.H., Haggart, J.W., Kring, D.A. & Beattie, M.J. (2004): Isotopic evidence bearing on Late Triassic extinction events, Queen Charlotte Islands, British Columbia, and implications for the duration and cause of the Triassic/Jurassic mass extinction. *Earth Planet Sci. Lett.*; Vol. 224, pp. 589-600.

Assessing groundwater vulnerability by SINTACS method in the Lower Savinja Valley, Slovenia

Ocenjevanje ranljivosti podzemne vode z metodo SINTACS v Spodnji Savinjski dolini, Slovenija

Jože Uhan[1], Jože Pezdič[2], Massimo Civita[3]

[1]Environmental Agency of the Republic of Slovenia, Vojkova cesta 1b, SI-1000 Ljubljana, Slovenia; E-mail: joze.uhan@gov.si
[2]University of Ljubljana, Faculty of natural sciences, Department of Geology, Aškerčeva cesta 12, SI-1000 Ljubljana, Slovenia; E-mail: joze.pezdic@guest.arnes.si
[3]Land, Environment and Geo-engineering Department, Politecnico di Torino, Italy, E-mail: massimo.civita@polito.it

Received: April 28, 2008 **Accepted:** August 28, 2008

Abstract: Three alluvial groundwater bodies in Slovenia have been assessed as a groundwater body with poor chemical status, mainly due to high concentrations of nitrate and other pollutants from intensive agricultural land use. In more than half of the national monitoring sampling sites in groundwater bodies, the annual average concentrations exceed 50 mg/l nitrate. In spite of the limitation in fertilisation, there is no evidence of a significant decreasing trend in nitrate concentrations in groundwater. The EU Water Framework Directive (WFD) requires further characterization of those groundwater bodies which have been identified as being at risk in order to establish a more precise assessment of the significance of such risk. The Lower Savinja Valley shallow alluvial aquifer with poor groundwater chemical status has been selected as a test case for such further characterization. This article discusses the issues of groundwater vulnerability assessment by the SINTACS method and sensitivity analysis of the model parameters. The result of the research offers a new basis for planning of detailed monitoring and protection measures, as well as good orientation for further methodological investigation.

Izvleček: V Sloveniji je bilo predvsem zaradi vsebnosti nitratov in drugih onesnaževal iz intenzivne kmetijske pridelave na treh aluvijalnih podzemnih vodnih telesih ocenjeno slabo kemijsko stanje. Na več kot polovici vzorčnih mest državnega monitoringa povprečne letne vsebnosti nitrata presegajo 50 mg/l. Nitrati kljub omejitvam

Scientific paper

pri gnojenju na nobenem vodnem telesu nimajo značilnega trenda zniževanja. Evropska vodna direktiva (WFD) zahteva podrobnejšo karakterizacijo vseh vodnih teles, za katera je bilo ugotovljeno tveganje za nedoseganje zastavljenih okoljskih ciljev. Za omenjena telesa podzemne vode naj bi izdelali bolj podrobno oceno značilnosti oz. pomembnosti tega tveganja. Za testni primer podrobnejše karakterizacije telesa podzemne vode s tveganjem je bil izbran plitvi aluvijalni vodonosnik Spodnje Savinjske doline s slabim kemijskim stanjem podzemne vode. Članek obravnava rezultate ocene ranljivosti podzemne vode z metodo SINTACS in rezultate analize občutljivosti modelnih parametrov. Rezultati raziskave nudijo novo podlago za načrtovanje programa podrobnejšega monitoringa in programa zaščitnih ukrepov, kakor tudi novo usmeritev nadaljnim metodološkim raziskavam.

Key words: groundwater, vulnerability, contamination, SINTACS, sensitivity analysis
Ključne besede: podzemna voda, ranljivost, kontaminacija, SINTACS, analiza občutljivosti

INTRODUCTION

Three out of twentyone Slovenian groundwater bodies have been identified as a groundwater body at risk in the first national groundwater chemical status assessment (KRAJNC et al., 2005). The central part of the smallest Slovenian groundwater body - Savinja Valley - has been selected as a test case for further characterization according to the WFD (DIRECTIVE 2000/60/EC, 2000), (Figure 1). It is about a 100 square kilometer-wide shallow alluvial aquifer system with about 5 percent of the total groundwater volume of all Slovenian alluvial aquifers. An important part of the regional water demand of the Savinja Valley is satisfied by pumping groundwater from the sandy gravel aquifers of the plain, where, even a decade ago, conflicts of interest occurred among the local population. The region of the Lower Savinja Valley is primarily renowned as the "valley of hops" with intensive agricultural activities and urbanization (Figure 2).

National groundwater level monitoring as well as groundwater quality monitoring in the Lower Savinja Valley have been permanently performed by the Environmental Agency of the Republic of Slovenia since 1955 and 1990 respectively. Activities in the last decade have been initiated to complete the conceptual model of the aquifer and initial characterization of the groundwater body. Studies included a review of the results of the previous hydrogeological investigations in the area, additional hydrogeological field mapping and water balance analysis (UHAN, 1996; PRESTOR et al., 2005).

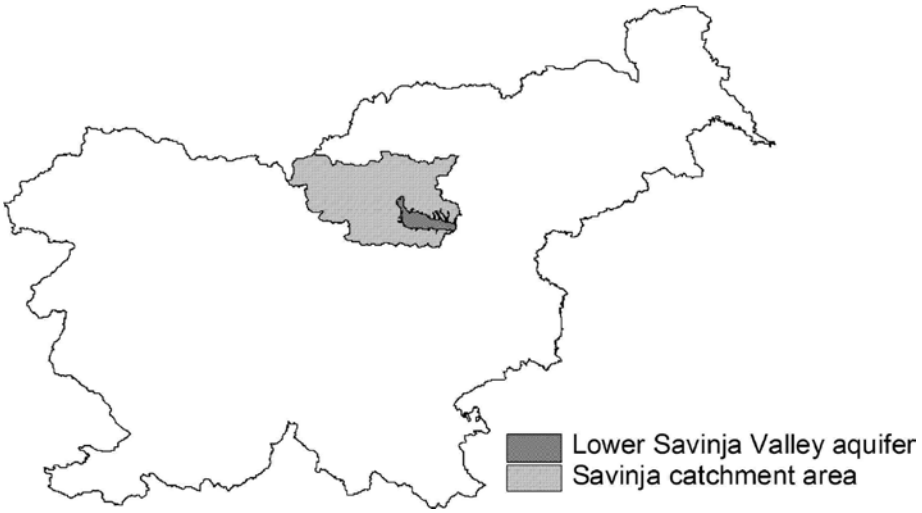

Figure 1. Position of the Lower Savinja Valley aquifer and their part of the Savinja river watershed
Slika 1. Vodonosnik Spodnje Savinjske doline in njeno prispevno hidrološko območje Savinje

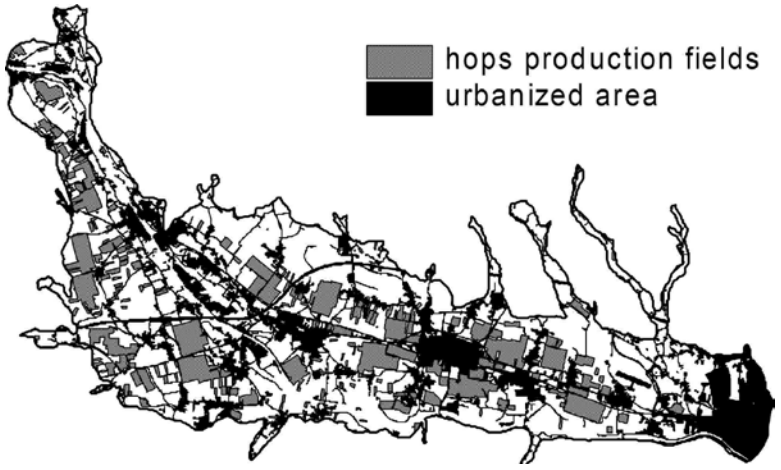

Figure 2. The hops production fields and urbanized areas in the Lower Savinja Valley
Slika 2. Hmeljišča in urbanizirana območja Spodnje Savinjske doline

In order to meet the requirements of the Water Framework Directive, the Lower Savinja Valley groundwater quality and quantity status assessment were made in the year 2005 (ANDJELOV et al., 2006; KRAJNC et al., 2007). Good quantitative but poor chemical statuses were assessed. The reason for the bad chemical status of the groundwater was found in high nitrate and pesticide concentrations, with an average 55.17 mg/l and maximum 143.02 mg/l for nitrates and an average 0.49 µg/l and maximum 2.63 µg/l for the sum of pesticides.

Following the first chemical status assessment results in 2005, further characterization has started with detailed groundwater vulnerability assessment using the Geographical Information System. We utilised the parametric method to assess intrinsic groundwater vulnerability and single-parameter sensitivity analysis. The purpose of the research was to improve knowledge about the natural protection ability of the unsaturated zone and about the pressure impacts, originating especially from diffuse pollution sources, in order to improve planning of protection measures.

METHODOLOGY

Groundwater vulnerability represents the intrinsic geological and hydrogeological characteristics of the aquifer. Its concept has been widely used in assessing the likely impact of pollution pressures during the groundwater characterization process and in the regional groundwater protection strategy. The SINTACS scheme of aquifer pollution vulnerability mapping was established for hydrogeological, climatic and impacts settings, typical for the Mediterranean countries (CIVITA, 1990). This assessment procedure incorporates seven parameters, relevant for the contaminant attenuation and vertical flow capacity (Table 1). In the vulnerability assessment procedure, the Savinja Valley area was discretised with a regular mesh grid of 100×100 m. The grid square cell structure of the SINTACS input data has been designed in order to use several weight strings. The weight strings have been prepared in order to satisfactorily describe the effective hydrogeological and impacting situation as set up by the sum of data. The present release of SINTACS presents five weight strings for normal impact, relevant impact, drainage from the surface network, deep karstified terrain and fissured terrain. For each of the 7.887 grid squares, element normalized SINTACS index was calculated and differently vulnerable areas were assessed using SINTACS R5 parametric methods (CIVITA & DE MAIO, 2000).

RESULTS AND DISCUSSION

Deep to the groundwater (SINTACS parameter S)

Groundwater is not deep under the surface in the Lower Savinja Valley. For the processing of the results of groundwater level measurements from fourteen measurement stations, a weighted moving average method has been used. In the period 1986-2005, the groundwater level was the highest in the north-central part (0.69 metre) and deepest in the central part of the valley (7.25 metre). The average depth to the groundwater at the majority (71.66 %) of the 100×100 metre grid cells amounts

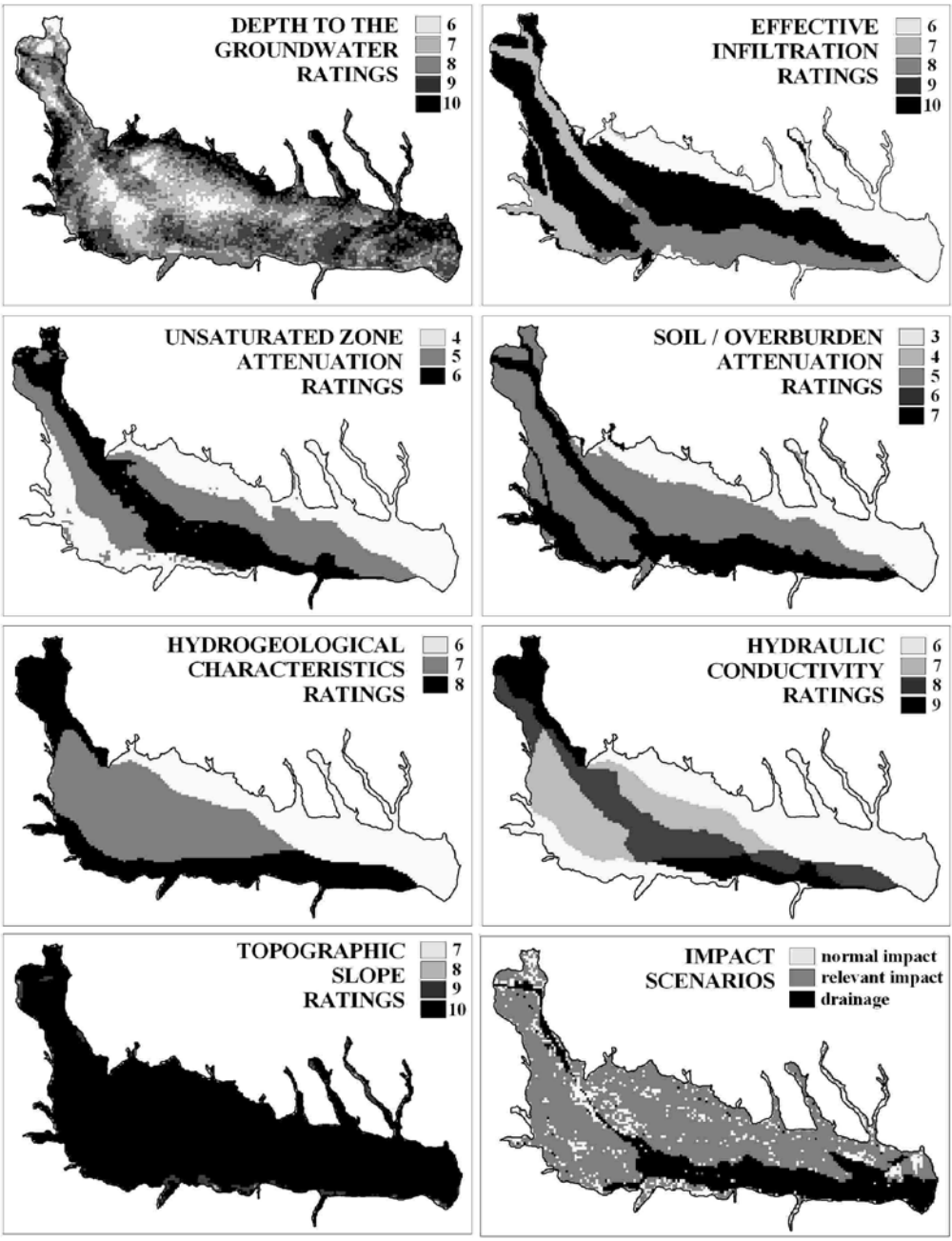

Figure 3. Parametric maps of SINTACS groundwater vulnerability model for the Lower Savinja Valley aquifer
Slika 3. Karte parametrov SINTACS modela ranljivosti podzemne vode vodonosnika Spodnje Savinjske doline

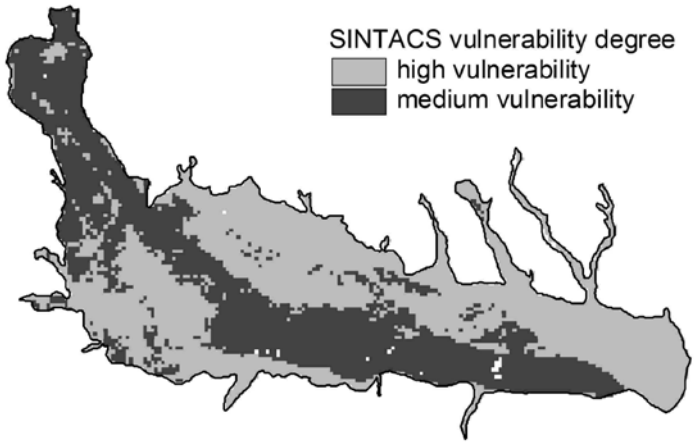

Figure 4. Distribution of the groundwater vulnerability index in the Lower Savinja Valley
Slika 4. Prostorska razporeditev indeksa ranljivosti podzemne vode v Spodnji Savinjski dolini

Table 1. Main characteristics of SINTACS parameters in the Lower Savinja Valley aquifer
Tabela 1. Osnovne značilnosti parametrov SINTACS v Spodnji Savinjski dolini

SINTACS Parameter	**Characteristics**
Depth to the groundwater table	average 3.9 m
Effective infiltration	average annual precipitation 1233 mm, average annual air temperature 9 °C
Unsaturated zone attenuation capacity	mainly holocene alluvial sandy gravel with clay component
Soil/overburden attenuation capacity	eutric cambisol, eutric fluvisol, eutric gleysol
Hydrogeological characteristics of the aquifer	unconfined aquifer, max. thickness of gravel, sand and clay sediments is 28 m, average 8 m
Coefficient of hydraulic conductivity	holocene: $1.1 \cdot 10^{-3} \div 1.1 \cdot 10^{-2}$ m/s, pleistocene: $2.0 \cdot 10^{-5} \div 2.0 \cdot 10^{-4}$ m/s
Topographic slope	average 0.8 %

to less than 4.5 metre, which corresponds to the ratings 8, 9 and 10 with the highest vulnerability rate. The majority (31.63 %) of the grid cells is to be found in the range of 2.5 and 4.5 metres.

Effective infiltration action (SINTACS parameter I)

For the calculation of the effective infiltration out of precipitation and evapotranspiration data, we used the hydrogeological inverse balance method (Civita et al., 1999), while taking the hydrogeological characteristics of the aquifer or soil texture characteristics into consideration. We estimated the interdependence of the following factors on the Lower Savinja Valley study area: (1) yearly average precipitation and corrected yearly average air temperature for the period 1986-2005 and (2) average elevation of the nearest gauging stations. We calculated the evapotranspiration and the effective precipitation of each of the 100×100 grid cells, using the numerical model CALCO INFILTRAZIONE (Civita and De Maio, 2000) after Turc (1954), and got the effective infiltration through estimating the potential infiltration coeficient. The effective infiltration in the period 1986-2005 ranged between 121 mm and 387 mm. The most frequently represented ratings are rating 10, ranging between 235 and 316 mm (47.76 %), and rating 6, ranging between 111 and 136 mm of effective infiltration (25.03 %).

Unsaturated zone attenuation capacity (SINTACS parameter N)

The unsaturated zone of the Lower Savinja Valley aquifer consists mostly of holocen sandy gravel with clay component at the marginal parts of the aquifer. We attributed the N rating between 4 and 6 to the litotypes on the basis of litotypes vs. N ratings diagram (Civita and De Maio, 2000). The pleistocene sediments with the assumed rating of N=3 can also be found at the lower part of the unsaturated zone of the central west-central part of the aquifer. For the areas, where the unsaturated zone is consist of holocene and pleistocene litotypes, we calculated the weighted mean that refers to the thickness. The unsaturated zone with rating N=4 represents 39.20 % of the 100×100 grid cells and is therefore prevalent at the area of the Lower Savinja Valley, followed by the unsaturated zone with a rating N=5 (34.53 %) and the unsaturated zone with a rating N=6 (26.27 %).

Soil/overburden attenuation capacity (SINTACS parameter T)

The significant water movement and pollutant retaining processes are dependent on textural characteristics of the soil, where the clay component is of special importance. There are three significant pedocartographical units prevalent in the Lower Savinja Valley: eutric fluvisol, evtric cambisol and evtric gleysol. Representation of all the other pedosystematical units is strongly inferior. The value of parameter T, read out of the soil textures vs. ratings T diagram (Civita and De Maio, 2000), is defined on the basis of nine pedological profiles in the Lower Savinja Valley. There are three types of soil prevalent in these profiles: light to medium-heavy eutric fluvisol (T=7), medium-heavy eutric soil (T=5) and medium-heavy to heavy evtric gleysol (T=3). There are 100×100 m grid cells with the rating T=5 prevalent (47.76 %) in the Lower Savinja Valley, followed by grid cells with a rating of T=7 (27.21 %) and T=3 (25.03 %).

Hydrogeological characteristics of the aquifer (SINTACS parameter A)

We compared the hydrogeological structure of the studied area (KÄSS et al., 1976; UHAN, 1996) with the results of statistical analysis of the groundwaterlevel national monitoring hydrograms (UHAN, 1997). Two highly separable factors with more than 92 % explained variance of groundwater level were founded through principle component analysis. The interpretation of the second factor is prevailingly bound to the lower terrace aquifer with high permeability. By that the coincidence of factor scores with water levels and flows of the Savinja River was discovered. Hydrogeological conditions along the bed of the river *Savinja* between *Breg pri Polzeli* and the confluence with *Bolska* allow the influent flow of the *Savinja* river. In the riverbed of *Bolska* and *Savinja* the exfluent flow, supplemented with groundwater springs at the area of *Kaplja vas* and *Vrbje*, was registered from the conflence with *Bolska*. The statistical analyses of the principal components of the groundwaterlevel national monitoring hydrograms support the spatial interpretation especially of those hydrogeological elements, linked with the spatial distribution of the holocene sediments or hydraulic relation of the groundwater and surface water. We attributed values of parameter A between 6 and 8 to the hydrogeological homogene units upon the recommendation of CIVITA and DE MAIO (2000). We attributed the following areas with the following values of parameter A: (1) lower terrace area with holocene coarse-grained sediments and less clay and silt fractions and a more dynamic hydrogeological regime – value 8, (2) the area of upper terrace with pleistocen – value 7 and (3) the area of the highest terrace with more compacted pliocen sediments with more clay component – value 6. These litotypes are in the Lower Savinja Valley and are mainly equally distributed, with a slight prevalence of the rating 7, which represents the occurrence of the holocene sediment.

Hydraulic conductivity range of the aquifer (SINTACS parameter C)

The estimate of the hydraulic conductivity range of the holocene part of the the Lower Savinja Valley, based on pumping tests, is between $1.1 \cdot 10^{-3}$ and $1.1 \cdot 10^{-2}$ m/s, whereas the hydraulic conductivity range of the pleistocene part of the aquifer is estimated at between $2.0 \cdot 10^{-5}$ m/s and $2.0 \cdot 10^{-4}$ m/s. The conductivity coefficient of $1.2 \cdot 10^{-2}$ m/s was defined using the tracer test east of *Arja vas*. The pumping test gave similar results ($0.65 \cdot 10^{-2}$ m/s), while the granulometric analyses of particular sedimentological heterogenic samples from the exploration hole resulted in the conductivity coefficient ranging between $6.5 \cdot 10^{-5}$ m/s and $2.3 \cdot 10^{-2}$ m/s (KÄSS et al., 1976). The hydraulic conductivity range of the pliocene sediments is due to the clay components and sediment compaction even lower than that of the pleistocene sediments. The hydraulic conductivity range of the holocene part of the Lower Savinja Valley is with the SINTACS value of C=9 (13.28 % of the cells) relatively high and lowers itself at areas of holocene sedimentation and even moreso at the marginal parts of the sedimentation basin or at the areas of pliocen sedimentation. Most of the area has the value of C=6 (41.28 %), followed by C=7 (23.47 %) and C=8 (21,86 %).

Table 2. Scenarios and weights for SINTACS parameters (Civita and De Maio, 2000)
Tabela 2. Scenariji in uteži za parametre SINTACS (Civita and De Maio, 2000)

Parameters	S	I	N	T	A	C	X
normal impact scenario	5	4	5	3	3	3	3
relevant impact scenario	5	5	4	5	3	2	2
drainage from surficial network scenario	4	4	4	2	5	5	2

Hydrological role of the topographic slope (SINTACS parameter X)

The Lower Savinja Valley is a flat surface aquifer with unexpressive topographic slopes. There is a 99-metre difference between the highest elevation on the west and the lowest elevation on the east, but the slope of the surface of the valley is gradual. Morphological particularities are declivities between individual terraces, sometimes as high as 10 metres. The prevalent slope inclination is based on a digital elevation model analysis 0.5°, which in relation to the slope inclination and value of parameter X corresponds with the rating 10.

Impact scenarios and weight strings

We adjusted the groundwater vulnerability model to the hydrogeological conditions and impact scenarios of the discussed area and accepted first three impact scenarios (Civita and De Maio, 2000). We used the normal impact scenario or relevant impact scenario and drainage from the river network scenario for the shallow aquifer of the Lower Savinja Valley. As far as the first two scenarios are concerned, the stress has been layed especially upon the intensive agricultural use of land, irrigation and urbanisation. The third scenario was attributed to the influent flow of the Savinja River and its affluents, to wetlands and to flooded areas. The predominant part of the Lower Savinja Valley is heavily anthropogenicly loaded (75.0 %), while the rest of the aquifer area is moderately loaded (4.2 %) or distinctive possibilities of surface drainage into the aquifer exist (20.8 %).

Elaboration of the vulnerability map

The assessment of the seven SINTACS parameters and three selected scenario enables the calculation of groundwater vulnerability SINTACS index $I_{SINTACS}$, which for the particular 100×100 m grid cell represents a sum of ratings and weights for all seven SINTACS parameters:

$$I_{SINTACS} = \sum_{j=1}^{7} P_j \cdot W_j$$

where $I_{SINTACS}$ is the vulnerability index and P_j and W_j are the ratings and the weights respectively of the grid cell *i.*

The SINTACS index ranging between 139 and 215 with the average of 183 has been calculated for 7.887 100×100 m grid cells at the area of Lower Savinja Valley. The Lower Savinja Valley is in SINTACS estimation placed in 4th and 5th groundwater vulnerability class. At the northeast and southwest of the aquifer (56.5 %) a 4th vulnerabilty class is prevalent, while in the northwestern and central area (43.2 %),

especially in the narrower area of *Savinja* river and lower terrace, the vulnerability increases (Figure 4).

SENSITIVITY ANALYSIS

The selection of ratings and weights that have to be assigned to the seven parameters for the SINTACS index calculation is unavoidably subjective. We applied the single-parameter sensitivity analysis, which evaluates the influence of each parameter on the groundwater vulnerability map. The analysis used for the Lower Savinja Valley SINTACS groundwater vulnerability map was based on the theory developed by LODWICK et al. (1990) and effectivly used by NAPOLITANO and FABBRI (1996).

For each grid square element we calculate the effective weight W_p (in %) using the following formula:

$$W_p = \left(\frac{P_r \cdot P_w}{I_{SINTACS}} \right) \cdot 100$$

where P_r and P_w are the ratings and the weights respectively of the layer P assigned to the subarea i, and $I_{SINTACS}$ is the vulnerability index.

The highest sensitivity to the output of the model was found at the depth to the groundwater (S) and effective infiltration action (I), while lower sensitivity was found at hydrogeological characteristics of the aquifer (A) and soil/overburden attenuation capacity (T). The lowest sensitivity of the model was found at the unsaturated zone attenuation capacity (N), the hydraulic conductivity range of the aquifer (C) and hydrological role of the topographic slope (X), (Table 3).

CONCLUSIONS

In the Lower Savinja Valley aquifer case study an attempt has been made to assess the groundwater vulnerability and single-parameter sensitivity analysis. The first groundwater vulnerability assessment of this case study area using the SINTACS parametric method allows us to distinguish from two classes with different vulnerability degrees. The first zone of medium vulnerability is characterised mainly by the lower terrace with shallow groundwater, high surface/groundwater interaction and a thin protective soil layer. The second zone of medium vulnerability is characterised mainly by the upper terraces with deeper groundwater and thick soil layer

Table 3. Average sensitivity weights (in %) of SINTACS parameters in the Lower Savinja Valley aquifer
Tabela 3. Povprečne uteži občutljivosti (v %) za parametre SINTACS v Spodnji Savinjski dolini

Parameters	W_S	W_I	W_N	W_T	W_A	W_C	W_X
Average actual weights	21,54	21,22	10,96	11,18	13,19	10,93	10,99

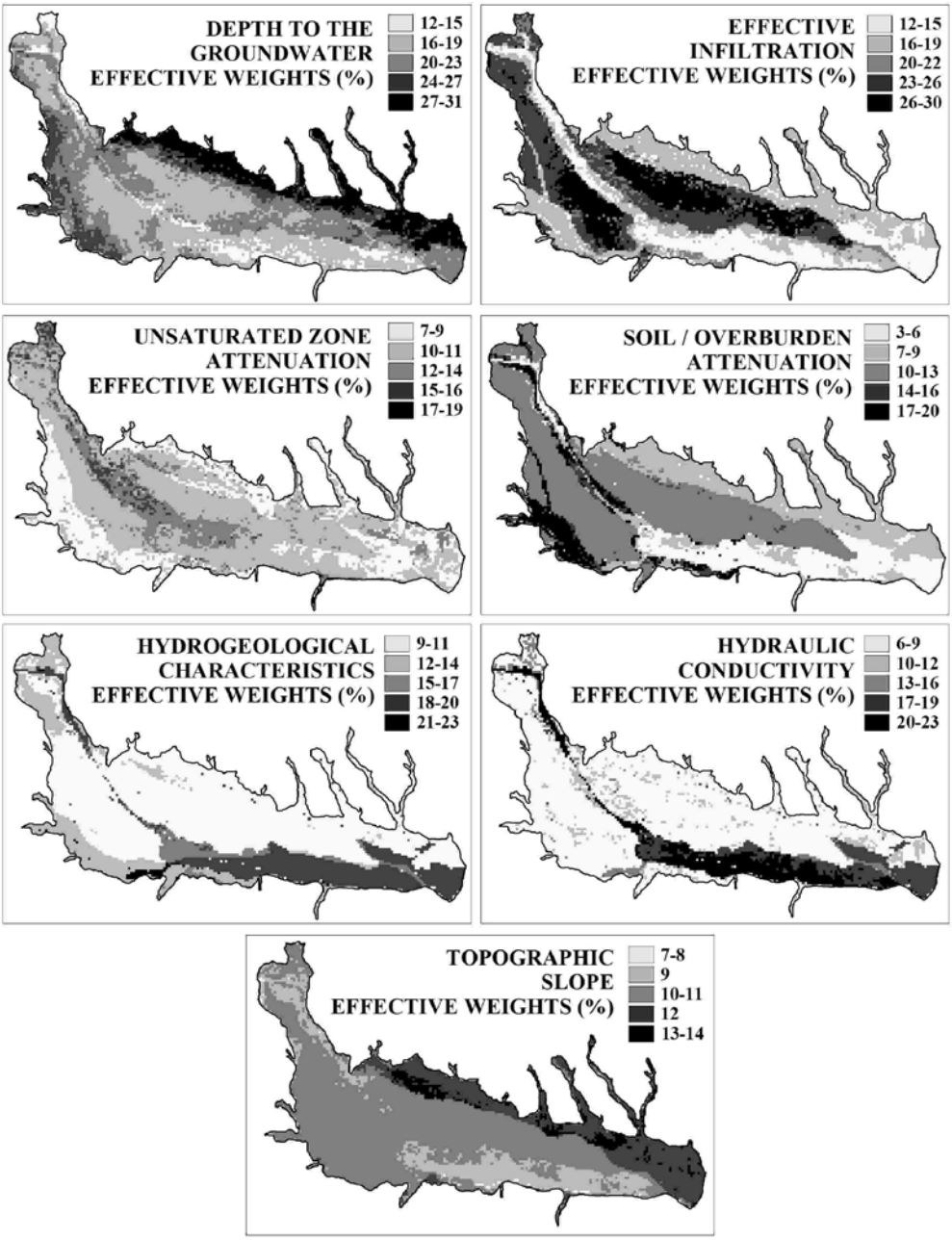

Figure 5. Sensitivity weights maps of SINTACS parameter for the Lower Savinja Valley aquifer

Slika 5. Karte uteži občutljivosti parametrov SINTACS za vodonosnik Spodnje Savinjske doline

with increased clay component. 48.9 percent of the hops production fields and 41.4 percent of the urbanised area are situated on the high groundwater vulnerable area of the Lower Savinja Valley aquifer.

The most sensitive parameters in the SINTACS groundwater vulnerability model of the Lower Savinja Valley are depth to the groundwater and effective infiltration action. The results of single-parameter sensitivity analysis enable better understanding of the vulnerability model results, enable consistent evaluation of the analytical result and give a new orientation for further methodological contamination research by using statistical and numerical model results with selected SINTACS groundwater vulnerability parameters.

It is pointed out that detailed vulnerability mapping, including analysis of hydrochemical data, especially nitrate concentration in groundwater, linked to the assessment of pressures and impacts, is a very good basis for establishing detailed monitoring programmes and programmes of measurement to achieve the WFD objectives of good groundwater status for groundwater bodies at risk.

Povzetek

Ocenjevanje ranljivosti podzemne vode z metodo SINTACS v Spodnji Savinjski dolini, Slovenija

V okviru študijskega primera vodonosnika v Spodnji Savinjski dolini smo ocenjevali ranljivost podzemne vode in analizirali občutljivost parametrov ocenjevalne sheme. Naravno ranljivost podzemne vode smo ocenili po metodologiji SINTACS, analizo občutljivosti pa smo izvedli ločeno po posameznih parametrih ocenjevalne sheme. S tem smo poskusili izboljšati poznavanje prostorske spremenljivosti zaščitnih sposobnosti nezasičene cone z namenom boljšega načrtovanja monitoringa in ukrepov za zaščito podzemne vode v Spodnji Savinjski dolini.

Spodnja Savinjska dolina je ravninski vodonosnik z neizrazito topografijo. Na območju vodonosnika prevladujejo tri pedokartografske enote: obrečna evtrična tla, evtrična rjava tla ter evtrični hipoglej. Nezasičena cona je sestavljena pretežno iz holocenskega peščenega proda z glinasto primesjo na obrobnih delih vodonosnika. Glede na hidrogeološko homogenost izstopa območje spodnje terase z debelozrnatimi prodnimi holocenskimi usedlinami z manj meljaste in glinaste primesi ter z bolj dinamičnim hidrogeološkim režimom, območje srednje terase s prisotnostjo tudi pleistocenskih usedlin ter območje zgornje terase z bolj kompaktnimi in bolj glinastimi holocenskimi usedlinami. Hidravlična prepustnost je ocenjena na podlagi črpalnih poskusov in za holocenske plasti znaša od $1{,}1 \cdot 10^{-3}$ do $1{,}1 \cdot 10^{-2}$ m/s, za pleistocenske plasti pa od $2{,}0 \cdot 10^{-5}$ do $2{,}0 \cdot 10^{-4}$ m/s. Efektiva infiltracija je bila v ocenjevalnem obdobju 1986-2005 med 120 in 390 mm, povprečna globina do podzemne vode pa je bila na pretežnem delu vodonosnika (71,66 %) manjša od 4,5 metre,

Uporabili smo scenarij zmernega ali povečanega antropogenega obremenjevanja ter scenarij dreniranja površinske vode v vodonosnik Spodnje Savinjske doline. Prete-

žni del Spodnje Savinjske doline je močno antropogeno obremenjen (75,0 %), preostali del območja vodonosnika je zmerno obremenjen (4,2 %) ali pa prevladujejo izrazite možnosti dreniranja površinske vode v vodonosnik (20,8 %).

Ocene sedmih parametrov ocenjevalne sheme po metodi SINTACS in izbranih treh scenarijev je omogočila izračun SINTACS indeksa ranljivosti podzemne vode, ki za posamezno ocenjevalno celico 100×100 metrov predstavlja vsoto vrednosti parametra in uteži za vseh sedem podatkovnih slojev. Za 7.887 celic 100×100 metrov na območju Spodnje Savinjske doline je bil izračunan SINTACS indeks v razponu od 139 do 215 s povprečjem 183. Območje aluvijalnega vodonosnika Spodnje Savinjske doline se po oceni SINTACS uvršča v 4. in 5. razred ranljivosti. V severovzhodnem in jugozahodnem delu vodonosnika prevladuje 4. razred ranljivosti, v severovzhodnem in osrednjem območju pa se ranljivost poveča.

Vpliv posameznih vhodnih parametrov na izhodni rezultat analitičnega modela smo ocenili z analizo občutljivosti posameznih parametrov v modelu ranljivosti. Največjo občutljivost na ranljivost podzemne vode v Spodnji Savinjski dolini ima parameter globine do podzemne vode in parameter efektivne infiltracije, manjša občutljivost pa je bila ugotovljena pri parametru hidrogeoloških lastnosti in lastnosti tal. Najmanjšo občutljivost imajo v tem ocenjevalnem modelu parameter lastnosti nezasičene cone, parameter hidravlične prepustnosti in parameter nagiba površja.

References

Andjelov, M., Gale, U., Kukar, N., Trišić, N., Uhan, J. (2006): Ocena količinskega stanja podzemnih voda v Sloveniji = Groundwater quantitative status assessment in Slovenia. *Geologija*.; Vol. 49/2, Ljubljana, str. 383-391.

Andjelov, M., Kerkeš, G., Kranjc, M., Uhan, J. 82007): Ocena stanja vodnih virov in vodne pravice. *Vodni dnevi 2007 - Zbornik referatov*. Portorož, str. 157-174.

Civita, M. (1990): La valutacione della vulnerabilita degli aquiferi all'inquinamento. *Proc. 1st Con. Naz. »Protezione E Gestione delle Acque Sotterranee: Metodologie, Technologie e Obiettivi«, Marano sul Panaro*.; pp. 39-86.

Civita, M., De Maio, M., Vigna, B. (1999): Una methodologia GIS per la valutazione della ricarica attiva degli acquiferi. *Atti del 3º convegno nazional sulla protezione e gestione delle acque sotterranee per il III millennio. Quaderni di geologia applicata*.; pp. 291-303.

Civita, M., De Maio, M., SINTACS R5 (2000): Quaderni di tecniche di protezione ambientale. *72. Pitagora Editrice*. Bologna, 226 p.

Directive 2000/60/EC of the European Parliament and of the Council (WFD) (2000): *Official Journal of the European Communities*.; 72 p.

Käss, W., Drobne, F., Bukvič, B. (1976): Markierung unterirdischer Wässer Untersuchungen in Slowenien 1972-1975. B. Markierung von

Porengrund-wässern, 1. Untersuchungen im Quartär des Savinja Tals. *Third International Symposium of Underground Water Tracing*.; pp. 219-238.

KRAJNC, M., GACIN, M., DOBNIKAR-TEHOVNIK, M. (2007): Monitoring kakovosti podzemne vpde v Sloveniji v letih 2004 in 2005 = Groundwater quality monitoring in Slovenija in years 2004 and 2005. *Report of the Environmental Agency of the Republic of Slovenia*. Ljubljana, 272 p.

LODWICK, W.A., MONSON, W., SVOBODA, L. (1990): Attribute error and sensitivity analysis of map operations in geographical information systems: suitability analysis. *Int. J. Geogr. Inform. Syst*.; Vol. 4, pp. 413-428.

NAPOLITANO, P., FABBRI, A.G. (1996): Single-parameter sensitivity analysis for aquifer vulnerability assessment using DRASTIC and SINTACS. V: *HydroGIS: Application of geographic information systems in hydrology and water resources management*. Edited by K. Kovar and H.P. Nachtnebel. IAHS Publication, No. 235, pp. 559-566.

PRESTOR, J., JANŽA, M., URBANC, J., MEGLIČ, P. (2005): Delineation of groundwater bodies in Slovenia. *Workshop on Groundwater Bodies in Europe and Adjacent Countries*. Berlin, poster.

TURC, L. (1954): Le bilan d'eaux des sols: relation entre les precipitations l'evaporation et l'ecoulement. *Annales Agronomiques*.; Vol. 5, pp. 491-595.

UHAN, J. (1996): Hidrološko – hidrogeološke osnove monitoringa podzemne vode v Spodnji Savinjski dolini. *Zaključno poročilo, Hidrometeorološki zavod RS Ljubljana*. 87 str.

UHAN, J. (1997): Analiza glavnih komponent podatkov o gladini podzemne vode v Spodnji Savinjski dolini = Principal components analysis of groundwater level data in the Spodnja Savinjska dolina. *Geol. zb*.; Vol. 13, str. 40-45.

Petrološke in mineraloške značilnosti Peračiškega tufa

Petrological and mineralogical characteristics of Peračica tuff

Vanja Kastelic[1]

[1]Univerza v Ljubljani, Naravoslovnotehniška fakulteta, Oddelek za geologijo, Aškerčeva cesta 12, SI-1000 Ljubljana, Slovenija; E-mail: vanja.kastelic@ntf.uni-lj.si

Received: May 11, 2008 **Accepted:** August 21, 2008

Izvleček: Peračiški tuf pripada seriji Smrekovških piroklastičnih kamnin. Starost kamnin je oligocenska, prostorska odmaknjenost obeh tipov kamnin pa posledica desnega zmika ob Savskem prelomu. Peračiški tuf sodi med drobno do srednjezrnate – pelitne do psamitne tufe. Sestava plagioklazov kaže 65 % vsebnost albitske komponente, kar jih uvršča med dacitno-andezitsko sestavo. Kamnine so sekundarno spremenjene. Zeleno barvo jim daje mineral klorit, ki v veliki meri nadomešča primarni biotit, v vzorcih pa so prisotni tudi minerali glin in zeoliti. Posamezni različki Peračiškega tufa so rjave barve, kar je posledica karbonatizacije kamnine, opaženi pa so tudi redki vzorci po strukturi kristalnega tufa z nekaj milimetrskimi luskami klorita.

Abstract: Peračica tuff series is a part of a bigger Smrekovec piroclastic rock series. The age of rocks is Oligocene and recent space-distribution of the piroclastic rocks depict dextral strike-slip along Sava Fault line. Peračica tuffs are fine to medium grained (pelitic to psamitic) tuffs with dacite to andesite composition. Rocks exhibit secondary changes in mineral composition. Green colour of tuffs is caused by chlorite content and this mineral is substituting primary biotite. Rock samples also contain minerals from clay mineral group and also zeolites. One of Peračica tuff variety is brown in colour which is caused from intense carbonatization processes, a type with a few millimetre in size grains of chlorite belongs to a crystal tuff variety according to its structure.

Ključne besede: Peračiški tuf, mineralna sestava, rentgenska difrakcija, sekundarne spremembe

Key words: Peračica tuff, mineral composition, X-ray diffraction, secondary mineral changes

Professional paper

DOSEDANJE RAZISKAVE IN REGIONALEN PREGLED

Smrekovške vulkanoklastične kamnine, kamor prištevamo tudi Peračiške tufe, so vezane na proces vulkanizma, ki je pričel delovati v morskem okolju, kjer je nastal vulkanski masiv z enim stratovulkanom. Sestava magme se je zaradi frakcionirane kristalizacije bazaltne taline s časom spreminjala od bazaltne prek bazaltno-andezitne in kisle andenzitne do dacitne taline (KRALJ, 1997).

Prve opise Peračiških tufov zasledimo pri MORLOTU (1850), ki jih opisuje kot posebne zelenkaste, tufom podobne kamnine, nastale s preobrazbo krhkega eocenskega skrilavca (MORLOT, 1850). S proučevanjem Peračiških tufov sta se v nadaljnih letih ukvarjala še Peters, ki jih je določil kot sedimentne tvorbe sestavljene iz drobcev glinastih skrilavcev in dioritnih kamnin (PETERS, 1856), ter Lipold, ki je omenjene kamnine starostno uvrstil v spodnji miocen (LIPOLD, 1857). V nadaljnih letih so sledile raziskave slovenskih geologov. S to tematiko sta se ukvarjala predvsem JOŽE DUHOVNIK (1964), ki je izdelal geološko skico ozemlja in se ukvarjal s preiskavami plagioklazev s pomočjo Fedorove metode, ter DOLAR-MANTUANI v razpravi Peračiški tufi (1937). V tej razpravi se je ukvarjala predvsem z določevanjem kemizma tufov in s pomočjo tako dobljenih rezultatov ter z merjenjem vsebnosti anortitne komponente plagioklazov ugotovila, da kamnine pod imenom Peračiški tufi ustrezajo dacitni ali andezitni sestavi.

V novejšem času na temo podrobnejših raziskav Peračiških tufov ni bilo objavljenega nobenega članka, omenjajo pa se v raziskavah smrekovških piroklastičnih kamnin kot njihovi ekvivalenti (HINTERLECHTER-RAVNIK & PLENIČAR, 1967). Na podlagi sestave obeh kamnin sta sklepala na skupen izvor in ugotovila, da je središče vulkanizma moralo ležati severno od Julijskih Alp, saj plasti oligocenskega andezitnega tufa niso bile najdene severneje od Savskega preloma, le južneje v Radovljiški kotlini, medtem ko so izdanki Smrekovškega tufa bili najdeni severneje od Savskega preloma, ob katerem naj bi prišlo do desnega zmika in s tem razmika obeh vulkanoklastičnih serij kamnin. PLACER (1996) je potrdil domnevo da je Celjski prelom le vzhodni podaljšek Savskega preloma, in s tem oligocenske plasti Radovljiške kotline, v kateri se nahajajo andezitni Peračiški tufi, odrezani in premaknjeni del oligocenskih plasti in serije Smrekovških vulkanoklastičnih kamnin iz Celjske kotline. Na podlagi tega je bil določen hipotetični premik ob Savskem prelomu za 65-70 km. Savski prelom je najjužnejši od spremljajočih prelomov Periadriatskega lineamenta. Dobljen premik je bil ugotovljen s pomočjo razdalje med zahodnima robovoma Radovljiške kotline in Smrekovškega oligocenskega bazena, ter vzporejanja oligocenskih plasti omenjenih enot.

Izdanki Peračiških vulkanoklastičnih kamnin so vezani na območje Radovljiške kotline v NW Sloveniji (slika 1). Regionalno območje pripada južnim obronkom Karavank in se pojavlja severno od Savskega preloma. Na severu zasledimo različke piroklastičnega materiala že skoraj ob vznožju gore Dobrča (DOLAR-MANTUANI, 1937). Proti jugovzhodu jim nato sledimo ob toku reke Peračice vse do Grofije,

kjer se strnjeno območje nastopanja omenjenih kamnin konča nekoliko zahodneje od vasi Peračica. Proti jugozahodu nato sledimo predvsem tufskim peščenjakom do vasi Črnivec, od tam proti severozahodu pa piroklastične kamnine zasledimo še vse do vasi Spodnji Otok in še severneje do Dvorske vasi. Poleg tufov zasledimo na omenjenem območju še tufske peščenjake, tufske breče in vmesne plasti gline sivice, tako da ne moremo govoriti o strnjenem območju nastopanja samih tufov. Na omenjenem območju je bil v preteklosti aktiven Bogatajev kamnolom, kjer so pridobivali različek sivega homogenega masivnega tufa.

Na območju Peračiškega slapa so vidni prehodi med različki piroklastičnega materiala. Na dnu slapa se pojavlja plast kompaktne sive gline, nad njo ležijo plasti drobnozrnatega tufa s posameznimi večjimi mineralnimi zrni, nad njimi pa izdanjajo plasti drobnozrnatega tufa. Po Duhovniku

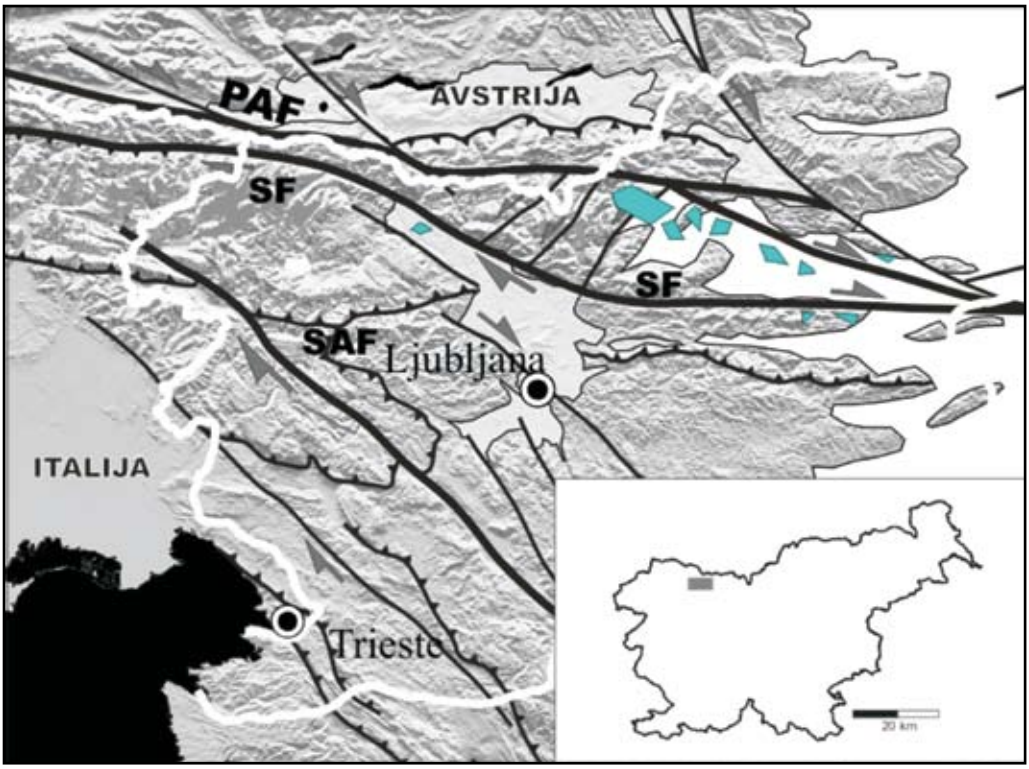

Slika 1. Regionalna skica raziskanega območja. Z modro barvo so podane lokacije Oligocenskih vulkanoklastičnih kamnin Smrekovške serije (po Buser, 1977; Mioć in Žnidaršič, 1987; Premru, 1983). SF=Savski prelom; PAF=Periadriatska prelomna cona; SAF=Južno-alpska narivna meja.

Figure 1. Regional scheme of the investigated area. Blue color depicts locations of Oligocene vulcanoclastics rocks of Smrekovec series (after Buser, 1977; Mioć in Žnidaršič, 1987; Premru, 1983). SF=Sava Fault; PAF=Periadriatic fault zone; SAF=South-alpine thrust zone.

(1964) najdemo večja strjena območja tufov še na področju okoli Špika in severneje, kjer se v glavnem menjata drobnozrnati in srednjezrnati tuf z redkimi vložki tufske breče, medtem ko pri vhodu v Peračiško dolino pri vasi Črnivec prevladuje predvsem tufski peščenjak.

Namen vzorčenja Peračiškega tufa je bil določitev mineraloške sestave različkov tufa, ki se razlikujejo že makroskopsko. Vzorci za mikroskopske in rentgenske analize in so bili vzeti v obeh odkopih Bogatajevega kamnoloma. Odkriti so bili trije različki tufa; svetlozelen drobnozrnat tuf, svetlozelen drobnozrnat tuf z posameznimi tudi do 1 centimeter velikimi temnejšimi izraziteje zelenimi mineralnimi zrni ter različek rjavega drobnozrnatega tufa. Lokacije vzorčenja so bile izbrane tako, da so mesta vzorčenja vključevala vse tri makroskopsko vidne rezličke tufa v različnih delih znotraj posameznih plasti. Prve štiri vzorce sem vzela v vzhodnem delu odkopa; vzorec številka ena je tipičen svetlozelen primerek tufa vzet iz sredine južnega dela stene. Vzorca 2 in 3 sta po barvi rjavkasta, vzeta iz zgornjega dela južne stene, vzorec številka 4 pa je vzet izven glavne stene ter vsebuje makroskopsko vidna večja mineralna zrna v drobnozrnati osnovi. Vzorce 5, 6 in 7 sem vzela v zahodnejšem odkopu kamnoloma. Vsi od teh so značilne svetlo zelene barve, vzorec št. 7 vsebuje še manganove dendrite.

MIKROSKOPSKE ANALIZE

Mikroskopske analize so bile opravljene z mikroskopom znamke Nikon Eclipse E600 POL vpresevni polarizirani svetlobi. V zbruskih svetlozelenih drobnozrnatih tufov prevladujejo zrna kremena. Večina kremenovih zrn je nepravilnih oblik, posamezna kažejo zaobljeno obliko, medtem ko so posamezna kristalna zrna idiomorfna. Prisotna so zrna z normalno in valovito potemnitvijo, ki nakazujejo pogoje povišanega usmerjenega tlaka. Povprečna velikost kremenovih zrn znaša od 30 do 60 μm, posamezna zrna pa dosežejo velikosti tudi do 300 μm. V zbruskih so opazni letvasti kristali enostavno dvojčičnega plagioklaza, ki se po velikosti zrn ne razlikuje močno od velikosti zrn kremena; povprečna velikost teh mineralnih zrn doseže vrednost 70 μm, maksimalna velikost zrn pa znaša plagioklazovih zrn znašajo od 300-500 μm. Zrna plagioklazov so povečini polisintetsko dvojčična s kotom potemnitve med 26° do 28° (slika 2d), kar nakazuje na sestavo plagioklazov, ki vsebujejo več kot 55 % albitske komponente (MACKENZIE & ADAMS, 2005). Od femičnih mineralov so prisotna posamezna zrna biotita, vendar je velika večina tega minerala že sekundarno spremenjena - kloritizirana. Ponekod je klorit nadomestil biotit že do take mere, da zasledimo le še luske klorita, ki se nahajajo v združbah posameznih pasov in imajo v celotnem zbrusku enako orientacijo. Te združbe so velike tudi do 380 μm. V manjši meri so v zbruskih prisotni še sericit ter opaki minerali. Osnova je zelo kriptokristalna in pod mikroskopom je mineralna sestava te neprepoznavna. Zbruski kažejo orientiranost; tako osnova kot tudi posamezna mineralna zrna, zlasti luske klorita (slika 2a).

Vzorci drobnozrnatih svetlozelenih tufov, ki se od ostalih makroskopsko ločijo po prisotnosti večjih lusk temneje zelenega minerala. Kremenova zrna so povečini

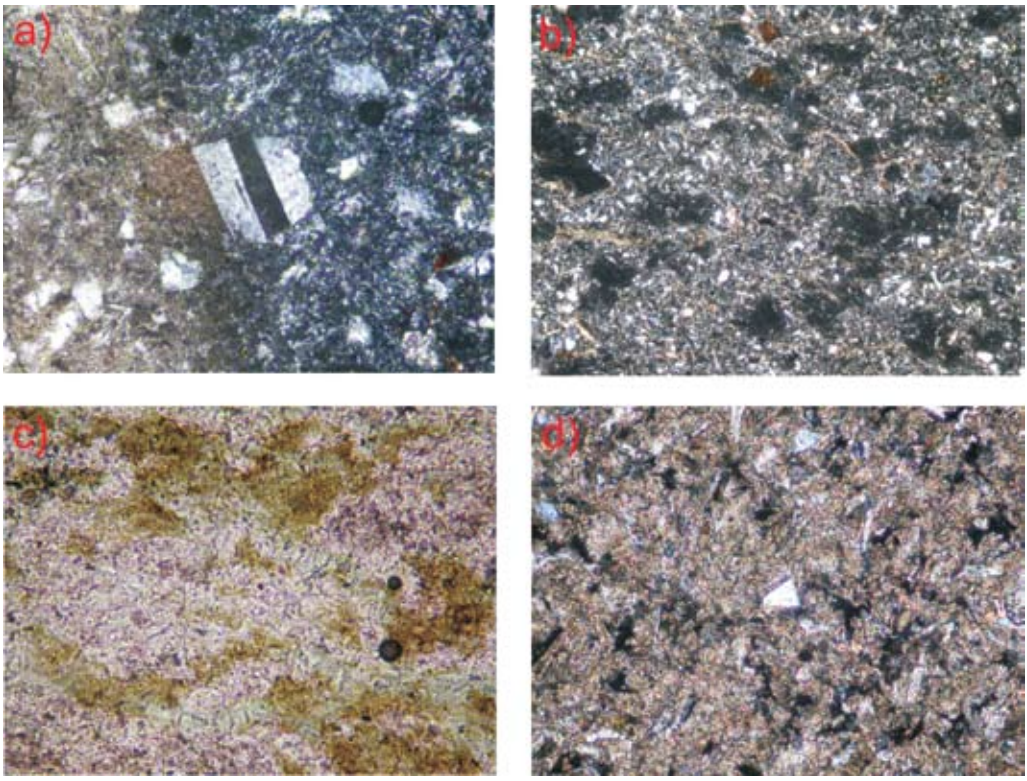

Slika 2. Mikroskopski posnetki različkov Peračiškega tufa. a) zrno dvojčičnega plagioklaza, ki po vrednosti kota potemnitve kaže na njegovo srednjo sestavo v albitno-anortitnem zveznem nizu; povečava 200×, slikano pod navzkrižnimi nikoli. b) kremenova zrna in zrna plagioklazev, ki prevladujejo med mineralnimi zrni ter letvičasta zrna biotita, ki kažejo povitost in usmerjenost. Vidna so tudi polja nepresevnih mineralnih združb ter posamezna zrna železovih oksidov in hidroksidov. Osnova je drobnozrnata do nekristaljena ter ponekod sekundarno spremenjena; povečava 40×, slikano pod navzkrižnimi nikoli. b) različek drobnozrnatega tufa, ki je močno sekundarno karbonitiziran; povečava 100×, slikano pod navzkrižnimi nikoli. c) zelen, najbolj razširjen različek Peračiškega tufa. Vzorec kaže zelena polja, ki so rezultat nadomeščanja primarnega biotita s kloritom; povečava 200×. d) različek drobnozrnatega tufa, ki je močno sekundarno karbonitiziran; povečava 100×, slikano pod navzkrižnimi nikoli.

Figure 2. Thin-section images of Peračica tuffs. a) grain of twined plagioclase that on the basis of extinction angle points to middle composition in the albite-anortite series; magnification 200×, crossed polars. b) quartz and plagioclase that prevail among mineral grains and flatty grains of biotite that display wrapping and orientation. Patches of opaque mineral associations are seen in the thin-section, as-well as grains of iron oxides and hydroxides. The matrix is fine grained to uncrystallized and in places secondary changed; magnification 40×, crossed polars. c) the green, most common variety of Peračica tuff rock series. In the thin-section primary biotite grains are replaced by chlorite; magnification 200×. d) grain of twined plagioclase that on the basis of extinction angle points to middle composition in the albite-anortite series; magnification 200×, crossed polars. d) fine grained variety of tuff rocks that displays high degree of secondary changes in the form of carbonatization; magnification 100×, crossed polars.

ksenomorfnih do hipidiomorfnih oblik, z normalno in valovito potemnitvijo velikosti od 100-350 μm. Prisotna so tudi polisintetsko dvojčična zrna plagioklazov s kotom potemnitve 25°, kar nakazuje na sestavo glinencev, ki vsebujejo več kot 65 % albitske komponente (MACKENZIE & ADAMS, 2005). Posamezna zrna plagioklazev dosegajo velikosti 230 μm, največje zrno pa je veliko 760 μm. Od mafičnih mineralov so prisotna biotitova zrna velikosti 230 μm, ki so večinoma že kloritizirana, ponekod tudi do take meje, da so od biotita ostali le še posamezni otočki ter biotitov višji relief. Klorit se v vzorcih pojavlja tudi kot primaren mineral, predvsem ga zasledimo v posameznih luskah dimenzij do 75 μm. Od ostalih mineralov so prisotna še posamezna zrna muskovita, ki v povprečju dosegajo 50 μm.

Pri vzorcih svetlozelenih tufov pri katerih so makroskopsko vidna temnejša polja ter vključki je pri opazovanju pod mikroskopom brez analizatorja vidna drobnozrnata osnova, posamezna kremenova zrna ter dokaj številni nepresevni vključki. Opazne so tudi številne, značilno svetlozelene luske klorita. Pri opazovanju pod navzkrižnimi nikoli je še bolj opazna drobnozrnata osnova z nizkimi interferenčnimi barvami od bele do črne prvega reda. Med mineralnimi zrni prevladujejo zrna kremena, ki so povečini ksenomorfnih do hipidiomorfnih oblik z normalno in valovito potemnitvijo, povprečne velikosti 170 μm. Po količini nastopanja so na drugem mestu zrna plagioklazov. Ta so povečini polisintetsko dvojčična s kotom potemnitve 28°, kar_nakazuje na sestavo plagioklazov, ki vsebujejo več kot 55 % albitske komponente. Velikosti plagioklazovih zrn znašajo od 300-500 μm. Razpoznavna so tudi posamezna zrna biotita. Nekatera so ohranjena še v celoti, medtem ko je od drugih ostal le še prvotni relief, drugače pa so povsem nadomeščena z kloritom (slika 2c). Velikosti teh zrn so 100-500 μm. Klorit se pojavlja tudi kot primaren mineral v obliki lusk, prisotna pa so tudi posamezna zrna muskovita.

Svetlorjav različek Peračiškega tufa kaže zelo drobnozrnato osnovo med katero so opazna posamezna hipidiomorfna do ksenomorfna kremenova zrna velikosti 60-90 μm, sama osnova pa je močno karbonatizirana (slika 2b). Preostali minerali zaradi močne karbonatizacije niso razpoznavni.

Rezultati mineralne sestave se ujemajo s petrološkimi rezultati DOLAR-MANTUJANIJEVE (1937) in DUHOVNIKA (1964). Slednji je za tufe Bogatajevega kamnoloma ugotovil, da v njih prevladuje andezitsko ali dacitsko steklo, ki ima pozitivni relief. Vsebovana zrna imajo največje dimenzije do 0,6 mm. Poleg teh kamnina vsebuje približno 4-5 % zrn plagioklazov, 1-2 % klorita, ki je povečini nastal kot posledica preperevanja femičnih mineralov in nastopa v glavnem v luskah velikosti 0,05 mm. Ugotovil je še prisotnost zrn kremena, ki naj bi verjetno nastal iz opala preko kalcedona pri rekristalizaciji steklaste osnove. Tufi naj bi bili podvrženi procesu kaolinitizacije, v zbruskih pa je zasledil še kalcit in sericit, ki naj bi bil prav tako posledica preperevanja vulkanskega stekla, ter pirit, goethit in lepidokrokit. DOLAR-MANTUANIJEva (1937) je v okviru svoje preiskave izvedla še kemijsko analizo tufov, glavna ugotovitev te je nizka vsebnost K_2O v tufih. Tudi DUHOVNIK (1964) je v okviru svoje raziskovalne naloge izvedel kemijsko analizo. Ugotovil je, da so tufi predvsem bogati z SiO_2, MgO, CaO in FeO, ki je vključen v Fe_2O_3.

Tabela 1. Vsebnost mineralov ugotovljena s pomočjo rentgenske difrakcije po vzorcih
Table 1. Mineral composition of 7 samples of Peračica tuff rocks determined by X-ray diffraction

Št. Vzorca	**1**	**2**	**3**	**4**	**5**	**6**	**7**
Mineral							
kremen SiO_2	+	+	+	+	+	+	+
kalcijski albit $(Na ,Ca) Al (Si, Al)_3O_8$	+				+	+	+
analkim $Na(Si_2Al)O_6.H_2O$	+	+	+	+	+	+	+
klorit $(Mg,Al)_6(Si,Al)_4O_{10}(OH)_8$	+	+	+	+		+	+
muskovit $KAl_2Si_3AlO_{10}(OH)_8$	+	+	+	+	+	+	
kalcit $CaCO_3$		+	+				
dickit $Al_2Si_2O_5(OH)_4$				+			
montmorillonit $(Na,Ca)_{0.33}(Al,Mg)_2(Si_4O_{10})(OH)_2 \cdot nH_2O$		+					
nontronit $Ca_{.5}(Si_7Al_{.8}Fe_{.2})(Fe_{3.5}Al_{.4}Mg_{.1})O_{20}(OH)_4$				+		+	

Rezultati rentgenske difrakcije

Vzorce sem analizirala z metodo praškovne rentgenske difrakcije. Uporabljen je bil rentgenski difraktometer PHILIPS s sledečimi parametri snemanja: napetost 40 kV, tok 30 mA, valovna dolžina uporabljene rentgenske svetlobe CuKα 1,5418 Å, sekundarni grafitni monokromator in proporcionalni števec, snemanje pa je potekalo v kotnem območju 2°-70° 2 Θ, s hitrostjo 3° 2 Θ/min. Rentgenograme sem analizirala s pomočjo računalniškega programa μPDSM. Na ta način sem analizirala vseh sedem vzorcev. Dobljeni rezultati so si precej podobni, izstopata le vzorca 2 in 3 (tabela 1).

Na vseh rentgenogramih so prisotni vrhovi, ki jih ustvari rentgenska svetloba uklonjena na vzporednih mrežnih ravninah (v nadaljevanju vrhovi), ki pripadajo kremenu. Prisotni so tudi vrhovi, ki pripadajo analkimu, kloritu ter plagioklazom, ki glede na njihove *d* vrednosti predstavljajo plagioklaze srednje sestave. V vzorcih 2 in 3 najvišja vrhova na rentgenogramu pripadata mineralu kalcitu, kar potrjuje intenziven proces karbonatizacije, ki je bila opažena že pri mikroskopskih analizah. Z metodo rentgenske difrakcije so bili je bila v vzorcih zaznana tudi prisotnost glinenih mineralov, katerih vrhove na rentgenogramih opazimo pri *d* vrednostih 7-15 Å.

Posamezni minerali glin s pomočjo RTG difrakcije niso bili izdvojeni, z izjemo montmorillonita v vzorcu številka 2. Poleg vseh omenjenih mineralov, sta bila v vzorcih dokazana tudi dickit in nontronit.

Mineralna sestava peračiških tufov določena z metodo praškovne rentgenske difrakcije je predstavljena v tabeli 1.

Rezultati rentgenske difrakcije se ujemajo z mineralno sestavo ugotovljeno pod mikroskopom. Potrjena je prisotnost kremena, ki predstavlja večino med mineralnimi zrni, ter prisotnost plagioklazov, natančneje kalcijskega albita. Ta ugotovitev se sklada z že dosedanjim uvrščanjem tufov med andezitske tufe.

S pomočjo rentgenske analize je tudi razvidno, da je v tufih prisoten mineral iz skupine zeolitov – analkim. Prisotnost tega minerala lahko povezujemo z odlaganjem vulkanoklastičnega materiala v vodnem okolju (IIJIMA, 1978) in delovanjem hidrotermalnih procesov ter sprememb (IIJIMA, 1984; UTADA, 1987) kar se prav tako navezuje na že prejšnje teorije o nastanku in sekundarnih spremembah smrekovških piroklastičnih kamnin (KRALJ, 1997). Pod mikroskopom mineralnih zrn analkima nisem opazila; po tem sklepam, da je gotovo prisoten v kriptokristalni osnovi tufov. Spremenjena osnova tufov v glavnem sestoji iz sericita, analkima, že pod mikroskopom pa je bilo videti, da je osnova tudi rahlo motna in verjetno vsebuje tudi iz minerale glin. To domnevo potrjujejo tudi vrhovi pri d vrednostih 7-10 Å, ki so prisotni na rentgenogramih. Pod mikroskopom sem opazila tudi zrna biotita, ki pa so bila v veliki meri sekundarno spremenjena tako, da je od posameznih zrn ostal le njihov prvotni relief. Pri rentgenski analizi med zastopanimi minerali v nobenem od sedmih vzorcev nisem kot rešitev dobila minerala biotita. Kot možni mineral, ki je nadomestil prvotni biotit se pri rešitvi rentgenogramov pojavlja tudi mineral nontronit, ki pripada skupini smecktitov in vsebuje katione železa. Sestava tega minerala se lahko spreminja, ker lahko absorbira različne količine vode, pogosto pa se pojavlja v koloidnih agregatih, natančneje kot fine vlaknate strukture. Njegova barva je odvisna od vsebovane količine železovih ionov, tako je lahko motno bel, rumen ali zeleno rumen. Zaradi vseh sprememb, ki jih je prvoten piroklastičen material, ki je vseboval predvsem minerale kot so kremen, plagioklazi in biotit preterpel med odlaganjem v vodnem okolju, transportu in ostalih dejavnikih je prišlo do številnih kemijskih reakcij - nadomeščanj. Poleg tega imajo muskovit, biotit, sericit in illit podobno strukturo, kar ustreza istim lokacijam značilnim vrhov na rentgenogramih in je zaradi tega posamezne minerale težko izdvojiti. Med rezultati rentgenske analize se pogosto nahaja tudi muskovit, ki sem ga pod mikroskopom opazila samo kot posamezna manjša mineralna zrna. Obema mineraloma glede na podobno strukturo na rentgenogramih pripadajo vrhovi pri podobnih *d* vrednostih, tako da jih je samo na podlagi analize rentgenske difrakcije medseboj težko ločiti.

Pri rešitvah rentgenske analize izstopata med ostalimi vzorca 2 in 3. Ta dva se razlikujeta od ostalih že po lastni barvi kamnine. Že pod mikroskopom je bila

razvidna močna karbonatizacija teh dveh vzorcev, ki jo je rentgenska analiza le še potrdila. Po količini v omenjenih vzorcih prevladuje kalcit, v manjši meri pa so prisotni še kremen, albit, analkim ter minerali glin, katerih prisotnost nakazuje sekundarne spremembe mineralov osnove. Tako močna karbonatizacija kot je opazna pri vzorcih številka 2 in 3 je gotovo nastala kot rezultat delovanja hidrotermalnih raztopin, ki so se verjetno v zgoraj ležečih karbonatnih kamninah obogatile z Ca ioni, ki so v tufih povzročili proces karbonatizacije predvsem njihove osnove.

Kvantitativna analiza prisotnosti posameznega minerala ni bila opravljena, ker pa so bili vsi vzorci posneti pod istimi pogoji in z enakimi nastavitvami, je primerjalna ocena zastopanosti posameznega minerala v vzorcih možna. V vzorcih, ki so bili karbonatizirani močno prevladuje mineral kalcit. Med ostalimi minerali v teh vzorcih sta na drugem mestu po prisotnosti minerala kremen in analkim, medtem ko je prisotnost sekundarnih mineralov glin in klorita majhna. Pri vzorcih, ki sekundarno niso bili izpostavljeni karbonatizaciji prevladuje mineral kremen, ki mu sledijo analkim, albit ter nato v manjših merah klorit in minerali glin.

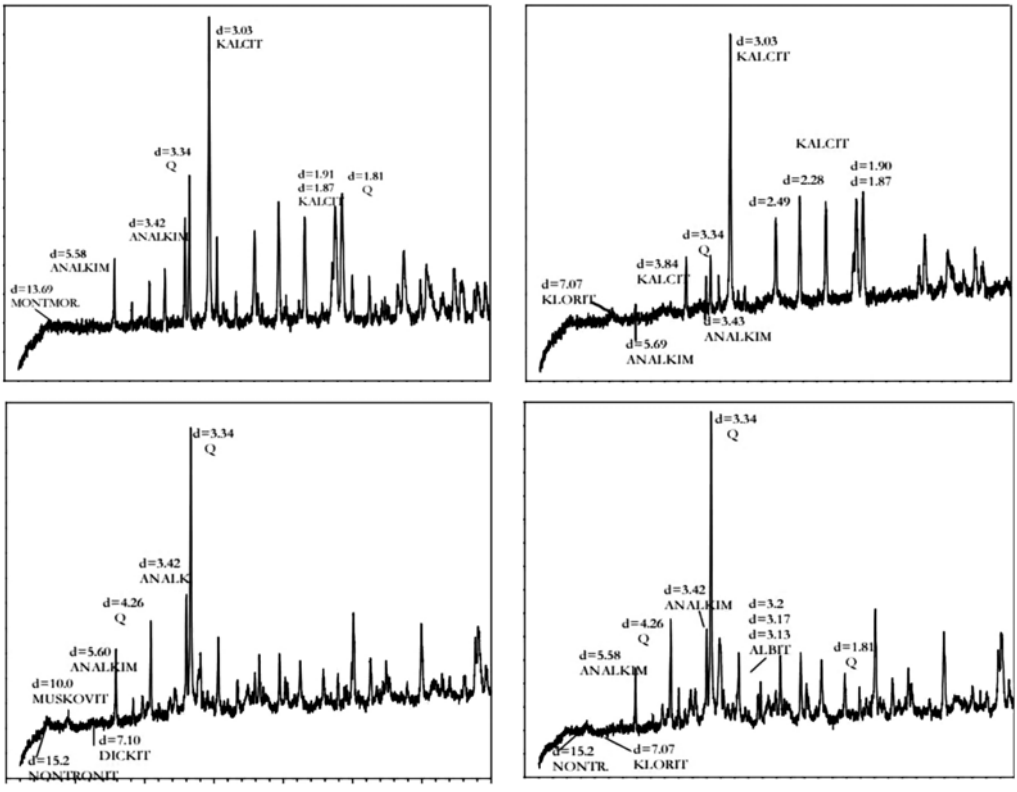

Slika 3. Rentgenogrami vzorcev 2 (levo zgoraj), 3 (desno zgoraj), 4 (levo spodaj) in 6 (desno spodaj) z označenimi reprezentativnimi vrhovi posameznih mineralov
Figure 3. X-ray diffraction results for different tuff samples; No. 2 (left upper corner), No. 3 (right upper corner), No. 4 (left lower corner), No. 6 (right lower corner)

ZAKLJUČKI

Peračiški tufi so del večjega, Smrekovškega kompleksa piroklastičnih kamnin. Njihov sestavni material naj bi izviral iz področja severno od njihove današnje lege in ga datirajo v obdobje oligocena. Ob koncu oligocena ali v miocenu je prišlo do desnozmičnega premika ob Savskem prelomu in posledica tega je današnja lega in razporeditev tufov in spremljajočega piroklastičnega materiala na Slovenskem ozemlju in na območju Hrvaškega Zagorja, kjer so prav tako našli omenjeni piroklastični material. Andeziti in piroklastiti se pojavljajo na veliki prelomni coni Hum na Sotli-Varaždinske toplice (PAMIČ, 1997) in ta cona se smatra za vzhodneje nadaljevanje Smrekovške prelomne cone tj. najvzhodnejši del Periadriatskega prelomnega sistema. Ta piroklastični material je iste starosti, mineralne sestave in se pojavlja z enakimi klastičnimi sedimenti.

Pri optični analizi tufov sem opazila izredno drobnozrnato strukturo omenjene kamine. Velikosti posameznih mineralnih zrn ne presegajo 1mm, pogosto pa dosegajo velikosti samo 100 μm in jih tako uvrščamo med pelitne (drobnozrnate), redko tudi med psamitne (srednjezrnate) tufe. Glede na razmerje posameznih sestavnih komponent sem uvrstila vzorce med steklaste tufe, vzorec številka 4 pa bi sodil med kristalne tufe. Pod mikroskopom izmerjen kot potemnitve plagioklazov znaša približno 25°, kar nakazuje na vsebnost 65 % albitske komponente. To se sklada z dacitno-andezitsko kemijsko sestavo tufov in uvrščanjem le teh kot andezitske različke piroklastičnega materiala. Pod mikroskopom so tudi lepo vidne sekundarne spremembe, predvsem biotitovih zrn. Ta so v veliki meri nadomeščena s sekundarnimi minerali, katerih pa z izjemo klorita nisem prepoznala. S pomočjo rentgenske analize sem ugotovila da je mineral, ki je v glavnem nadomestil biotit, klorit, kot možen mineral, ki bi prav tako lahko nastal pri nadomeščanju biotita pa bi bil lahko tudi nontronit, ki pripada skupini smektitov in vsebuje Fe katione in mineral klorit. Rentgenska analiza je pokazala tudi prisotnost velike količine minerala iz skupine zeolitov-analkima, kar nakazuje na usedanje materiala v vodnem okolju in/ali sekundarne hidrotermalne spremembe vulkanskega stekla. Prisotnost glinenih mineralov v vzorcih nakazuje sekundarne spremembe prvotne mineralne sestave kot vpliv delovanja hidrotermalnih procesov in preperevanja.

Rezultati mineraloške sestave serije Peračiških tufov se skladajo z mineraloško sestavo kamnin Smrekovške serije. Za kamnine Smrekovške serije je značilna prisotnost mineralov kremena, albita, klorita ter zeolitov in njihova analiza je potrdila intruzijo vulkanskega materiala v z vodo nasičene morske sedimente ter delovanje hidrotermalnih raztopin (KRALJ, 1997). Podobna sestava ter struktura kamnin serije Peračiških tufov potrjuje njihov soroden izvor.

SUMMARY

Petrological and mineralogical characteristics of Peračica tuff

Peračica tuff rocks were investigated by methods of microscopic analysis and X-

ray diffraction to determine their petrological and mineralogical characteristics and to determine the differences between individual tuff types that can be found in the investigated area.

Macroscopically three variations of Peračica tuff were recognized. The most abundant is the light green fine graded tuff type that was and is widely used also as building and decoration stone. Variation of this type is a light green tuff type with fine graded matrix and darker green mineral grains in size of a few millimetres to a centimetre, while the third tuff type displays fine graded matrix and it brownish in colour. Microscopical analyses confirm that tuffs are composed of fine graded matrix. The mineral grains recognized in thin section belong to quartz and plagioclase, which are two minerals most abundant in samples. Measured extinction angles of plagioclases give values of around 25°, which corresponds to medium composition the plagioclases in the albite-anortite series and is therefore in agreement with andesitic composition of tuff rocks. Other mineral grains recognizable in thin section include small grains of muscovite, sericite and biotite, but the later shows intensive degradation and replacement by chlorite. Intensive processes of carbonatization of both matrix as well as mineral grains was already observed in thin section and reconfirmed by method of X-ray diffraction. This method also shown the presence of mineral analcime, which speaks of sedimentation processes of volcanic material in aquatic environment (Iijima, 1978) or influence from hydrothermal fluid activity (Iijima, 1984; Utada, 1987).

Results of petrological and mineralogical characteristics of Peračica tuff series are similar to the ones obtained from investigations of Smrekovec rock series (Kralj, 1997), while entire geographical extension of similar volcanoclastic rocks of Oligocene age are scattered over a larger area and covering also parts of N - NE Croatia (Pamič, 1997). Their position is an indirect indicator for dextral strike slip activity of faults belonging to the southern part of Periadriatic fault system and is post Oligocene in age.

Zahvala

Zahvala gre dr. Meti Dobnikar za recenzijo, ki je močno izboljšala kvaliteto članka.

Viri

Buser, S. (1977): *Tolmač k osnovni geološki karti SFRJ, list Celje*. Zvezni geološki zavod Beograd, 72 str.

Dolar-Mantuani, L. (1937): Peračiški tuf. *Vesnik geološkog inštituta Kraljevine Jugoslavije*.; Vol. 5, Beograd.

Duhovnik, J. (1964): *Andezitski tufi v Peračici na Gorenjskem*. Arhiv inštituta za geologijo Univerze v Ljubljani.

Hinterlechtner-Ravnik, A. in Pleničar, M. (1967): Smrekovški andezit in njegov tuf. *Geologija*.; Vol. 10, str. 219-237, Geološki zavod Ljubljana, Ljubljana.

IIJIMA, A. (1978): Geological occurrencesof zeolites in marine enviroments. In: L.B. Sand and F.A. Mupton (eds): *Natural zeolites.* Pergamon, pp. 245-258, Oxford.

IIJIMA, A. (1984): A petrochemical ascpect of the zeolite formation in volcanoclastic rocks. In: *Proceedings of the 27th International Geological Congress*.; Vol. 4, pp. 29-52, VNU Science Press, Utrecht.

KRALJ, P. (1997): Zeoliti v vulkanoklastičnih kamninah smrekovškega podgorja. *Geologija*.; Vol. 40, str. 268-281, Geološki zavod Ljubljana, Ljubljana.

LIPOLD, M.V. (1857): Bericht Über Die Geologischen Aufnahmen. In: Ober-Krain Im Jahre 1856. *Jb. Geol. R. A*.; Vol. 8, Wien.

MACKENZIE, W.S. and ADAMS, A.E. (2005): *A Colour Atlas of Rocks and Minerals in Thin Section – 8th impression*. Manson Publishing, London, 192 pp.

MIOĆ, P. in ŽNIDARČIČ, M. (1987): *Tolmač k osnovni geološki karti SFRJ, list Slovenj Gradec*. Zvezni geološki zavod Beograd, 74 str.

MORLOT, A. (1850): Über die geologischen Verhältnisse von Oberkrain. *Jb. Geol. R-A*.; pp. 389-411, Wien.

PAMIĆ, J. (1997): Vulkanske stijene savsko-dravskog Međuriječja 1. *Časopis "Nafta"*.; Zagreb.

PETERS, K. (1856): Bericht Über Die Geologischen Aufnahmen. In: Kärnten, Krain Und Dem Görzer Gebite Im Jahre 1885. *Jb. Geol. R. A*.; Vol. 7, Wien.

PLACER, L. (1996): O premiku ob Savskem prelomu. *Geologija*.; Vol. 39, str. 283-287, Geološki zavod Ljubljana, Ljubljana.

PREMRU, U. (1983): *Tolmač k osnovni geološki karti SFRJ, list Ljubljana*. Zvezni geološki zavod Beograd, 70 str.

UTADA, M. (1987): Zeolitization in the continental margin, with special reference to those in the Green tuff region in Japan. *Yerbilimleri*.; Vol. 14, pp. 35-43, Tsakuba.

The use of the logistic function for forecasting vertical movements of surface

Uporaba logistične funkcije pri napovedovanju vertikalnih premikov površine

Milivoj Vulić[1], Jernej Korelc[2]

[1]University of Ljubljana, Faculty of Natural Sciences and Engineering, Aškerčeva cesta 12, SI-1000 Ljubljana, Slovenia; E-mail: milivoj.vulic@ntf.uni-lj.si
[2]Municipality Velenje, Titov trg 1, SI-3320 Velenje, Slovenia; E-mail: jernej.korelc@velenje.si

Received: December 14, 2007 **Accepted:** August 6, 2008

Abstract: We are familiar with a lot of different methods, which are used for forecasting vertical movements of a surface. These movements are caused by mining or building of an underground object. In this article we will in detail write about the logistic function and with its help we will describe time dependent vertical movements.

Izvleček: Poznamo veliko različnih metod, ki se uporabljajo za napovedovanje vertikalnih premikov površine, ki nastanejo zaradi rudarjenja ali izgradnje podzemnega objekta. V tem članku bomo podrobneje pisali o logistični funkciji in z njo opisali vertikalne premike v odvisnosti od časa.

Key words: logistic function, vertical movements, prognostic methods
Ključne besede: logistična funkcija, vertikalni pomiki, prognozne metode

Introduction

Experts are engaged in dynamics of subsidence of field and buildings which are results of mining from the very early stages of mining. Therefore in single areas different prognostic methods were developed to forecast movements of the field above the underground object.

In continuation it will be presented how we can forecast developing of vertical movements above the underground object with help of a logistic function. Basics of the logistic function will be described in the beginning (its structure and form). With help of this function we will then describe time dependent vertical movements. In the example, that will be presented, we will compare data achieved in the field above an underground object and calculated values achieved with help of the logistic function. In conclusion

we analyse, if this method of forecasting vertical movements offers us good and useful results so we can continue using it in future.

DESCRIPTION OF THE LOGISTIC FUNCTION

Structure of the logistic function

The logistic function consists of two parts: exponential and boundary exponential function. In the exponential function the growing is exponential which means that the growth rate is actually proportional to the size of the function value. In the second part of the logistic function the graph is approaching some fixed capacity, stated in advance. We achieve this by subtracting the exponential function from the fixed capacity. The function that we get in this way combines the first part of exponential growth, when the outputs are small, with the second part of exponential growth, when the outputs are approaching a certain limit.

Algebraic presentation

$$f(x) = \frac{a}{1 + b \cdot c^{-x}}$$

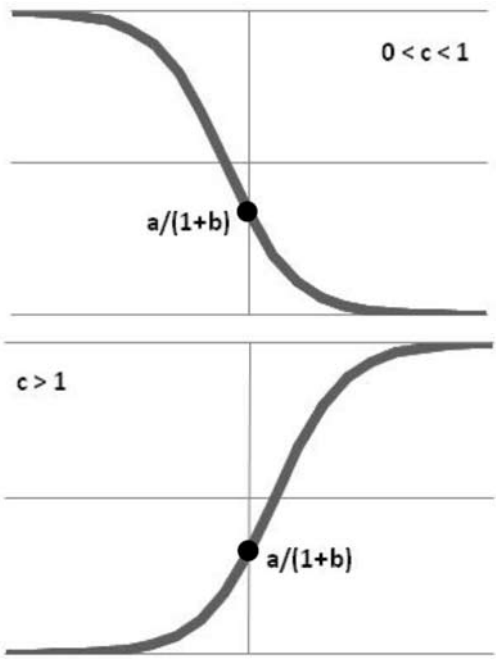

Figure 1. Influence of parameter ***c*** on logistic function
Slika 1. Vpliv parametra ***c*** na logistično funkcijo

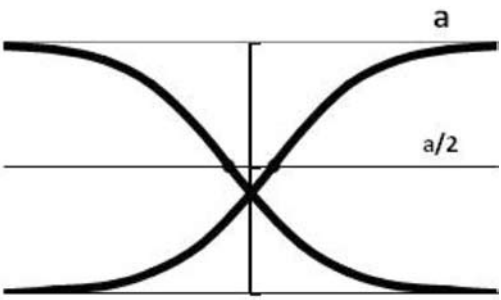

Figure 2. Inflection point
Slika 2. Prevojna točka

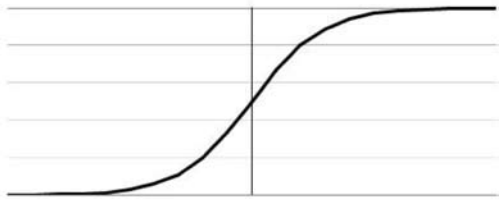

Figure 3. Shape of the logistic function
Slika 3. Oblika logistične funkcije

The algebra of the logistic function combines characteristics of exponential and power functions. This means that we are in the field where descriptions of complex problems are composed from more different functions.

To win a graph with the characteristic S-shape, we have to use three parameters of the logistic family which are connected to one another.

The parameters ***b*** and ***c*** are the base of the component of the exponential function $b \cdot c^{-x}$ and they define the point where the graph intercepts the y-axis. Base ***c*** is limited with positive values, so as long as $c > 1$, c^x grows and c^{-x} decays. Similarly if $0 < c < 1$, c^x decays and c^{-x} grows.

With other words this means: if c^{-x} grows ($0 < c < 1$), so does the denominator and a function as a whole is driven towards 0. If c^{-x} decays ($c > 1$), the denominator approaches 1 and the function as a whole converges towards the value of the numerator (parameter ***a***).

The rate at which a logistic function falls from or rises to its limiting value is completely determined by the exponential function in the denominator. More exactly, by the parameters ***b*** and ***c***.

The curve changes at its half from being convex to concave or the other way round, depending of the growing or decaying of the function.

The gradient change always appears on halfway of the logistic function. This point of critical change in the function's behaviour is called the inflection or gradation point.

By using this we can calculate the exact location of the point of inflection:

$$\frac{a}{1 + bc^{-x}} = \frac{a}{2}$$

$$1 + bc^{-x} = 2$$

$$bc^{-x} = 1$$

$$c^{-x} = b^{-1}$$

$$c^{x} = b$$

$$c^{x} = \log_c b$$

Graphic presentation

Logistic graphs follow a characteristic S-shape which is often called S-function or sigmoid function.

The S shape may either rise from the x-axis to the limiting value, or drop from the limiting value to the x-axis. The limiting value may change. The rate at which the curve travels between the two horizontal asymptotes may vary, but this basic sigmoid shape is found in all logistic graphs.

Logistic law and description of time depending vertical movements

$$u'_3(t) = au_3(t) - bu_3{}^2(t_0) \dots\dots\dots u_3(t=0) = u_{3,0} \tag{1}$$

u_3 ..... vertical movement
$au_3(t)$…….....growing part
$bu_3{}^2(t_0)$..... suffocating part, which prevents unlimited growth

Parameters ***a*** and ***b*** are constants which have an exactly fixed dimension:

$$a \rightarrow [T^{-1}]$$
$$b \rightarrow [M^{-1}T^{-1}] \tag{2}$$

After integration of the equation (1) we get the logistic function (ČIBEJ, 1988):

$$u_3(t) = \frac{au_{3,0}}{bu_{3,0} + (a - bu_{3,0}) \cdot \exp(-a(t - t_0))} \tag{3}$$

Equation (3) is not practical for forecasting vertical movements because it contains too many reciprocally independent parameters. Therefore it would be right to assign the vertical movement in early stages $\boldsymbol{u_0}$ some minimal starting value, which would be considered in all observing points. As in case $u_{3,0} = 0$ also $u_3(t) = 0$ we will arrange to $\boldsymbol{u_{3,0}}$ a very small value, which will be different as zero.

So we adopt: $u_{3,0} = 0{,}2$ mm

Because of a shorter record we introduce factor $\boldsymbol{\lambda}$ with the following record:

$$\lambda = \frac{u_{3,max}}{u_{3,0}} = \frac{u_{3,max}}{0{,}2} \frac{[M]}{[M]} \tag{4}$$

We also define the maximum subsidence:

$$u_{3,max} = \lim_{t\to\infty} \frac{a u_{3,0}}{b u_{3,0} + (a - b u_{3,0}) \cdot \exp(-a(t - t_0))} = \frac{a u_{3,0}}{b u_{3,0}} = \frac{a}{b} \tag{5}$$

For the parameter ***b*** we introduce the following substitution:

$$u_{3,max} = \frac{a}{b} \tag{6}$$

$$b = \frac{a}{u_{3,max}} \tag{7}$$

Previous results of vertical movements on the surface, that we analyzed, have showed that one half of vertical movements is being developed in time t_c. Because the developing of vertical movements is the fastest in time t_c. After that time it begins slowing down. This characteristic of the process of subsidence we use to determinate the parameter ***a***.

From the mentioned it follows:

$$\begin{aligned} t &= t_c \\ u_3(t_c) &= \frac{1}{2} u_{3,max} \end{aligned} \tag{8}$$

For the inflection point the logistic functions gets by taking into account equation (8), introduction of substitution (7) and introduction of the factor λ "λ" the following shape:

$$\frac{1}{2} u_{3,max} = \frac{a \frac{u_{3,max}}{\lambda}}{\frac{a}{u_{3,max}} \cdot \frac{u_{3,max}}{\lambda} + \left(a - \frac{a}{u_{3,max}} \cdot \frac{u_{3,max}}{\lambda}\right) \cdot \exp(-a(t_c - t_0))} \tag{9}$$

$$\frac{1}{2} = \frac{\frac{1}{\lambda}}{\frac{1}{\lambda} + \left(1 - \frac{1}{\lambda}\right) \cdot \exp(-a(t_c - t_0))} \tag{10}$$

From equation (10) we can express value ***a*** in dependence to ***λ***according to the following procedure:

$$\frac{1}{\lambda}+\left(1-\frac{1}{\lambda}\right)\cdot\exp\left(-a(t_c-t_0)\right)=2\cdot\frac{1}{\lambda}$$

$$\left(1-\frac{1}{\lambda}\right)\cdot\exp\left(-a(t_c-t_0)\right)=\frac{1}{\lambda}$$

$$\exp\left(-a(t_c-t_0)\right)=\left(\frac{1}{\lambda-1}\right) \qquad (11)$$

$$a=-\frac{ln\left(\frac{1}{\lambda-1}\right)}{(t_c-t_0)}$$

After performing it we have all parameters of a S-shaped time diagram.

Example of using the logistic function

An example of comparison of observations with the logistic S function will be presented upon the example of point C20, where it means:

$u_{3,0}$..... adopted starting value of movement
$u_{3,max}$..... maximum measured subsidence of a particular point
t_0 ..... day, when the first measurement was made
t ..... time of running measurement
t_c ..... day when subsidence comes to half of its value
λ..... factor introduced for shorter recording
a..... constant
b..... constant

$u_{3,0}$ = 0,2 mm

$$u_{3,max} = -38\ mm \rightarrow \frac{u_{3,max}}{2} = -19\ mm$$

$$u_{3,max} = -38\ mm \rightarrow \frac{u_{3,max}}{2} = -19\ mm$$

$t_c = 160\ dan^{-1}$ $t_c = 160\ dan^{-1}$ …. day of the inflection point – we read this from the measuring table

$$\lambda=\frac{|u_{3,max}|}{u_{3,0}}=\frac{|-38|}{0{,}2}=190$$

$$a = -\frac{ln\left(\frac{1}{\lambda - 1}\right)}{(t_c - t_0)} = -\frac{ln\left(\frac{1}{190 - 1}\right)}{(160 - 0)} = 0{,}0327609$$

$$b = \frac{a}{|u_{3,max}|} = \frac{0{,}0327609}{|-38|} = 0{,}0008621$$

$$u_3(t) = \frac{au_{3,0}}{bu_{3,0} + (a - bu_{3,0}) \cdot \exp\left(-a(t - t_0)\right)}$$
$$= \frac{0{,}0327609 \cdot 0{,}2}{0{,}0008621 \cdot 0{,}2 + (0{,}0327609 - 0{,}0008621 \cdot 0{,}2) \cdot \exp\left(-0{,}0327609 \cdot (t - t_0)\right)}$$

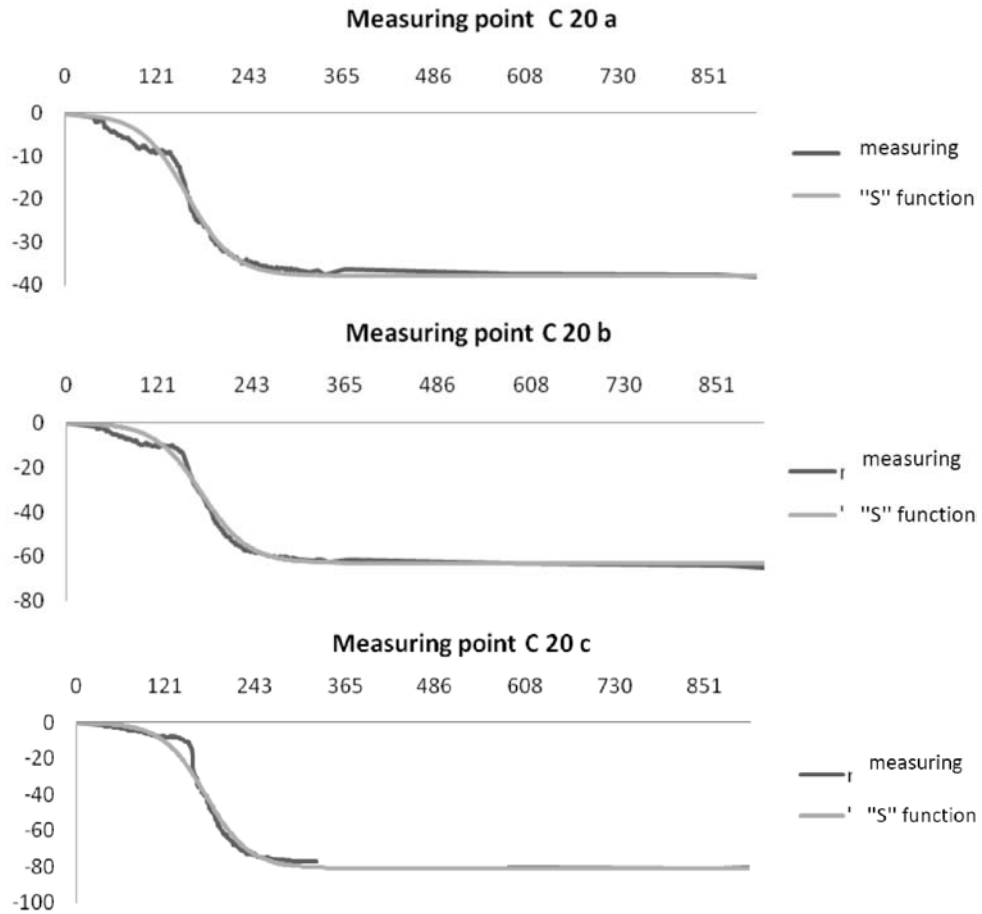

Figure 4. Comparing measured and calculated graph
Slika 4. Primerjava meritvenega in izračunanega grafa

CONCLUSIONS

As we see, the graphs of a single point are rather well agreeing with one another. From this fact we can presume, that this method can be used for forecasting of vertical movements above an underground object. But we mustn't forget that we get such results only by anticipating maximum subsidence and that could be a problem in some cases. We can therefore conclude that this method is based upon a theoretical part as well as inevitably upon an empirical part.

POVZETEK

Uporaba logistične funkcije pri napovedovanju vertikalnih premikov površine

Za primer in analizo uporabnosti logistične funkcije pri napovedovanju vertikalnih premikov, je bilo narejenih preko 20.000 meritev na več kot sto različnih točkah. Rezultati, ki smo jih dobili z logistično funkcijo (S – funkcija), se z dejanskimi meritvami zelo dobro ujemajo. Pri večini točk se empirična in teoretična krivulja skoraj popolnoma ujemata, kot je vidno tudi pri zgoraj navedenem primeru (slika 4). Največkrat pride do odstopanja v zaključnem delu grafa, ko se funkcija že umirja. Graf S - funkcije doseže mejno vrednost pred dejanskimi meritvami.

Slaba stran takšnega napovedovanja je, da moramo empirično ugotoviti maksimalni ugrezek. Če to vrednost poznamo, se rezultati zelo dobro ujemajo. Torej metoda temelji na teoretičnem in neizogibno tudi na empiričnem delu.

Vendar, tudi če naredimo veliko število meritev in lahko iz krivulje razberemo, da so vertikalni premiki površine minimalni, ne moremo z zagotovostjo trditi, da se ti premiki na meritvenem območju umirjajo. Zaradi tega so potrebne nadaljnje meritve in analize rezultatov.

REFERENCES

ČIBEJ, J.A.(1988): Diferencialne enačbe in matematično modeliranje. *Obzornik matematike in Fizike.; Vol.* 35, No. 5, pp. 129-136.

KORELC, J. (2008): *Prispevek k napovedovanju dinamike ugrezanja zaradi rudarjenja: diplomsko delo*. Naravoslovnotehniška fakulteta, Ljubljana.

MUELLER, W. (2004): *The MathWorks, Inc. Natick, MA.* Available on World Wide Web: http://www.wmueller.com/precalculus/families/l_80.html

PODOJSTRŠEK, R. (2007): *Prognoziranje dinamičnega ugrezanja točk na vplivni površini nad rudarskimi deli: diplomsko delo*. Naravoslovnotehniška fakulteta, Ljubljana.

ZAPUŠEK, P. (2003): *Vertikalni premiki površine na vplivnem območju izgradnje predorov: diplomsko delo*. Naravoslovnotehniška fakulteta, Ljubljana.

Author`s Index, Vol. 55, No. 3

INSTRUCTIONS TO AUTHORS

RMZ-MATERIALS & GEOENVIRONMENT (RMZ- Materiali in geookolje) is a periodical publication with four issues per year (established 1952 and renamed to RMZ-M&G in 1998). The main topics of contents are Mining and Geotechnology, Metallurgy and Materials, Geology and Geoenvironment.
RMZ-M&G publishes original Scientific articles, Review papers, Technical and Expert contributions (also as short papers or letters) **in English**. In addition, evaluations of other publications (books, monographs,...), short letters and comments are welcome. A short summary of the contents in Slovene will be included at the end of each paper. It can be included by the author(s) or will be provided by the referee or the Editorial Office.
**** Additional information and remarks for Slovenian authors:***
English version with extended »Povzetek«, and additional roles (in Template for Slovenian authors) ***can*** *be written. Only exceptionally the articles in the Slovenian language with summary in English will be published. The contributions in English will be considered with priority over those in the Slovenian language in the review process.*

Authorship and originality of the contributions. Authors are responsible for originality of presented data, ideas and conclusions as well as for correct citation of data adopted from other sources. The publication in RMZ-M&G obligate authors that the article will not be published anywhere else in the same form.

Specification of Contributions

Optimal number of pages of full papers is 7 to 15, longer articles should be discussed with Editor, but 20 pages is limit.
Scientific papers represent unpublished results of original research.
Review papers summarize previously published scientific, research and/or expertise articles on the new scientific level and can contain also other cited sources, which are not mainly result of author(s).
Technical and Expert papers are the result of technological research achievements, application research results and information about achievements in practice and industry.
Short papers (Letters) are the contributions that contain mostly very new short reports of advanced investigation. They should be approximately 2 pages long but should not exceed 4 pages.
Evaluations or critics contain author's opinion on new published books, monographs, textbooks, exhibitions...(up to 2 pages, figure of cover page is expected).
In memoriam (up to 2 pages, a photo is expected).

Professional remarks (Comments) cannot exceed 1 page, and only professional disagreements can be discussed. Normally the source author(s) reply the remarks in the same issue.

Supervision and review of manuscripts. All manuscripts will be supervised. The referees evaluate manuscripts and can ask authors to change particular segments, and propose to the Editor the acceptability of submitted articles. Authors can suggest the referee but Editor has a right to choose another. **The name of the referee remains anonymous.** The technical corrections will be done too and authors can be asked to correct missing items. The final decision whether the manuscript will be published is made by the Editor in Chief.

The Form of the Manuscript

The manuscript should be submitted as a complete hard copy including figures and tables. The figures should also be enclosed separately, both charts and photos in the original version. In addition, all material should also be provided in electronic form on a diskette or a CD. The necessary information can conveniently also be delivered by E-mail.

Composition of manuscript is defined in the attached Template

The original file of Template is temporarily available on E-mail addresses:
peter.fajfar@ntf.uni-lj.si,
barbara.bohar@ntf.uni-lj.si

References - can be arranged in two ways:
- first possibility: alphabetic arrangement of first authors - in text: (Borgne, 1955),
or
- second possibility: [1] numerated in the same order as cited in the text: example[1]

Format of papers in journals:

Le Borgne, E. (1955): Susceptibilite magnetic anomale du sol superficiel. *Annales de Geophysique*, 11, pp. 399-419.

Format of books:

Roberts, J. L. (1989): Geological structures, *MacMillan*, *London*, 250 p.

Text on the hard print copy can be prepared with any text-processor. The electronic version on the diskette, CD or E-mail transfer should be in MS Word or ASCII format. **Captions of figures and tables** should be enclosed separately. **Figures (graphs and photos)** and tables should be original and sent separately in addition to text. They can

be prepared on paper or computer designed (MSExcel, Corel, Acad).
Format. Electronic figures are recommended to be in CDR, Al, EPS, TIF or JPG formats. Resolution of bitmap graphics (TIF, JPG) should be at least 300 dpi. Text in vector graphics (CDR, Al, EPS) must be in MSWord Times typography or converted in curves.
Color prints. Authors will be charged for color prints of figures and photos.
Labeling of the additionally provided material for the manuscript should be very clear and must contain at least the lead author's name, address, the beginning of the title and the date of delivery of the manuscript. In case of an E-mail transfer the exact message with above asked data must accompany the attachment with the file containing the manuscript.
Information about RMZ-M&G:
Editor in Chief prof. dr. Peter Fajfar (tel. ++386 1 4250-316) or
Secretary Barbara Bohar Bobnar, un. dipl. ing. geol. (++386 1 4704-630),
Aškerčeva 12, Ljubljana, Slovenia

or at E-mail addresses:
peter.fajfar@ntf.uni-lj.si,
barbara.bohar@ntf.uni-lj.si

Sending of manuscripts. Manuscripts can be sent by mail to the **Editorial Office** address:

- RMZ-Materials & Geoenvironment
  Aškerčeva 12,
  1000 Ljubljana, Slovenia

or delivered to:

- **Reception** of the Faculty of Natural Science and Engineering (for RMZ-M&G)
  Aškerčeva 12,
  1000 Ljubljana, Slovenia
- E-mail - addresses of Editor and Secretary
- You can also contact them on their phone numbers.

TEMPLATE

The title of the manuscript should be written in bold letters (Times New Roman, 14, Center)

NAME SURNAME[1], …. , & NAME SURNAME[X]
(TIMES NEW ROMAN, 12, CENTER)

[x]Faculty of ... , University of ... , Address…, Country, e-mail: ...
(Times New Roman, 11, Center)

THE LENGTH OF FULL PAPER SHOULD NOT EXCEED TWENTY (20, INCLUDING FIGURES AND TABLES) PAGES (OPTIMAL 7 TO 15), SHORT PAPER FOUR (4) AND OTHER TWO (2) WITHOUT TEXT FLOWING BY GRAPHICS AND TABLES.

Abstract (Times New Roman, Normal, 11): The text of the abstract is placed here. The abstract should be concise and should present the aim of the work, essential results and conclusion. It should be typed in font size 11, single-spaced. Except for the first line, the text should be indented from the left margin by 10 mm. The length should not exceed fifteen (15) lines (10 are recommended).

Key words: a list of up to 5 key words (3 to 5) that will be useful for indexing or searching. Use the same styling as for abstract.

INTRODUCTION (TIMES NEW ROMAN, BOLD, 12)

Two lines below the keywords begin the introduction. Use Times New Roman, font size 12, Justify alignment.
There are two (2) admissible methods of citing references in text:

1. by stating the first author and the year of publication of the reference in the parenthesis at the appropriate place in the text and arranging the reference list in the alphabetic order of first authors; e.g.:
   "Detailed information about geohistorical development of this zone can be found in: Antonijević (1957), Grubić (1962), ..."
   "… the method was described previously (Hoefs, 1996)"

2. by consecutive Arabic numerals in square brackets, superscripted at the appropriate place in the text and arranging the reference list at the end of the text in the like manner; e.g.:
   "... while the portal was made in Zope[3] environment."

Materials and methods (Times New Roman, Bold, 12)

This section describes the available data and procedure of work and therefore provides enough information to allow the interpretation of the results, obtained by the used methods.

Results and discussion (Times New Roman, Bold, 12)

Tables, figures, pictures, and schemes should be incorporated in the text at the appropriate place and should fit on one page. Break larger schemes and tables into smaller parts to prevent extending over more than one page.

Conclusions (Times New Roman, Bold, 12)

This paragraph summarizes the results and draws conclusions.

Acknowledgements (Times New Roman, Bold, 12, Center - optional)

This work was supported by the ****.

References (Times New Roman, Bold, 12*)*

In regard to the method used in the text, the styling, punctuation and capitalization should conform to the following:

FIRST OPTION - in alphabetical order

Casati, P., Jadoul, F., Nicora, A., Marinelli, M., Fantini-Sestini, N. & Fois, E. (1981): Geologia della Valle del'Anisici e dei gruppi M. Popera - Tre

Cime di Lavaredo (Dolomiti Orientali). *Riv. Ital. Paleont.*; Vol. 87, No. 3, pp. 391-400, Milano.

Folk, R. L. (1959): Practical petrographic classification of limestones. *Amer. Ass. Petrol. Geol. Bull.;* Vol. 43, No. 1, pp. 1-38, Tulsa.

SECOND OPTION - in numerical order

[1] Trček, B. (2001): *Solute transport monitoring in the unsaturated zone of the karst aquifer by natural tracers.* Ph.D. Thesis. Ljubljana: University of Ljubljana 2001; 125 p.

[2] Higashitani, K., Iseri, H., Okuhara, K., Hatade, S. (1995): Magnetic Effects on Zeta Potential and Diffusivity of Nonmagnetic Particles. *Journal of Colloid and Interface Science 172*, pp. 383-388.

Citing the Internet site:

CASREACT-Chemical reactions database [online]. Chemical Abstracts Service, 2000, updated 2.2.2000 [cited 3.2.2000]. Accessible on Internet: http://www.cas.org/CASFILES/casreact.html.

Povzetek (Times New Roman, 12)

A short summary of the contents in Slovene (up to 400 characters) can be written by the author(s) or will be provided by the referee or by the Editorial Board.

TEMPLATE for Slovenian Authors

The title of the manuscript should be written in bold letters (Times New Roman, 14, Center)

Naslov članka (Times New Roman, 14, Center)

Name Surname[1],…. , & Name Surname[X] (Times New Roman, 12, Center)
Ime Priimek[1], …, Ime Priimek[X] (Times New Roman, 12, Center)

[X]Faculty of ... , University of ... , Address…, Country; e-mail: ...
(Times New Roman, 11, Center)
[X]Fakulteta…, Univerza…, Naslov…, Država; e-mail: …
(Times New Roman, 11, Center)

THE LENGTH OF ORIGINAL SCIENTIFIC PAPER SHOULD NOT EXCEED TWENTY (20, INCLUDING FIGURES AND TABLES) PAGES (OPTIMAL 7 TO 15), SHORT PAPER FOUR (4) AND OTHER TWO (2) WITHOUT TEXT FLOWING BY GRAPHICS AND TABLES.
DOLŽINA IZVIRNEGA ZNANSTVENEGA ČLANKA NE SME PRESEGATI DVAJSET (20, VKLJUČNO S SLIKAMI IN TABELAMI), KRATKEGA ČLANKA ŠTIRI (4) IN OSTALIH PRISPEVKOV DVE (2) STRANI.

Abstract (Times New Roman, Normal, 11): The text of the abstract is placed here. The abstract should be concise and should present the aim of the work, essential results and conclusion. It should be typed in font size 11, single-spaced. Except for the first line, the text should be indented from the left margin by 10 mm. The length should not exceed fifteen (15) lines (10 are recommended).

Izvleček (TNR, N, 11): Kratek izvleček namena članka ter ključnih rezultatov in ugotovitev. Razen prve vrstice naj bo tekst zamaknjen z levega roba za 10 mm. Dolžina naj ne presega petnajst (15) vrstic (10 je priporočeno).

Key words: a list of up to 5 key words (3 to 5) that will be useful for indexing or searching. Use the same styling as for abstract.

Ključne besede: seznam največ 5 ključnih besed (3-5) za pomoč pri indeksiranju ali iskanju. Uporabite enako obliko kot za izvleček.

Introduction – Uvod (Times New Roman, Bold, 12)

Two lines below the keywords begin the introduction. Use Times New Roman, font size 12, Justify alignment. All captions of text and tables as well as the text in graphics must be prepared in English and Slovenian language.
Dve vrstici pod ključnimi besedami se začne Uvod. Uporabite pisavo TNR, velikost črk 12, z obojestransko poravnavo. Naslovi slik in tabel (vključno z besedilom v slikah) morajo biti pripravljeni v slovenskem in angleškem jeziku.

Figure (Table) X. Text belonging to figure (table)
Slika (Tabela) X. Pripadajoče besedilo k sliki (tabeli)

There are two (2) admissible methods of citing references – obstajata dve sprejemljivi metodi navajanja referenc:

1. by stating the first author and the year of publication of the reference in the parenthesis at the appropriate place in the text and arranging the reference list in the alphabetic order of first authors; e.g.:
1. z navedbo prvega avtorja in letnice objave reference v oklepaju na ustreznem mestu v tekstu in z ureditvijo seznama referenc po abecednem zaporedju prvih avtorjev; npr.:
   "Detailed information about geohistorical development of this zone can be found in: Antonijević (1957), Grubić (1962), ..."
   "… the method was described previously (Hoefs, 1996)"

or/ali

2. by consecutive Arabic numerals in square brackets, superscripted at the appropriate place in the text and arranging the reference list at the end of the text in the like manner; e.g.:
2. z zaporednimi arabskimi številkami v oglatih oklepajih na ustreznem mestu v tekstu in z ureditvijo seznama referenc v številčnem zaporedju navajanja; npr.;
   "... while the portal was made in Zope[3] environment."

Materials and methods (Times New Roman, Bold, 12)

This section describes the available data and procedure of work and therefore provides enough information to allow the interpretation of the results, obtained by the used methods.
Ta del opisuje razpoložljive podatke, metode in način dela ter omogoča zadostno količino informacij, da lahko z opisanimi metodami delo ponovimo.

Results and discussion – Rezultati in razprava (Times New Roman, Bold, 12)

Tables, figures, pictures, and schemes should be incorporated (inserted, not pasted) in the text at the appropriate place and should fit on one page. Break larger schemes and tables into smaller parts to prevent extending over more than one page.
Tabele, sheme in slike je potrebno vnesti (z ukazom Insert, ne Paste) v tekst na ustreznem mestu. Večje sheme in tabele je potrebno ločiti na manjše dele, da ne presegajo ene strani.

Conclusions – Sklepi (Times New Roman, Bold, 12)

This paragraph summarizes the results and draws conclusions.
Povzetek rezultatov in zaključki.

Acknowledgements – Zahvale (Times New Roman, Bold, 12, Center - optional)

This work was supported by the ……..
Izvedbo tega dela je omogočilo ……

References - Viri (Times New Roman, Bold, 12)

With regard to the method used in the text, the styling, punctuation and capitalization should conform to the following:
Glede na uporabljeno metodo citiranja referenc v tekstu upoštevajte eno od naslednjih oblik:

FIRST OPTION (recommended) – PRVA MOŽNOST (priporočena) – in alphabetical order (v abecednem zaporedju)

Casati, P., Jadoul, F., Nicora, A., Marinelli, M., Fantini-Sestini, N. & Fois, E. (1981): Geologia della Valle del'Anisici e dei gruppi M. Popera – Tre Cime di Lavaredo (Dolomiti Orientali). *Riv. Ital. Paleont.*; Vol. 87, No. 3, pp. 391-400, Milano.

Folk, R. L. (1959): Practical petrographic classification of limestones. *Amer. Ass. Petrol. Geol. Bull.;* Vol. 43, No. 1, pp. 1-38, Tulsa.

SECOND OPTION – DRUGA MOŽNOST - in numerical order (v numeričnem zaporedju)

[1] Trček, B. (2001): *Solute transport monitoring in the unsaturated zone of the karst aquifer by natural tracers.* Ph.D. Thesis. Ljubljana: University of Ljubljana 2001; 125 p.

[2] Higashitani, K., Iseri, H., Okuhara, K., Hatade, S. (1995): Magnetic Effects on Zeta Potential and Diffusivity of Nonmagnetic Particles. *Journal of Colloid and Interface Science 172*, pp. 383-388.

Citing the Internet site:
CASREACT-Chemical reactions database [online]. Chemical Abstracts Service, 2000, updated 2.2.2000 [cited 3.2.2000]. Accessible on Internet: http://www.cas.org/CASFILES/casreact.html.

Citiranje Internetne strani:
CASREACT-Chemical reactions database [online]. Chemical Abstracts Service, 2000, obnovljeno 2.2.2000 [citirano 3.2.2000]. Dostopno na svetovnem spletu: http://www.cas.org/CASFILES/casreact.html.

Povzetek – Summary (Times New Roman, 12)

An extended summary of the contents in Slovene (from one page to approximately 1/3 of the original article length).
Razširjeni povzetek vsebine prispevka v Angleščini (od ene strani do približno 1/3 dolžine izvirnega članka).

Rešitve za opazovanje premikov in deformacij

GNSS senzor
Leica GMX902 GG

GPS senzor
Leica GMX901
in 360° reflektor
Leica GZR122

Nagibni senzor
Leica NIVEL200

Samodejni tahimeter
Leica TCA1201 M

Programska oprema
Leica GNSS Spider

Programska oprema
Leica GeoMoS

geo servis

Authorized Leica Geosystems Distributor

- when it has to be **right**

Leica Geosystems

Geoservis, d.o.o.
Litijska cesta 45, 1000 Ljubljana
t. (01) 586 38 30, i. www.geoservis.si


RTH

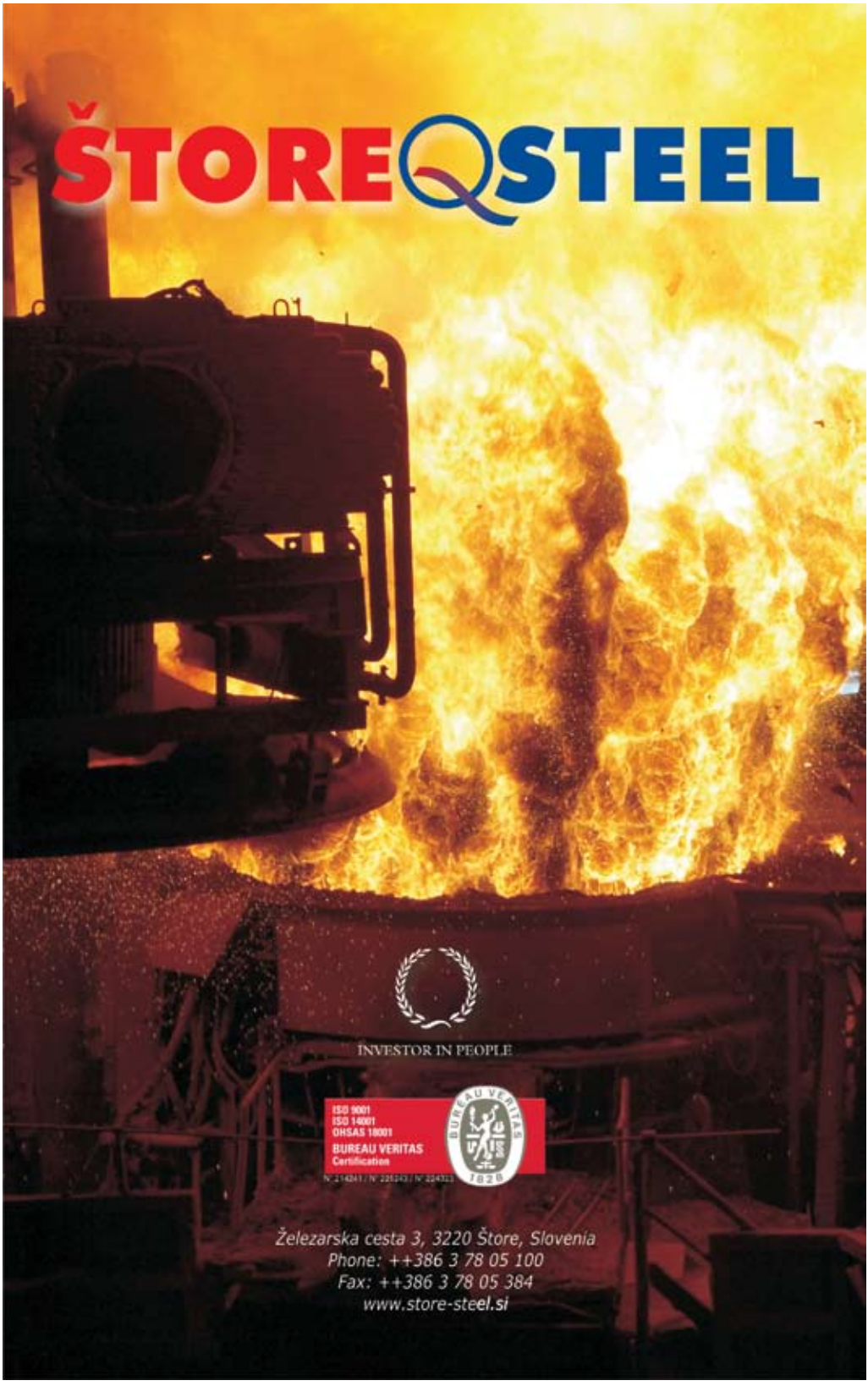
ŠTORE STEEL
INVESTOR IN PEOPLE
ISO 9001
ISO 14001
OHSAS 18001
BUREAU VERITAS
Certification
Železarska cesta 3, 3220 Štore, Slovenia
Phone: ++386 3 78 05 100
Fax: ++386 3 78 05 384
www.store-steel.si

prof. dr. Andrej Paulin

Tehniški metalurški slovar *(CD-ROM za WINDOWS)*

slovensko - angleško - nemški

Technical metallurgical dictionary *(CD-ROM for WINDOWS)*

Slovenian - English - German

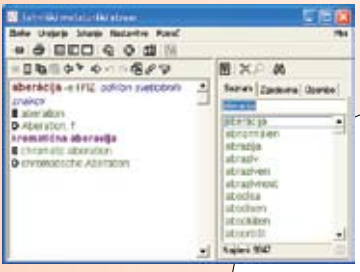

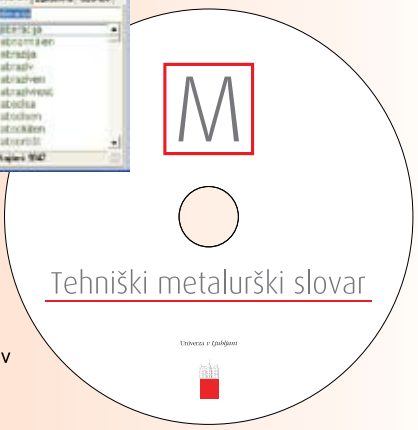

Več kot 10.000 gesel s področij:
- metalurgije,
- tehniških materialov,
- tehnike površin,
- analiznih metod,
- strojništva,
- kemije,
- elektrotehnike,
- ekologije,
- standardizacije,
- predpisov,
- ekonomike in
- uporabe računalništva pri tehnoloških postopkih.

Osnovne značilnosti oz. prednosti elektronske različice slovarja so preprost in izjemno hiter dostop do iskanega gesla, besede ali zveze, tudi pri zahtevnejših pogojih, ter velika prilagodljivost vmesnika uporabnikovim potrebam in željam. Slovar uporablja pregledovalnik ASP32 in je združljiv s številnimi drugimi slovarji v tem sistemu.

Cenik elektronskega slovarja:
Enouporabniška lokalna verzija - 58,00 EUR
5 licenc mrežna verzija - 390,00 EUR
10 licenc mrežna verzija - 535,00 EUR
20 licenc mrežna verzija - 680,00 EUR
30 licenc mrežna verzija - 825,00 EUR
40 licenc mrežna verzija - 970,00 EUR
50 licenc mrežna verzija - 1.115,00 EUR

Leto izdaje: 2007
Issued in 2007

Prices for the electronic dictionary:
Single user local version - 58,00 EUR
5 users network version - 390,00 EUR
10 users network version - 535,00 EUR
20 users network version - 680,00 EUR
30 users network version - 825,00 EUR
40 users network version - 970,00 EUR
50 users network version - 1.115,00 EUR

More than 10 000 technical terms on:
-metallurgy
-technical materials
-surface engineering
-analytical methods
-mechanical engineering
-chemical engineering
-electrical engineering
-environmental engineering
-standardization
-technical regulations
-economics, and
-computer engineering in technological processes

Basic characteristics or advantages, respectively, of electronic version of the dictionary is simple and very fast access to sought term, word or to complex term, also in more demanding conditions, and a great adaptability of the interface to user's needs and wishes. The dictionary uses ASP32 search system that is compatible to numerous other dictionaries in this system.

Za naročila in dodatne informacijenas kontaktirajte preko e-pošte:
For orders and additional information please contact us by e-mail: ***omm@ntf.uni-lj.si***